

AD-A058 515

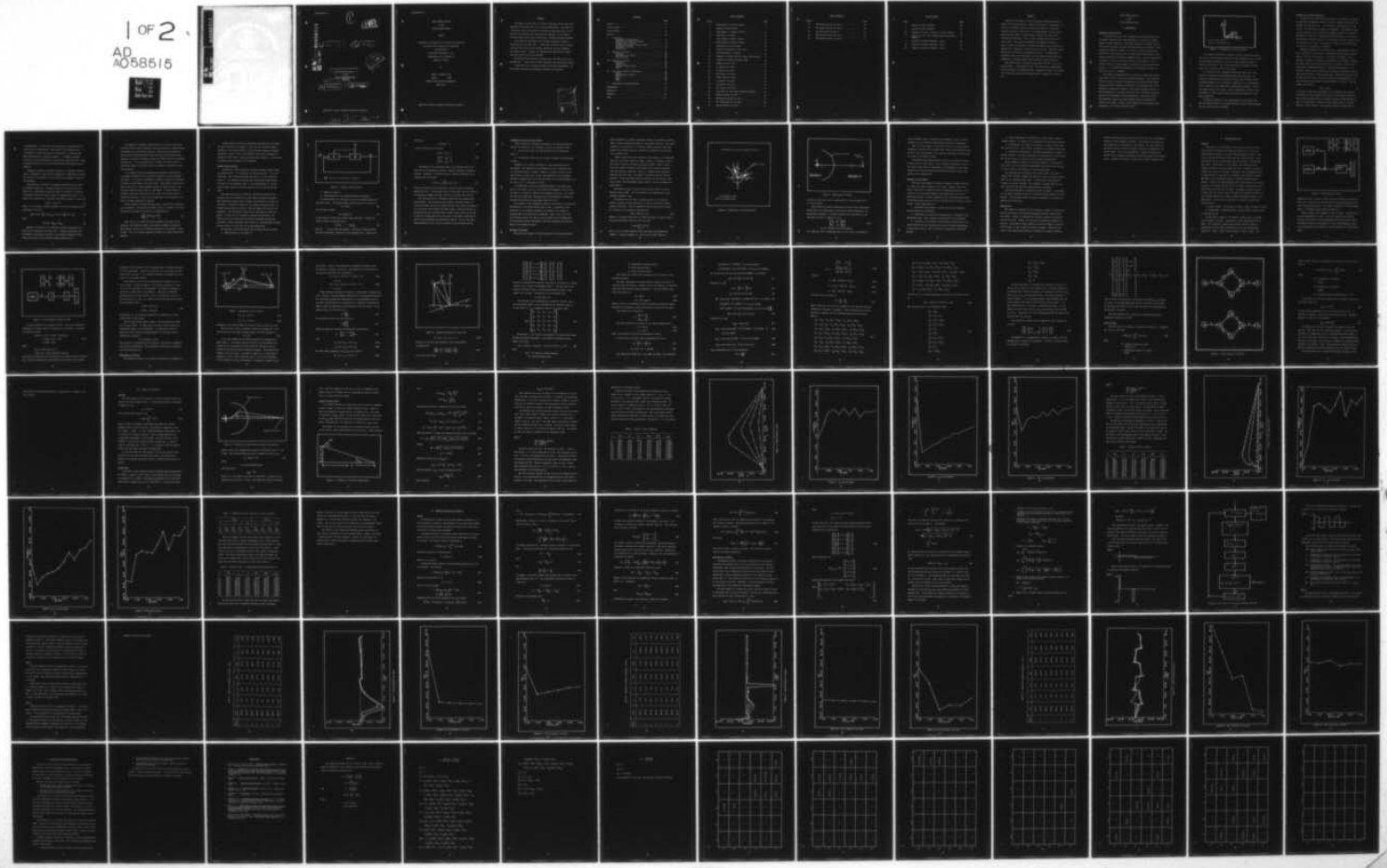
AIR FORCE INST OF TECH WRIGHT-PATTERSON AFB OHIO SCH--ETC F/8 16/4.1
DUAL CONTROL ANALYSIS OF AN AIR TO GROUND MISSILE.(U)

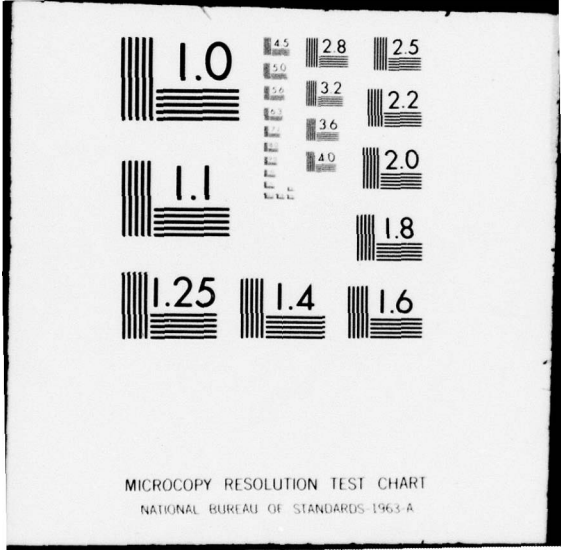
MAR 78 J P KAUPPILA
AFIT/6A/EE/78-1

UNCLASSIFIED

NL

1 OF 2
AD
A058515





MICROCOPY RESOLUTION TEST CHART
NATIONAL BUREAU OF STANDARDS-1963-A

C

LEVEL III

ADA 058515

11 Mar 78

12 128p

AD No. _____
DDC FILE COPY

DDC
APPROVED
SEP 12 1978
AFIT/GA/EE

6 DUAL CONTROL ANALYSIS
OF AN
AIR TO GROUND MISSILE.

9 -master's THESIS.

14 AFIT/GA/EE/78-1

10 James P. Kauppila
Capt ~~USAF~~

Approved for public release; distribution unlimited

78 08 04 059
012 225 Gu

AFIT/GA/EE/78-1

DUAL CONTROL ANALYSIS
OF AN
AIR TO GROUND MISSILE

THESIS

Presented to the Faculty of the School of Engineering
of the Air Force Institute of Technology
Air University
in Partial Fulfillment of the
Requirements for the Degree of
Master of Science

by

James P. Kauppila, B.S.

Captain USAF

Graduate Astronautical Engineering

March 1978

Approved for public release; distribution unlimited

Preface

The intent of this study is to find a trajectory profile which will minimize the terminal error of an air-to-ground missile. This thesis is a follow-on study to the research conducted by Major Rony Dayan, I.A.F. His work was concerned with evaluating the parameters of an advanced missile guidance and control system using a maximum likelihood estimator.

This thesis was sponsored by the Avionics Laboratory, Wright-Patterson Air Force Base, Ohio. I would like to give my sincere thanks to Captain Gary Reid for his untiring assistance and help throughout this entire project. Without his enthusiasm and intellectual insight, this work would not have been possible.

My typists, Miss Patsy Rose and Miss Cheryl Gilliland, did an outstanding job. I thank them for their assistance and professional support.

I would also like to thank my fiancée, Miss Sandra Sundermeyer, for her patience and moral encouragement throughout this research.

ACCESSION for	
NTIS	White Section <input checked="" type="checkbox"/>
DDC	Buff Section <input type="checkbox"/>
UNANNOUNCED	<input type="checkbox"/>
JUSTIFICATION	
BY	
DISTRIBUTION/AVAILABILITY CODES	
Dist. and/or SPECIAL	
A	

Contents

	Page
Preface	ii
List of Figures	iv
List of Tables	vi
Abstract	vii
I. Introduction	1
Background and Motivation	1
Estimation of Unknown Parameters	3
Optimal Control Systems	6
Fundamental Concepts of Dual Control	9
Statement of Problem	9
Organization	14
II. Analysis of Problem	16
Overview	16
Development of P Matrix	19
Plan of Attack	29
III. Single Turn Analysis	33
Overview	33
Initial Turn	33
Terminal Guidance Phase	35
Case 1	37
IV. First-Order Gradient Optimization	50
Theory	50
Application to Problem	53
Case 1	59
Case 2	60
Case 3	60
V. Conclusions and Recommendations	74
Bibliography	76
Appendix A	77
Appendix B	90
VITA	117

List of Figures

Figure		Page
1	Misalignment of Inertial Frames	2
2	Automatic Control System	7
3	Misalignment of Guidance Platform	11
4	Description of Problem	12
5	Block Diagram of Phase I Flight	17
6	Block Diagram of Phase II Flight	18
7	Propagation of Error Ellipse	20
8	Geometrical Analysis of Lift Vector	22
9	Driving Sequence of P Matrix	30
10	Schematic of Flight Paths for Single Turn Analysis.	34
11	Schematic of Terminal Guidance Phase.	35
12	Flight Paths for Case 1	39
13	σ_x Versus α for Case 1	40
14	σ_y Versus α for Case 1	41
15	CEP Versus α for Case 1	42
16	Flight Paths for Case 2	44
17	σ_x Versus α for Case 2	45
18	σ_y Versus α for Case 2	46
19	CEP Versus α for Case 2	47
20	Flow Chart for First-Order Gradient Technique . . .	58
21	Control History for Case 1	63
22	CEP Versus Cycle-No for Case 1	64
23	PSI Versus Cycle-No for Case 1	65
24	Control History for Case 2	67

List of Figures

Figure		Page
25	CEP Versus Cycle-No for Case 2	68
26	PSI Versus Cycle-No for Case 2	69
27	Control History for Case 3	71
28	CEP Versus Cycle-No for Case 3	72
29	PSI Versus Cycle-No for Case 3	73

List of Tables

Table		Page
I	Results of Case 1 Analysis	38
II	Results of Case 2 Analysis	43
III	Comparison of Case 1 and Case 2 at End of Phase I	48
IV	Results of Case 1 with Terminal Maneuvering During Phase II	48
V	Results of Gradient Technique - Case 1	62
VI	Results of Gradient Technique - Case 2	66
VII	Results of Gradient Technique - Case 3	70

Abstract

Many errors are known to exist in Inertial Navigation Systems of modern air-to-ground missiles. These error sources, if undetected, contribute to navigation errors of position and velocity. This study analyses one source of INS errors -- the misalignment of the accelerometer reference frame. By maneuvering a missile, the error source becomes more observable. Thus, a better estimate can be made of the error source. This directly influences the estimate of position. Hence, in order to minimize the terminal navigation error, some control energy must be expended to identify the error source. This dual control problem may be viewed as an optimization problem. By formulating a performance index of the terminal error and control energy appropriate mathematical techniques should yield an optimal flight trajectory.

This thesis seeks to analyze the dual control nature of an air-to-ground missile. Two methods are used. The first uses a predetermined flight path which is incremental until a minimum is reached. The second is a first-order gradient which allows greater freedom in the control law.

DUAL CONTROL ANALYSIS
OF AN
AIR TO GROUND MISSILE

I. Introduction

Background and Motivation

The production of low cost, expendable, air-to-ground missiles is of primary consideration in the development of an effective standoff weapons systems capability. Since these systems are intended strictly for one time use only, low cost navigation systems are employed. These navigation systems are subject to a variety of error sources such as bias errors, scale factor errors, initial position and velocity errors, gravity anomalies, and transfer alignment errors. Each of these sources contribute to errors in the final position of the missile. If the terminal errors are large enough the missile will miss the target completely. It is therefore advantageous to find methods to reduce all sources of error to a minimum.

The transfer alignment problem is perhaps the single most significant source of error for low cost navigation systems. Even though the carrier aircraft is flying in straight and level unaccelerated flight there are inherent vibrations, wind gusts, and turbulence that create problems in aligning the platform of the inertial guidance system. If this misalignment is too large, then there will be incorrect values of specific force measured by the accelerometers. This will be used in the navigation computer and thus erroneous values of position and velocity will result. Figure 1 shows schematically the problem of misalignment of the inertial reference frames.

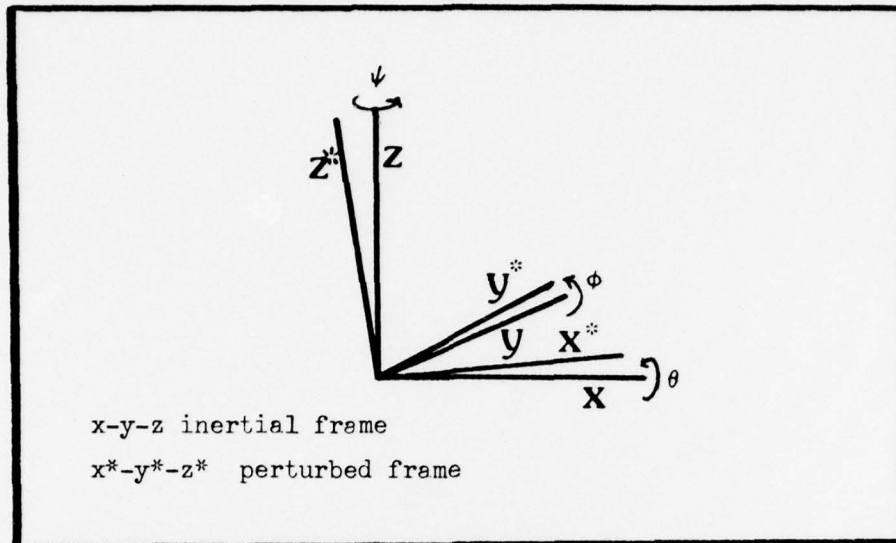


Figure 1. Misalignment of Inertial Frames

If an effective estimation algorithm is used to accurately predict the value of the misalignment angles then this information can be relayed to the navigation computer to arrive at a much improved estimate of position and velocity. This in turn would greatly enhance the probability of a successful "hit" of the target.

In a previous study, conducted by Major Rony Dayan I.A.F., the problem of estimating the misalignment angles was undertaken. By choosing an appropriate system model and using radar tracking the misalignment parameters can be estimated. However, it was not determined if the estimation can be improved by maneuvering the missile. This is the central theme of this study: that by maneuvering a missile it may be possible to induce large sensitivities and hence improve our estimation capability.

In order to establish a clear understanding of the problem some basic background material concerning estimation, optimal control systems, and dual control will be presented.

Estimation of Unknown Parameters

In order to gain understanding and explain the processes of natural and man-made environments, models are created. Models in this sense are mathematical descriptions of these processes. They may pertain to any system. The system may be physical or nonphysical. The important point is that models are made to explain the dynamic processes of the system. Mathematical models aid in understanding the performance of the system. By selecting a suitable criteria, it is possible to select an input which will optimize this factor. By optimal it is meant that the performance criteria will be maximized or minimized.

Modeling encompasses four problem areas: representation, measurement, estimation, and validation. Representation deals with the mathematical structure of the system. Is it static or dynamic, linear or nonlinear, discrete or continuous, deterministic or stochastic? Measurement deals with the physical quantities of the system. There are two basic types of physical quantities: signals and parameters. It is difficult to give a precise definition of signals and parameters because many times they tend to overlap one another. Basically signals are time varying quantities which can easily be measured and parameters are constants which are known only to a certain degree of accuracy. Take for example the relation

$$F(t) = Ma(t) \quad (1)$$

If we apply a known force and measure the acceleration then force and acceleration are the "signals" and the mass is the unknown "parameter." With accurate measurements of the signals, accurate estimations may be made of the parameters. However, in most systems there is a certain amount of "noise" present. This presents a degree of uncertainty in

our measurements. In this case, the uncertainty is described by the covariance of the measurement. This would be the stochastic case. It is desirable to reduce the amount of uncertainty to a desired level. Exact measurements are simply not possible. In summary, parameter estimation is the determination of those physical quantities that cannot be measured directly but can be determined from quantities that can be measured.

Parameter estimation, sometimes referred to as parameter identification, encompasses a large block of engineering. Depending on the type and structure of the system, it may or may not be possible to identify the parameters.

Many numerical techniques for parameter identification are based on parameter sensitivity. Parameter sensitivity is the study of any property of a mathematical model which might be altered by a change of the parameter values from their nominal or assumed values (8:1). If a system can be described by a nonlinear differential equation of the form:

$$\dot{X}(t,b) = f(x,b,t) \quad (2)$$

where b is the unknown, constant parameter, then the relationship may be linearized to the form:

$$\frac{d}{dt} \xi(t,b_0) = \frac{\partial f}{\partial x}(x,b,t)|_{b_0} \xi(t,b_0) + \frac{\partial f}{\partial b}(x,b,t)|_{b_0} \quad (3)$$

where

$$\xi(t,b_0) = \frac{\partial x}{\partial b}(t,b)|_{b_0} \quad (4)$$

Equation 3 is known as the "sensitivity system" and equation 4 is known as the "sensitivity function" (8:4). Parameter sensitivity may be defined as the Fréchet derivative of the unknown mathematical model output with respect to the unknown constant parameter (8:1).

One approach to parameter identification is to view it as an optimization problem in which parameter values are selected to either maximize or minimize some selected cost function. This may be the difference between some predetermined model output and the actual measured output. Generally an iterative technique is used and involves the use of parameter sensitivities. If our sensitivities are "large" then there will be a noticeable change in our output and we can compute our parameter values more accurately.

It is apparent from the discussion that parameter identification is extremely important if it is desired to obtain an accurate mathematical model. In the case of navigation, parameter values of the equations of motion are the unknown sources of error. Such things as bias values, scale factor errors, and misalignment angles are known to exist in any Inertial Navigation System (INS) to some degree. If these values are estimated incorrectly then there will be errors in the model output of position and velocity. Thus for an accurate INS, it is necessary to be able to estimate parameters accurately.

In the navigation problem discussed above, accurate state estimation is also required. As described by Eykoff (3:446), a problem of this type with constant parameter vector \bar{a} may be reformulated as:

$$\begin{bmatrix} \dot{x} \\ \dot{a} \end{bmatrix} = \begin{bmatrix} f(x,u,a,u,t) \\ 0 \end{bmatrix} \quad (5)$$

Thus, even for a process with linear dynamics and linear in the parameter, the combined parameter and estimation problem is nonlinear. This suggests the use of an iterative technique for the solution of this problem. One of the methods suggested by Eykoff is a quasi-linearization approach.

In many cases the problem of optimizing performance by controlling the input variables is considered. When the system contains unknown parameters, the problem becomes a tradeoff between parameter estimation and optimal control. This is the theory of dual control presented by Feldbaum in 1960 (4:31). Before discussing this, however, a brief review of optimal control systems will be presented.

Optimal Control Systems

In Figure 2, a block diagram of a general automatic control system is presented (4:8). "B" represents the controlled object. "A" is the controller. The controller provides the input, U , to the controlled object B. "X" represents the controlled variable which characterizes the state of the controlled object B. The perturbations, Z , are measured as input noise and cause the output X to vary from the desired state.

The controlled object is fixed for a particular system but the controller may be selected from a large class of possible algorithms. When considering optimal control systems, the problem is to choose the controller, A, which will control B, in a known, predictable manner to minimize the performance criteria. Take for example the control of an automobile. The performance function may be efficiency or miles per gallon. In this case it is desired to maximize the function. The driver would be the controller and using his knowledge of speed and efficiency, traffic conditions, route selection, and maintenance required, he will be able to control the car at the optimal level.

In selecting a controller usually the following factors are used:

1. Characteristics of the object B

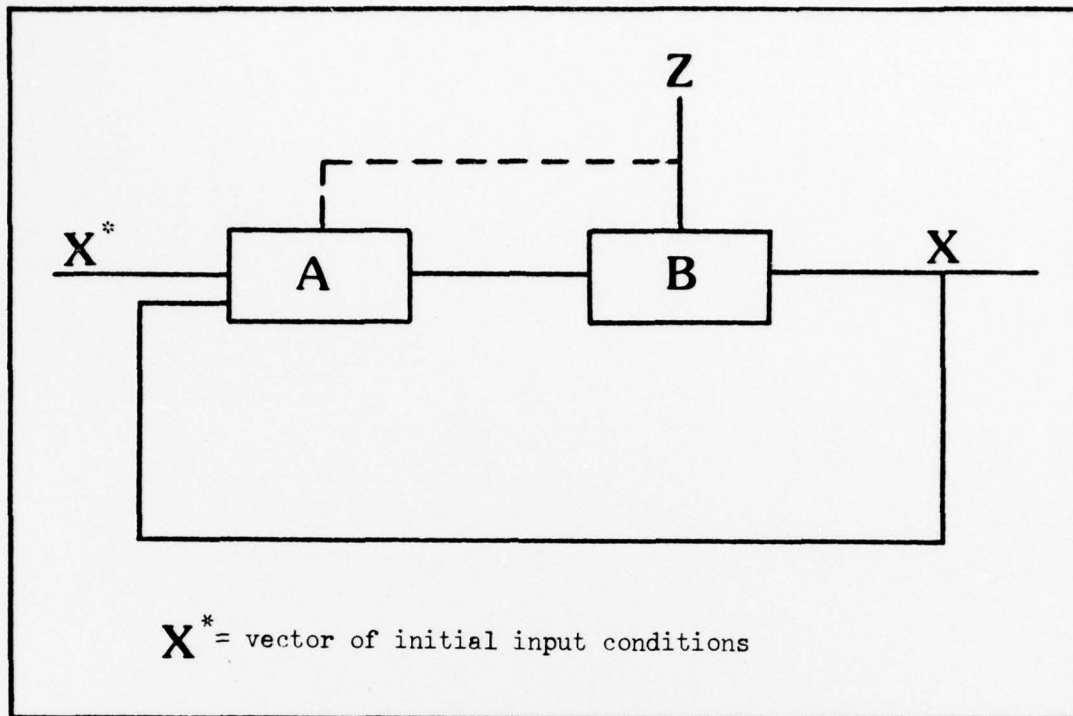


Figure 2. Automatic Control System

2. Demands on object B
3. Characteristics of the information about B entering A

The characteristics of the object B are the relations between the input and output. In general operator notation this may be written as

$$\bar{X} = f(\bar{u}, z) \quad (6)$$

or for dynamic systems

$$\dot{\bar{X}} = f(\bar{X}, \bar{u}, \bar{z}, t) \quad (7)$$

In any realistic system there will be some constraints. Usually the control \bar{u} may be restricted such as:

$$|U_1| \leq U_1 \dots \dots |U_m| \leq U_m \quad (8)$$

where $U_1 \dots U_m$ are selected constants. The state of the system may also have constraints, especially at the terminal state. These may be

written as

$$\Psi [\bar{x}, t_f] = 0 \quad (9)$$

or more specifically in the form

$$\begin{aligned} x_1(t_f) - x_{1f} &= 0 \\ x_2(t_f) - x_{2f} &= 0 \\ \vdots & \\ x_n(t_f) - x_{nf} &= 0 \end{aligned} \quad (10)$$

The demands on the controlled object B are characterized by the selection of the optimality criteria. Usually a minimum or maximum is desired. Typically J is selected based on terminal conditions and an integral term of the form:

$$J = \phi(x, t_f) + \int_{t_0}^{t_f} L(x, u, t) dx \quad (11)$$

The actual selection of the optimality criteria presents a difficult problem in itself. The important point is that once J has been selected the problem is finding the input control \bar{u} to minimize the function.

The characteristics of information entering A vary significantly among systems. Some systems may have complete information about the controlled object, while other systems may have only partial information. It is the latter that presents the most concern. With only partial information about the controlled object B some of the control action must be used for learning more about the nature of the object itself and not just strictly minimizing the performance function. This is the underlying assumption of dual control discussed in the following section.

Fundamental Concepts of Dual Control

When a system with incomplete knowledge of the controlled object B exists, the controller A is attempting to solve two problems (4:26):

1. To learn more about the characteristics of the controlled object B.
2. To determine future control actions to minimize the performance criteria.

Feldbaum (4:27) offers an analogy of a man interacting with his environment. Man studies the surroundings in order to influence them in a direction useful to himself. However, in order to direct his own actions better he must have a better understanding of his environment. Therefore, sometimes he acts on the environment not to take advantage of it but only to try to understand it better.

In considering a system with unknown parameters, the conflicting goals in the control law are to learn about the parameters and to direct the object in a manner to minimize the performance function. As a result the control law must have characteristics of distributing its energy for learning and achieving the performance objective (1:2).

As a measure of the information content of the object B, a probability distribution of the characteristics may be used. A reduction in the covariance of the parameter estimates is a measure of the amount of learning made by the dual control algorithm. Thus, in the case of an air-to-ground missile, the control action should be able to demonstrate the relationship between knowledge of the error parameters and the estimates of the navigation states.

Statement of Problem

This study will analyze an inertially guided air-to-ground missile,

with an unknown but constant misalignment angle of the guidance platform. Figure 3 shows a simplified drawing of the guidance platform. The overall objective of the analysis is to find the nominal trajectory which will minimize the terminal position covariance as indicated by the circular error probable (CEP).

Figure 4 shows the overall scenario of the problem to be considered. There are two distinct phases of flight. Phase I is a period in which the carrier aircraft can track the missile by radar. There is also a data link between the missile and aircraft which allows for updating state and parameter estimates. Phase II is without radar tracking or communications data link. The missile is controlled by pure inertial guidance. During this phase parameter estimates of bias values, scale factor errors, and misalignment angles remain at the last estimate made during Phase I.

The terminal target is fixed in space but the missile is free to maneuver during flight. This is especially true during Phase I where parameter estimates occur.

The objective of the study, as stated earlier, is to find the nominal trajectory profile which gives, a priori, the lowest terminal position covariance. This is measured by the CEP which can be written as a function of the position covariance as:

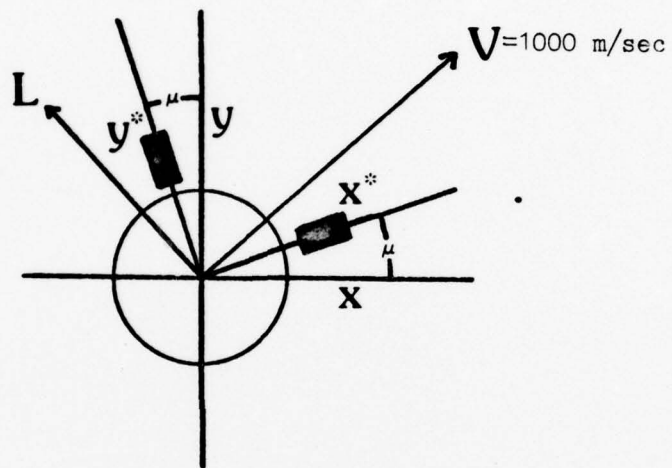
$$\text{CEP} = 0.588 (\sigma_x + \sigma_y) \quad (12)$$

However, a secondary objective is to limit the amount of control used so the total performance objective is of the form:

$$J = \text{CEP} + \int_{t_0}^{t_f} w_1 L^2 dt \quad (13)$$

where w_1 is a constant weighting value determined from engineering judgment. The major emphasis on J will be on the CEP; however, a

Two Dimensional Inertial Reference Platform



μ = misalignment angle
 X^*-Y^* perturbed frame

Figure 3. Description of Missile Platform

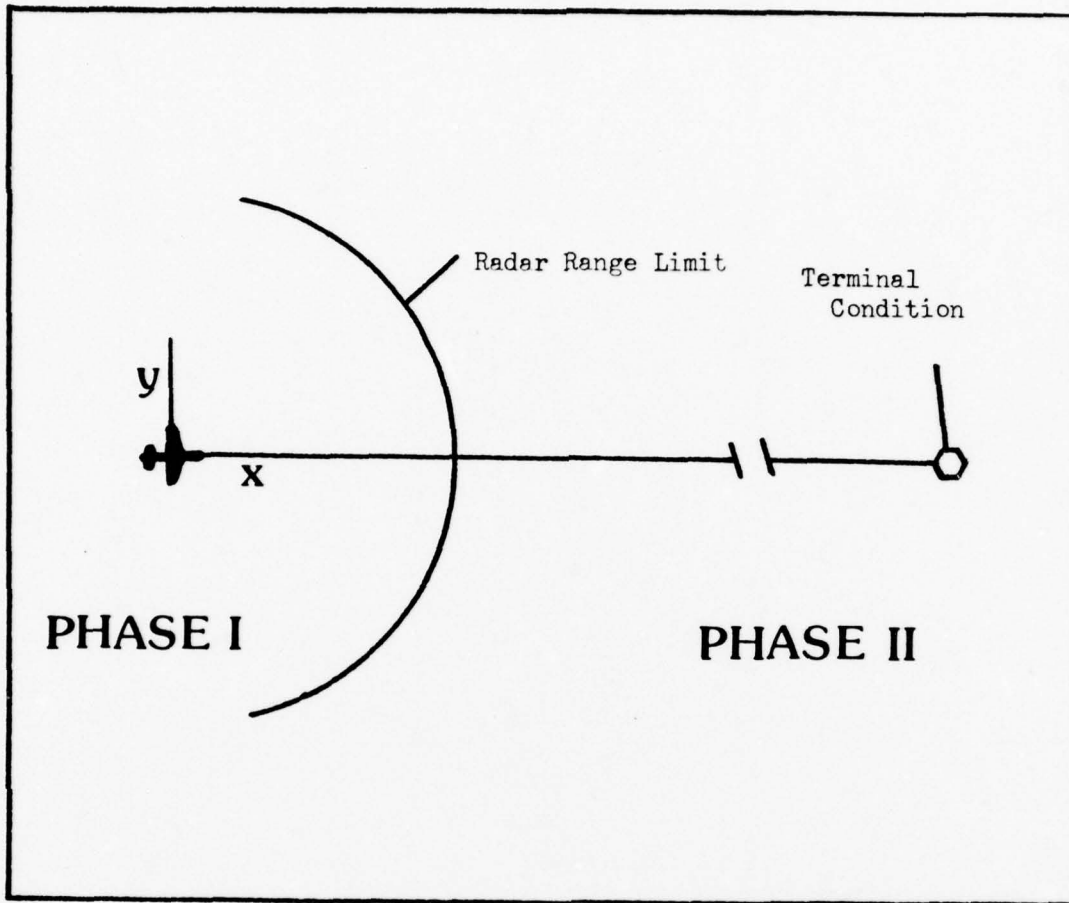


Figure 4. Description of Problem

realistic problem must also be concerned with a finite energy source for control input.

This problem has several characteristics which deserve explanation. During Phase I the maneuvering of the missile allows estimation of the system model parameters. The model equations for acceleration, to be developed in detail in Chapter II, are:

$$\begin{bmatrix} \dot{v}_x \\ \dot{v}_y \end{bmatrix} = \begin{bmatrix} 1 & -\mu \\ \mu & 1 \end{bmatrix} \begin{bmatrix} a_x \\ a_y \end{bmatrix} \quad (14)$$

a_x, a_y = specific force measurements

It is apparent that by commanding inputs to the x and y accelerometers

the misalignment angle, μ , becomes more observable. Hence, a better estimate of μ may be made by maneuvering the missile in some matter.

Phase II of the flight is "open loop"; that is, no more parameter estimates are fed back to the missile INS. Hence, any uncertainty which may still exist during Phase II will directly contribute to the success or failure of the missile system.

Considering these characteristics, it may be concluded that this problem is one of dual control. This is because during Phase I use of the control input directly contributes to the knowledge of the system parameters and hence influences the ultimate objective--to get to the target with the minimum CEP.

Approach to the Problem

This study could logically include all phases of flight from boost to cruise and terminal guidance to the target. However, since this study is primarily a feasibility study in applying the concept of dual control to an air-to-ground missile, the approach will be to use a simplified analysis. Several assumptions will be made which will limit the modeling process but still allow a detailed study of the dual control concept. These assumptions are:

1. The missile has boosted to cruise velocity and maintains a constant velocity of 1000 m/sec.
2. The missile is restricted to maneuvering in a horizontal, two-dimensional plane. Hence, gravity accelerations are not considered.
3. The control of the missile is restricted to deflection of the control surfaces and the resultant lift vector is always perpendicular to the velocity vector. The lift vector is restricted to 100 m/sec^2 maximum.

4. The accelerometers are misaligned by a small angle μ which is assumed constant. See Figure 3 for a description of the missile platform.

5. During Phase I of flight, the missile is tracked by radar from the carrier aircraft. The aircraft is modeled as a stationary point mass.

6. During the tracking phase, continuous measurements are taken of missile position. The radar measurements are taken directly in polar form but can be related to cartesian form by a simple transformation.

These assumptions simplify the analysis; however, if the concept of dual control can be successfully demonstrated then the door will be open to future study of this concept on a more detailed basis.

Two algorithms were employed to solve this problem. The first, a "single turn" analysis, commands the missile to turn to a desired α angle then fly to a specified range limit. It then flies to the target by turning to the proper heading. This technique, although simple in concept, allows for the numerical demonstration of the theory.

The second algorithm is a modified gradient technique. By searching in the negative gradient direction, the method should converge to a local minimum. This technique allows for greater flexibility in the amount of maneuvering during Phase I.

Organization

This thesis is organized into five chapters. Chapter I is the introduction, motivation, and underlying background material concerned with the problem. Chapter II formulates the problem in detail and describes the plan of attack. Chapter III discusses the single turn analysis for solution. This chapter brings together the theory of Chapter I and problem of Chapter II into a realistic numerical example. Chapter IV discusses a more sophisticated numerical technique for finding a solution.

Gradient optimization was used because of its fast rate of convergence during the initial phases of solution. The numerical difficulties of this method are also explained in this chapter. The last chapter summarizes the results, forms conclusions, and makes recommendations for further study. There are two appendices. Appendix A presents the details of the continuous measurement covariance equation of the Kalman filter. Appendix B presents a listing of the computer programs used.

II. Problem Formulation

Overview

The problem to be undertaken by this study is to find a control input which will minimize the terminal position error of an air-to-ground missile employing a low cost inertial navigation system. There are two inherent difficulties which preclude an easy solution. These difficulties are the time-of-flight and the knowledge of the misalignment angle. During Phase II of the flight, the covariance of the position estimates can only increase with time. Therefore, the time-of-flight must be kept to a minimum. Knowledge of the misalignment angle, μ , helps directly in reducing the covariance of the position estimates. Knowledge of the misalignment angle is achieved by maneuvering the missile. However, too much maneuvering will increase the time of flight. Therefore, the optimum solution will be a tradeoff between the amount of maneuvering versus the time of flight. In summary, the main objective of this study is to find a control law which will minimize the CEP of an air-to-ground missile with a small, constant misalignment angle of the INS platform. The control law will have to consider the conflicting difficulties of:

1. Time of flight: the shorter the time of flight the smaller the CEP.
2. Maneuvering: increased maneuvering during Phase I directly aids in reducing the CEP.

As described in Chapter I, the missile trajectory will be divided into two phases of flight. During Phase I radar measurements will be taken. The estimates of position and velocity will be a result of measurements from the INS accelerometers and the radar measurements themselves. Figure 5 shows a block diagram of Phase I flight. The

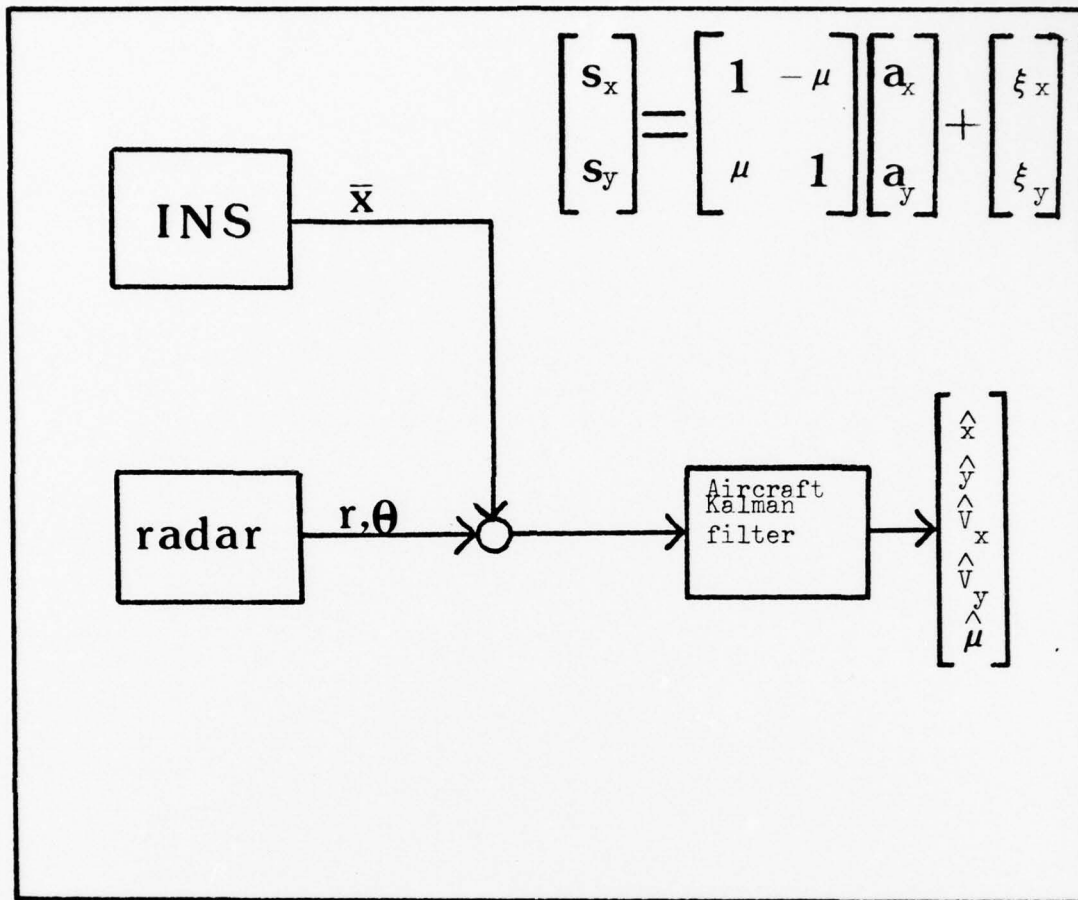


Figure 5. Block Diagram of Phase I

important feature of Phase I is that the state estimates and covariance matrix are a result of both the INS specific force measurements and the radar tracking measurements. As a result, knowledge of the misalignment angle μ is constantly being updated and improved.

Figure 6 shows a block diagram of Phase II flight. During Phase II, no radar measurements are taken. The state estimates are produced strictly by the specific force measurements taken by the INS platform. The important feature during Phase II is that the misalignment angle μ is not being updated but remains at the last estimate, $\hat{\mu}$, made during Phase I.

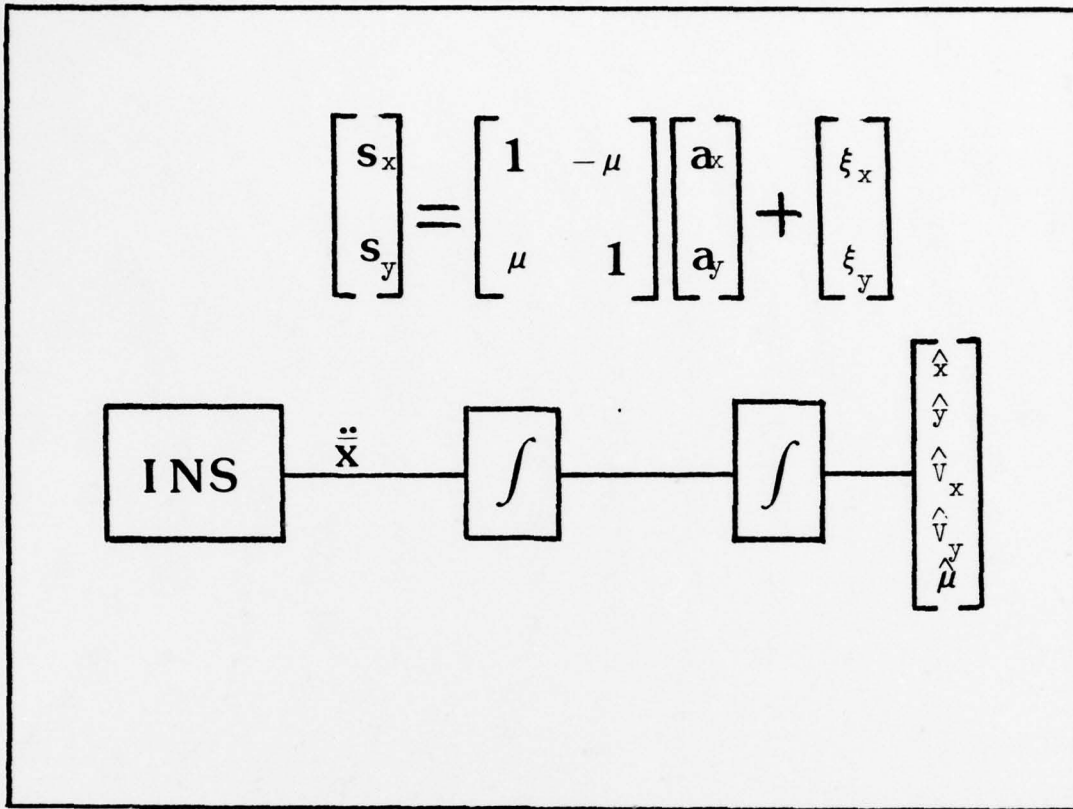


Figure 6. Block Diagram of Phase II Flight

Our main objective is to minimize the CEP. This can be achieved by minimizing the terminal position covariance of the estimate. Covariance is defined as (6:80):

$$\begin{aligned} \text{cov}(x,y) &= \Sigma (X_i - \mu_x)(Y_j - \mu_y)h(X_i, Y_j) \\ &= E [(X - \mu_x)(Y - \mu_y)] \\ &= E [XY] - \mu_x\mu_y \end{aligned} \tag{15}$$

where

μ_x, μ_y = mean value of x, y

$h(X_i, Y_j)$ = joint probability function

Covariance is a measure of the uncertainty of the random quantity involved.

For a Gaussian distributed random variable, 67.8 percent of the random

samplings of that variable will be contained within ± 1 standard deviation (σ) of the mean value. Obviously the smaller the σ the smaller the dispersion about the mean. It is therefore desirable to minimize the covariance for a successful missile.

The covariance of the x and y estimates may be thought of as an error ellipse. As shown in Figure 7, the initial covariance of x and y is an area of uncertainty of the estimate. The ellipse is propagated forward by a Kalman filter during Phase I. This will be developed mathematically in the next section. Now it is sufficient to say that the covariances of x and y are a function of the lift and time of flight, and misalignment angle μ :

$$\begin{aligned} \text{cov}(x) &= f(L, t_f, \mu) \\ \text{cov}(y) &= f(L, t_f, \mu) \end{aligned} \tag{16}$$

During Phase II, the covariance propagation is expressed as a linear system driven by white noise.

The two flight paths shown in Figure 7 show the intuitive effects on the error ellipse. In flight path A no lift is produced hence the misalignment angle μ is not observable. In flight path B the lift generated directly effects the observability of μ and hence aids in reducing the covariance.

$$L \rightarrow \hat{u} \rightarrow \text{cov}(x), \text{cov}(y)$$

The covariance is represented by the P matrix. This matrix is symmetric and positive semi-definite. The derivation of this matrix is presented in the following section.

Development of P Matrix

The dynamical relations of the missile position may be expressed as:

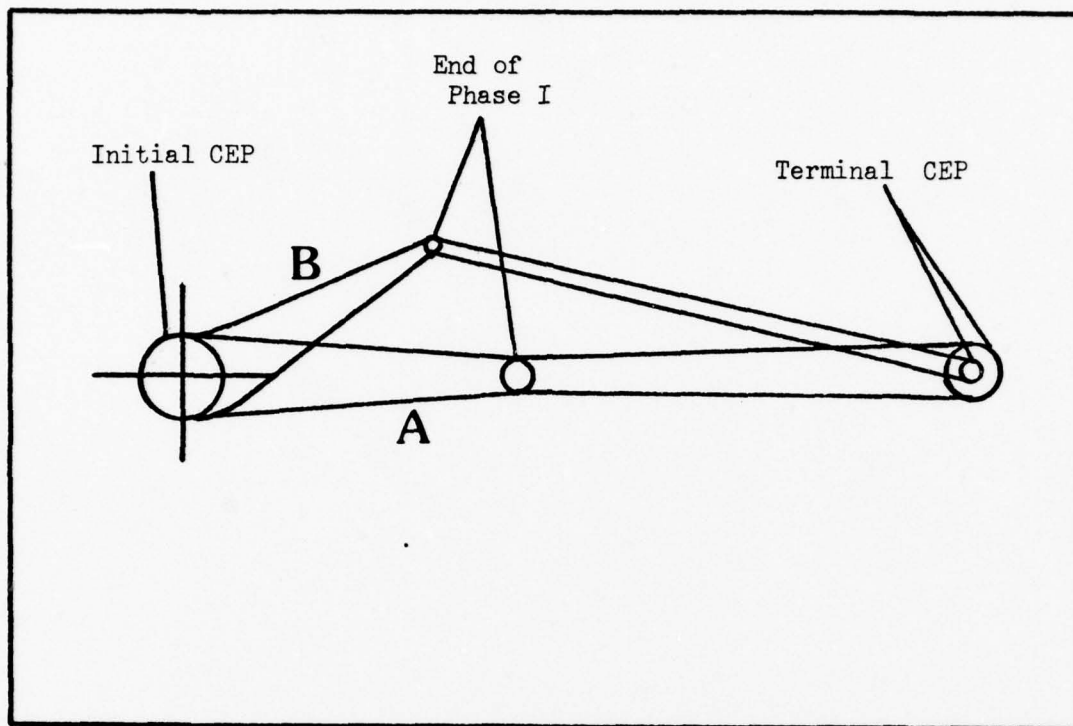


Figure 7. Propagation of Error Ellipse

$$\dot{X}_1 = V_1 = V \cos \theta \quad (17a)$$

$$\dot{X}_2 = V_2 = V \sin \theta \quad (17b)$$

Assuming θ is the angle between the velocity vector V and the X_1 axis.

Since the lift vector is assumed to always be perpendicular to the velocity vector, the change in heading angle, θ , may be expressed as:

$$\dot{\theta} = L/V \quad (18)$$

It was also assumed that the missile platform is misaligned by a small angle, μ . This means incorrect specific force measurements will be made by the accelerometers and this incorrect information will be relayed to the on-board missile navigation computer. More specifically looking at the lift vector, L as shown in Figure 8, L_1 is the desired component of lift in the X_1 direction and L_1^* is the actual component of lift measured by the X_1 accelerometer. As long as μ is small $L_1 \approx L_1^*$

and $L_2 \approx L_2^*$. However, the discrepancy is significant enough to cause the missile to navigate incorrectly. The equations for acceleration in the X_1 and X_2 directions are respectfully

$$\begin{aligned} S_x = \dot{V}_1 &= -V \sin \theta \dot{\theta} = -V \sin \theta \cdot L/V \\ &= L \sin \theta \end{aligned} \quad (19a)$$

$$\begin{aligned} S_y = \dot{V}_2 &= V \cos \theta \dot{\theta} = V \cos \theta \cdot L/V \\ &= L \cos \theta \end{aligned} \quad (19b)$$

These equations represent the desired or "truth model" representation of $\ddot{\bar{X}}$. Because of the misalignment problem, $\dot{\bar{V}}$ may be expressed differently. The relationship between the measurements in a non-misaligned frame and one which is misaligned may be considered as a coordinate transformation. Figure 8 shows the geometrical interpretation of the lift vector. In the nominal frame, the lift vector is:

$$\bar{L} = \begin{bmatrix} L_1 \\ L_2 \end{bmatrix} \quad (20)$$

In the perturbed frame, the lift vector is:

$$\bar{L} = \begin{bmatrix} L_{1*} \\ L_{2*} \end{bmatrix} \quad (21)$$

These two frames are related by the direction cosine matrix:

$$\bar{L} = \begin{bmatrix} \cos \mu & -\sin \mu \\ \sin \mu & \cos \mu \end{bmatrix} \bar{L}^* \quad (22)$$

thus

$$L_1 = \cos \mu L_{1*} - \sin \mu L_{2*} \quad (23a)$$

$$L_2 = \sin \mu L_{1*} + \cos \mu L_{2*} \quad (23b)$$

For small angle assumption, and $L_{1*} \approx L_1$ this results:

$$S_x = \dot{V}_1 = L_1 - \mu L_2 + \xi x \quad (24a)$$

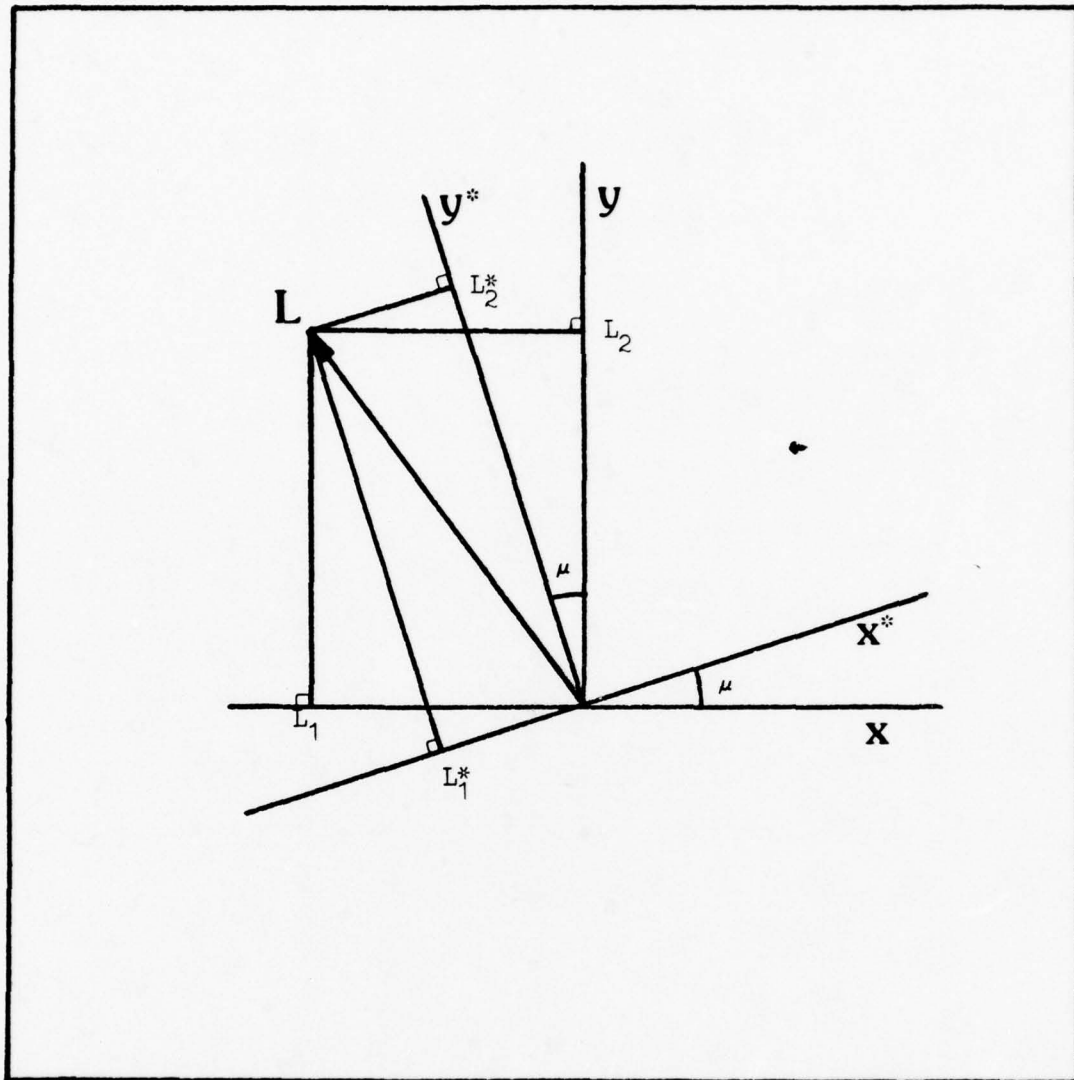


Figure 8. Geometrical Analysis of Lift Vector

$$S_y = \dot{v}_2 = \mu L_1 + L_2 + \xi_y \quad (24b)$$

where ξ_x , ξ_y are the noise inherent to the accelerometers.

in matrix form:

$$\begin{bmatrix} S_x \\ S_y \end{bmatrix} = \begin{bmatrix} 1 & -\mu \\ \mu & 1 \end{bmatrix} \begin{bmatrix} L_1 \\ L_2 \end{bmatrix} + \begin{bmatrix} \xi_x \\ \xi_y \end{bmatrix} \quad (25)$$

or in first order form:

$$\begin{bmatrix} \dot{x}_1 \\ \dot{x}_2 \\ \dot{v}_1 \\ \dot{v}_2 \\ \dot{\mu} \end{bmatrix} = \begin{bmatrix} 0 & 0 & 1 & 0 & 0 \\ 0 & 0 & 0 & 1 & 0 \\ 0 & 0 & 0 & 0 & -L_2 \\ 0 & 0 & 0 & 0 & L_1 \\ 0 & 0 & 0 & 0 & 0 \end{bmatrix} \begin{bmatrix} x_1 \\ x_2 \\ v_1 \\ v_2 \\ \mu \end{bmatrix} + \begin{bmatrix} 0 \\ 0 \\ L_1 \\ L_2 \\ 0 \end{bmatrix} + \begin{bmatrix} 0 \\ 0 \\ \xi_1 \\ \xi_2 \\ 0 \end{bmatrix} \quad (26)$$

Equation 26 represents the dynamical relations of a missile at a constant velocity with a constant misalignment angle, μ . The last term of the equation represents noise or undesired disturbances present to some degree in all systems. The equation is of the general form:

$$\dot{\bar{x}} = \bar{A}\bar{x} + \bar{B}u + \bar{G}\bar{\xi}$$

The covariance of the measurements of position, velocity, and of the misalignment angle μ can be expressed by the covariance matrix, P .

In this case P is a 5 x 5 symmetric matrix of the general form:

$$[P] = \begin{bmatrix} P_{11} & P_{12} & P_{13} & P_{14} & P_{15} \\ P_{21} & P_{22} & P_{23} & P_{24} & P_{25} \\ P_{31} & P_{32} & P_{33} & P_{34} & P_{35} \\ P_{41} & P_{42} & P_{43} & P_{44} & P_{45} \\ P_{51} & P_{52} & P_{53} & P_{54} & P_{55} \end{bmatrix} \quad (27)$$

During Phase I, the P matrix is propagated by a Kalman filter using INS data and radar measurements. The equation describing \dot{P} during Phase I is (7:273):

$$\dot{P}(t) = F(t)P(t) + P(t)F^t(t) - P(t)HR^{-1}HP(t) + GQG^t \quad (28)$$

where

$F(t)$ = "A" matrix of system equations

H = output position matrix

R = measurement covariance matrix

G = noise position matrix

Q = noise covariance matrix

The F matrix has already been developed as the "A" matrix of the missile INS system.

The radar measurements are taken directly in polar form, that is, range and angle information. Inherent to any radar system is a covariance associated with range and angle measurements. For this problem, these values are chosen as:

$$\sigma_R = 100 \text{ m} \quad (29a)$$

$$\sigma_\theta = 10^{-3} \text{ radians} \quad (29b)$$

However, since it is desirable to work in cartesian coordinates, expressions must be developed to relate the R matrix to the σ_R and σ_θ values.

The R matrix can be written as:

$$R = \begin{bmatrix} \sigma_x^2 & \sigma_{xy} \\ \sigma_{xy} & \sigma_y^2 \end{bmatrix} \quad (30)$$

The x and y positions are related to the radar measurements by:

$$x = r \cos \theta \quad (31a)$$

$$y = r \sin \theta \quad (31b)$$

Thus, an expression for $\sigma_{x_1}^2$ may be developed as follows:

To first order, the Taylor series approximation of Δx is:

$$\Delta x \approx \frac{\sigma_{x_1}}{\sigma_r} \Delta r + \frac{\sigma_{x_1}}{\sigma_\theta} \Delta \theta \quad (32)$$

$$\Delta x = \cos \theta \Delta r - r \sin \theta \Delta \theta \quad (33)$$

$$\sigma_{x_1}^2 = E[\Delta x_1 \cdot \Delta x_1] = E[(\cos \theta \Delta r - r \sin \theta \Delta \theta) (\cos \theta \Delta r - r \sin \theta \Delta \theta)] \quad (34)$$

$$\begin{aligned}
&= E[\text{Cos}^2 \theta \Delta R^2 + R^2 \text{Sin}^2 \theta \Delta \theta^2 - 2R \text{Sin} \theta \text{Cos} \theta \Delta \theta R] \\
&= \text{Cos}^2 \theta E[\Delta R^2] + R^2 \text{Sin}^2 \theta E[\Delta \theta^2] - 2R \text{Sin} \theta \text{Cos} \theta E[\Delta \theta \Delta R]
\end{aligned}$$

For uncorrelated and zero mean functions $E[\Delta \theta \Delta R] = 0$, therefore,

$$\sigma_{x_2}^1 = \text{Cos}^2 \theta \sigma_R^2 + R^2 \text{Sin}^2 \theta \sigma_\theta^2 \quad (35)$$

Similarly for $\sigma_{x_2}^2$:

$$\Delta X_2 = \frac{\sigma_{x_2}}{\sigma_R} \Delta R + \frac{\sigma_{x_2}}{\sigma_\theta} \Delta \theta \quad (36)$$

$$\Delta X_2 = \text{Sin} \theta \Delta R + R \text{Cos} \theta \Delta \theta \quad (37)$$

$$\sigma_{x_2}^2 = E[\Delta X_2 \cdot \Delta X_2] = E[(\text{Sin} \theta \Delta R + R \text{Cos} \theta \Delta \theta)(\text{Sin} \theta \Delta R + R \text{Cos} \theta \Delta \theta)] \quad (38)$$

$$= E[\text{Sin}^2 \theta \Delta R^2 + R^2 \text{Cos}^2 \theta \Delta \theta^2 + 2R \text{Sin} \theta \text{Cos} \theta \Delta R \Delta \theta]$$

$$= \text{Sin}^2 \theta E[\Delta R^2] + R^2 \text{Cos}^2 \theta E[\text{Cos}^2 \theta \Delta \theta^2] + 2R \text{Sin} \theta \text{Cos} \theta E \left[\begin{array}{c} \Delta R \\ \Delta \theta \end{array} \right]$$

$$\sigma_{x_2}^2 = \text{Sin}^2 \theta \sigma_R^2 + R^2 \text{Cos}^2 \theta \sigma_\theta^2 \quad (39)$$

Similarly for $\sigma_{x_1 x_2}$:

$$\sigma_{x_1 x_2} = E[\Delta X_1 \cdot \Delta X_2] \quad (40)$$

$$\sigma_{x_1 x_2} = E[\text{Cos} \theta \text{Sin} \theta \Delta R^2 - R^2 \text{Sin}^2 \theta \Delta \theta \Delta R + R \text{Cos}^2 \theta \Delta R \Delta \theta - R^2 \quad (40a)$$

$$\text{Sin} \theta \text{Cos} \theta \Delta \theta^2]$$

$$\sigma_{x_1 x_2} = \text{Cos} \theta \text{Sin} \theta E[\Delta R^2] - R^2 \text{Sin} \theta \text{Cos} \theta E[\Delta \theta^2] \quad (40b)$$

$$\sigma_{x_1 x_2} = \text{Cos} \theta \text{Sin} \theta \sigma_R^2 - R^2 \text{Sin} \theta \text{Cos} \theta \sigma_\theta^2 \quad (40c)$$

Now an expression for R^{-1} may be developed.

$$R^{-1} = \frac{\text{adj } R}{[R]} \quad (41)$$

$$R^{-1} = \frac{\begin{bmatrix} \sigma x_2^2 & -\sigma x_1 x_2 \\ -\sigma x_1 x_2 & \sigma x_1^2 \end{bmatrix}}{(\sigma x_1^2 \sigma x_2^2 - \sigma x_1^2 x_2)} \quad (41a)$$

letting

$$A = \sigma x_2^2 / (\sigma x_1^2 \sigma x_2^2 - \sigma x_1^2 x_2) \quad (41b)$$

$$B = \sigma x_1 x_2 / (\sigma x_1^2 \sigma x_2^2 - \sigma x_1^2 x_2) \quad (41c)$$

$$D = \sigma x_1^2 / (\sigma x_1^2 \sigma x_2^2 - \sigma x_1^2 x_2) \quad (41d)$$

the matrix may be written as:

$$R^{-1} = \begin{bmatrix} A & B \\ B & D \end{bmatrix} \quad (42)$$

Again noting that the P matrix is symmetrical only the upper diagonal elements are necessary to propagate. After multiplying the matrices developed in Equation 28, the following equations are derived for

Phase I:

$$\begin{aligned} \dot{P}_{11} &= 2P_{13} - P_{11} (AP_{11} + BP_{12}) - P_{12} (BP_{11} + DP_{12}) \\ \dot{P}_{12} &= P_{23} + P_{14} - P_{11} (AP_{12} + BP_{22}) - P_{12} (BP_{12} + DP_{22}) \\ \dot{P}_{13} &= P_{33} - L_2 P_{15} - P_{11} (AP_{13} + BP_{23}) - P_{12} (BP_{13} + DP_{23}) \\ \dot{P}_{14} &= P_{34} + L_1 P_{15} - P_{11} (AP_{14} + BP_{24}) - P_{12} (BP_{14} + DP_{24}) \\ \dot{P}_{15} &= P_{35} - P_{11} (AP_{15} + BP_{25}) - P_{12} (BP_{15} + DP_{25}) \\ \dot{P}_{22} &= 2P_{24} - P_{12} (AP_{12} + BP_{22}) - P_{22} (BP_{12} + DP_{22}) \\ \dot{P}_{23} &= P_{34} - L_2 P_{25} - P_{12} (AP_{13} + BP_{23}) - P_{22} (BP_{13} + DP_{23}) \\ \dot{P}_{24} &= P_{44} + L_1 P_{25} - P_{12} (AP_{14} + BP_{24}) - P_{22} (BP_{14} + DP_{24}) \end{aligned} \quad (43)$$

$$\begin{aligned}
\dot{P}_{25} &= P_{45} - P_{12} (AP_{15} + BP_{25}) - P_{22} (BP_{15} + DP_{25}) \\
\dot{P}_{33} &= -2L_2 P_{35} - P_{13} (AP_{13} + BP_{23}) - P_{23} (BP_{13} + DP_{23}) \\
\dot{P}_{34} &= -L_2 P_{45} + L_1 P_{35} - P_{13} (AP_{14} + BP_{24}) - P_{23} (BP_{14} + DP_{24}) \\
\dot{P}_{35} &= -L_2 P_{55} - P_{13} (AP_{15} + BP_{25}) - P_{23} (BP_{15} + DP_{25}) \\
\dot{P}_{44} &= +2L_1 P_{45} - P_{14} (AP_{14} + BP_{24}) - P_{24} (BP_{14} + DP_{24}) \\
\dot{P}_{45} &= +L_1 P_{55} - P_{14} (AP_{15} + BP_{25}) - P_{24} (BP_{15} + DP_{25}) \\
\dot{P}_{55} &= -P_{15} (AP_{15} + BP_{25}) - P_{25} (BP_{15} + DP_{25})
\end{aligned}$$

During Phase II, no radar measurements are taken so the equation for \dot{P} is:

$$\dot{P}(t) = F(t)P(t) + P(t)F^t(t) + GQG^t \quad (44)$$

Thus during Phase II, the \dot{P} equations become:

$$\begin{aligned}
\dot{P}_{11} &= 2P_{13} \\
\dot{P}_{12} &= P_{23} + P_{14} \\
\dot{P}_{13} &= P_{33} - L_2 P_{15} \\
\dot{P}_{14} &= P_{34} + L_1 P_{15} \\
\dot{P}_{15} &= P_{35} \\
\dot{P}_{22} &= 2P_{24} \\
\dot{P}_{23} &= P_{34} - L_2 P_{25} \\
\dot{P}_{24} &= P_{44} + L_1 P_{25} \\
\dot{P}_{25} &= P_{45} \\
\dot{P}_{33} &= -2L_2 P_{35}
\end{aligned} \quad (45)$$

$$\begin{aligned}
\dot{P}_{34} &= L_2 P_{45} + L_1 P_{35} \\
\dot{P}_{35} &= -L_2 P_{55} \\
\dot{P}_{44} &= 2L_1 P_{45} \\
\dot{P}_{45} &= L_1 P_{55} \\
\dot{P}_{55} &= 0
\end{aligned}$$

The main objective is to minimize the covariance of x and y , or the P_{11} and P_{22} states, at the terminal time. By looking carefully at the equations the interaction between the covariance of the error, P_{55} , and the P_{11} and P_{22} states become evident. The driving sequence is shown in Figure 9. It is therefore apparent that knowledge about the error parameter will directly effect the P_{11} and P_{22} states. It is also shown that lift is necessary to influence P_{11} and P_{22} . In the nominal, "no-lift" case, both L_1 and L_2 are 0 and P_{55} will not effect P_{11} or P_{22} . Therefore, it is only through maneuvering the missile that P_{55} will effect P_{11} and P_{22} .

The system state equation may be augmented by the \dot{P} equations to the form:

$$\begin{bmatrix} \dot{\bar{X}} \\ \dot{\bar{P}} \end{bmatrix} = \begin{bmatrix} F(t)\bar{X} \\ f(P, L, \sigma_0, \sigma_R) \end{bmatrix} + \begin{bmatrix} \bar{B} \bar{u} \\ 0 \end{bmatrix} + \begin{bmatrix} \bar{\xi} \\ \xi \end{bmatrix} \quad (46)$$

By assumption 1, the magnitude of velocity is constant, only the heading angle, θ , needs to be propagated. Therefore, the final system of interest is as follows:

$$\dot{\bar{X}} = \begin{bmatrix} \dot{X}_1 \\ \dot{X}_2 \\ \dot{X}_3 \\ \dot{X}_4 \\ \dot{X}_5 \\ \cdot \\ \cdot \\ \cdot \\ \cdot \\ \dot{X}_{18} \end{bmatrix} = \begin{bmatrix} \dot{X} \\ \dot{Y} \\ \dot{\theta} \\ P_{11} \\ P_{12} \\ \cdot \\ \cdot \\ \cdot \\ \cdot \\ P_{55} \end{bmatrix} = \begin{bmatrix} V \cos \theta \\ V \sin \theta \\ L/V \\ 2P_{13} - P_{11}(AP_{11} + BP_{12}) - P_{12}(BP_{11} + DP_{12}) \\ \cdot \\ \cdot \\ \cdot \\ \cdot \\ \cdot \end{bmatrix} \quad (47)$$

This 18 state vector equation is the basis for the numerical techniques to follow. By choosing appropriate initial values and a proper method for selecting the control vector \bar{L} then the objective of minimizing P_{11} and P_{22} will be achieved.

The state equations are nonlinear so an appropriate numerical integration method will be used.

Plan of Attack

The first step is to formulate a performance objective, J . Generally, the cost is of the form:

$$J = \phi[x, t_f] + \int_{t_0}^{t_f} L(u, x, t) dt \quad (48)$$

where

ϕ = terminal condition of state
vector at t_f

L = performance criteria of control
input

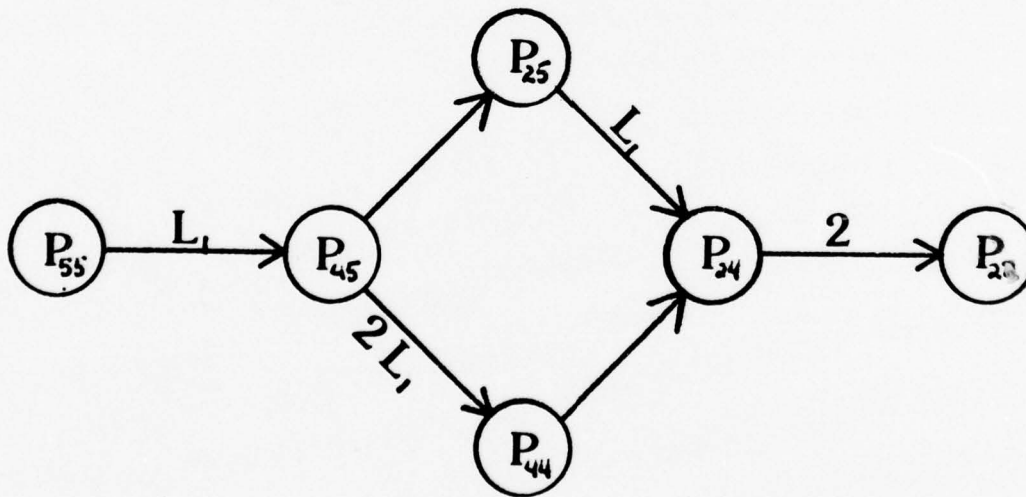
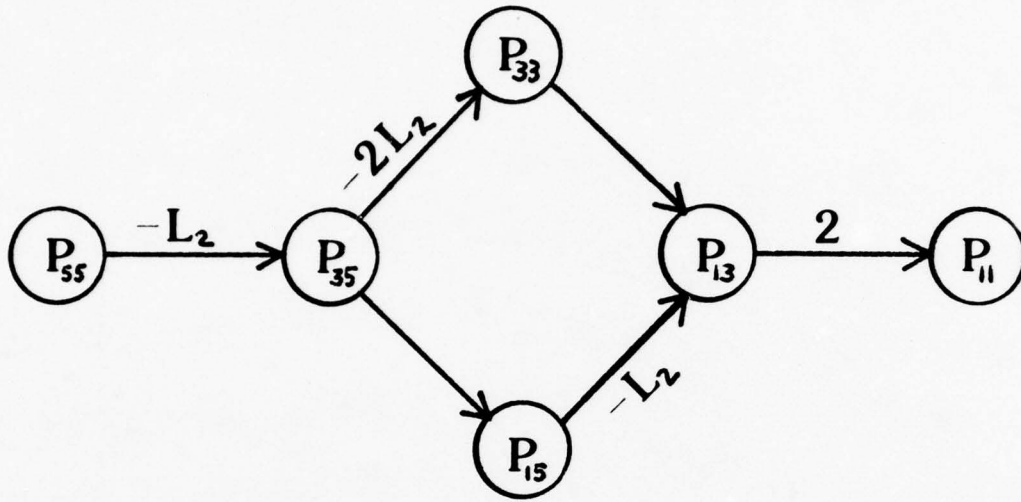


Figure 9. Driving Sequence of P Matrix

Since the main objective is minimization of the CEP, the cost function will be

$$J = 0.588 (\sigma_x + \sigma_y) \Big|_{t_f} + \int_{t_0}^{t_f} W_1 L^2 dt \quad (49)$$

where

σ_x = covariance of x estimate

$$= (P_{11})^{\frac{1}{2}}$$

σ_y = covariance of y estimate

$$= (P_{22})^{\frac{1}{2}}$$

W_1 = selected arbitrary weighting value = 10^{-5}

The integral term for this problem is just a quadratic function of the control input only

$$L(x,u,t) = W_1 L^2 \quad (50)$$

in this case the dimension of m , of the control vector \bar{u} is 1. As described in Chapter I, $|u_1| < u_1$ for any practical system. Choosing a maximum of a 10g turn for the missile

$$L_{\max} = 100 \text{ m/sec}^2 \quad (51)$$

Two methods will be used to determine the minimum of the cost function. The first will be a single turn analysis. In this concept, the missile is commanded to turn to a predetermined heading angle, α , fly to the radar limit, then turn to the target. Then the performance function is calculated. By increasing α slightly the technique should converge to an optimum α angle. This method does severely limit the amount of maneuvering but should demonstrate the dual control concept.

The second method will be a numerical gradient technique. This

will allow for greater maneuverability in searching for a minimum of the cost function.

III. Single Turn Analysis

Overview

The basic approach of this method is to find an optimal flight path based on an initial heading angle, α . The system equations, as described in Chapter II, are:

$$\dot{\frac{z}{x}} = f(x, u, t) \quad (51)$$

and the performance function J is:

$$J = CEP + \int_{t_0}^{t_f} W L^2 dt \quad (53)$$

Figure 10 shows the schematic idea behind the single turn concept.

Beginning with an initial turn rate, the missile is commanded to turn to a desired α angle. It flies a specified distance then begins a turn to intercept the terminal condition. Thus, the maneuvering will be accomplished during Phase I of the flight. The cost function is then evaluated. The process is repeated after incrementing α . The procedure is continued from $\alpha = 0$ to $\alpha = 1.0$ radians to show the general trend of the CEP versus the amount of maneuvering.

As seen from Figure 10, the amount of lift and the time-of-flight required will vary greatly between flight path A and flight path D. Therefore, the optimum flight path will be a tradeoff between these two factors.

Initial Turn

To provide a valid comparison between no-maneuvering and maneuvering an initial α angle of 0.0 was chosen. The increment size is 0.1 radian to a maximum of 1.1 radians. The maximum permissible lift is 100 m/sec^2 which yields a maximum turn rate of 0.100 rad/sec. To insure the proper

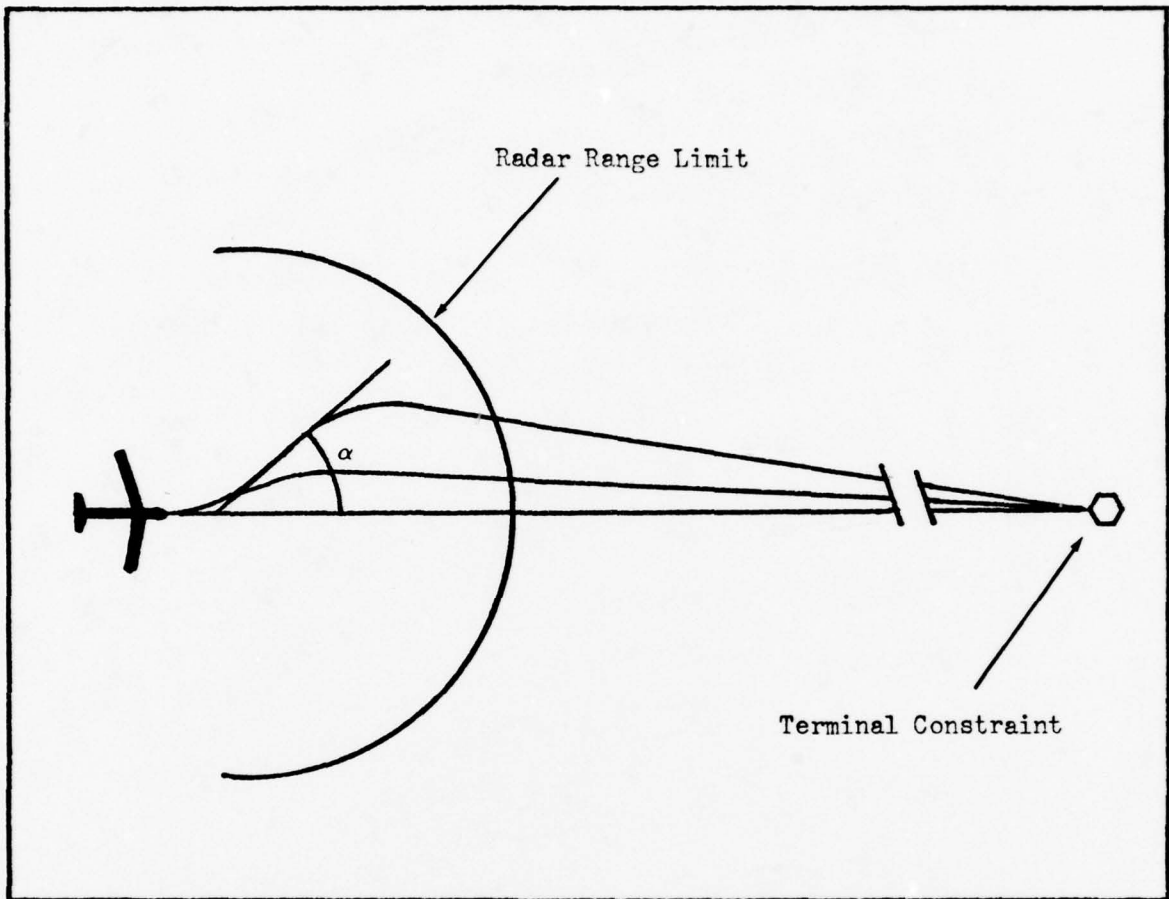


Figure 10. Schematic of Flight Paths for Single Turn Analysis

amount of turn, the commanded lift remains at 100 m/sec^2 until $(\alpha - \theta) < 0.100$. The following scheme was used to command the initial turn:

$$L = 1000 (\alpha - \theta) \quad (54)$$

where

θ = Current Heading Angle

with restriction

$$L_{\text{max}} = 100$$

Thus, if $\alpha = 0.5$ and $\theta = 0.45$ then $L = 50 \text{ m/sec}^2$. By using an integration step size of $\Delta t = 1.0 \text{ sec}$, this scheme will insure an accurate

turn. After the completion of the turn, no lift is commanded so the missile flies in a straight line to a predetermined range of 25,000 m. prior to turning towards the target.

Terminal Guidance Phase

It is during this phase of flight that the lift vector is commanded in such a manner to insure the terminal condition is met. Figure 11 shows the geometrical consideration for the guidance law. The scheme is centered on the θ_{req} angle. If the current θ angle can be made equal to the θ_{req} angle then the missile will be heading directly toward the target. Mathematically, the objective is to drive $(\theta - \theta_{req})$ to zero.

From Figure 11, two equations may be formulated based on position at the 25,000 m. range and estimating the final time t_f . These equations

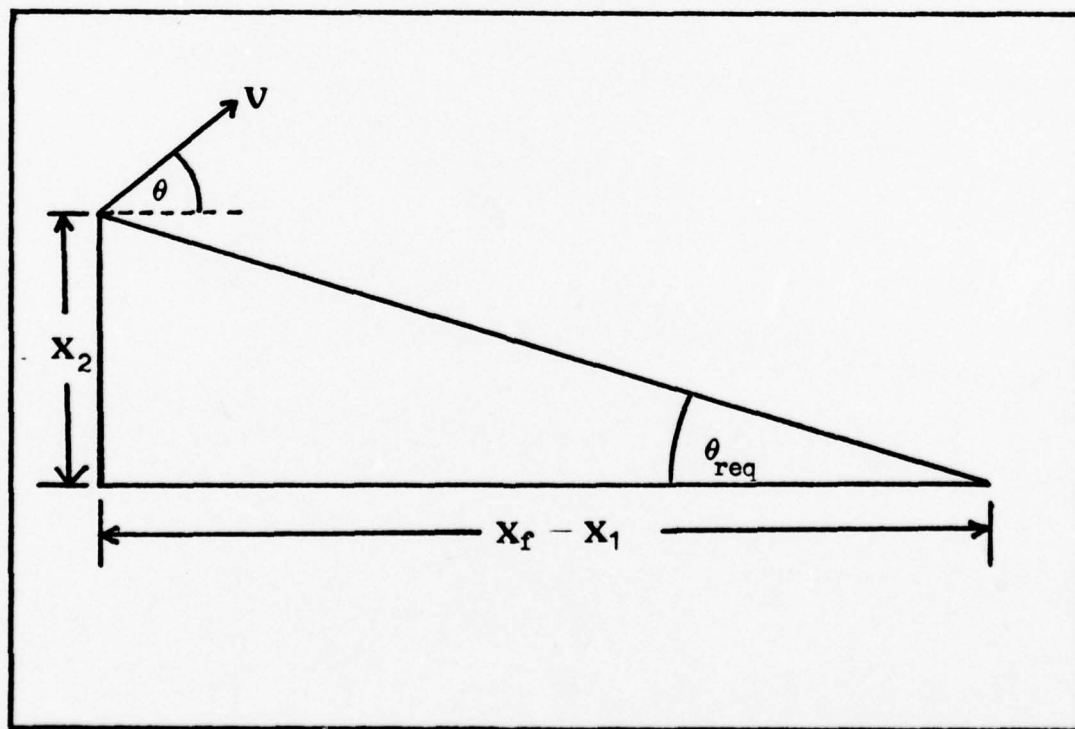


Figure 11. Schematic of Terminal Guidance Phase

are:

$$V \cos \theta_{\text{req}} = \frac{(x_f - x_1(t))}{(\hat{t}_f - t)} \quad (55)$$

$$V \sin \theta_{\text{req}} = \frac{-x_2(t)}{(\hat{t}_f - t)} \quad (56)$$

By squaring each side, an expression for \hat{t}_f may be found.

$$V^2 (\cos^2 \theta_{\text{req}} + \sin^2 \theta_{\text{req}}) = \frac{(x_f - x_1(t))^2 + x_2^2(t)}{(t_f - t)^2} \quad (57)$$

$$V^2 = x_f^2 - 2x_f x_1 + x_1^2 + x_2^2 / (t_f - t)^2 \quad (58)$$

$$\hat{t}_f^2 - 2t\hat{t}_f + \left[t^2 - [x_f^2 - 2x_f x_1 + x_1^2 + x_2^2] / V^2 \right] = 0 \quad (59)$$

using the quadratic formula and taking the positive root t_f becomes:

$$\hat{t}_f = 2t + \frac{\sqrt{4t^2 - 4t^2 + 4[x_f^2 - 2x_f x_1 + x_1^2 + x_2^2] / V^2}}{2} \quad (60)$$

letting

$$\text{RAD} = \sqrt{4(x_f^2 - 2x_f x_1 + x_1^2 + x_2^2) / V^2} \quad (61)$$

$$\hat{t}_f = t + \text{RAD} / 2 \quad (62)$$

knowing the current \hat{t}_f , the θ_{req} is:

$$\theta_{\text{req}} = \cos^{-1}((x_f - x_1) / ((t_f - t)V)) \quad (63)$$

The lift required, L_{req} , can now be calculated from

$$L_{\text{req}} = \frac{\theta_{\text{req}} - \theta}{\Delta t} V \quad (64)$$

With constraint

$$|L_{\max}| \leq 100 \text{ m/sec}^2$$

This algorithm will turn the missile at the maximum rate to intercept the target in minimum time of flight. To maximize the maneuvering during Phase I, this turn is initiated at a range of 25,000 m., thus the turn will be completed in Phase I and during Phase II only a minimum of lift will be required to maintain a target interception course.

To investigate the problem using this method, two cases were chosen. Case 1 has a radar range of 50,000 m. and terminal condition of $X_f = 101,000$ m. The initial range is 1000 m. thus for $\alpha = 0$ the time of flight is 100. sec. For Case 2, the radar range is decreased to 40,000 m. and the terminal condition is $X_f = 201,000$. The initial range remains at 1000 m. thus for $\alpha = 0$ the time of flight is 200. sec. The results of these two cases are presented in the following section.

Case 1

$$\begin{aligned} \text{Radar Range} &= 50,000 \text{ m.} \\ X_f &= 101,000. \text{ m.} \\ X_o &= 1,000. \text{ m.} \end{aligned}$$

The major results for Case 1 are presented in Table 1. With no maneuvering, $\alpha = 0$, the terminal CEP is 14.00. This decreases to 8.05 at $\alpha = 0.1$ and is the minimum value for Case 1. This shows a definite relationship between maneuvering, learning about the misalignment angle, and reducing the CEP. The most significant result is the σ_y value which decreases from 15.62 for $\alpha = 0$. to 2.78 for $\alpha = 0.1$. This in turn decreases the CEP significantly.

The cost is rising steadily but this is due to the integral term of control. It is hypothesized that the weighting value for the control integral is too high. The significant result is that a small amount of

maneuvering will minimize the CEP.

Figures 12 through 15 show graphically the results of Case 1. Figure 12 is a schematic of four flight paths for $\alpha = 0.1$, $\alpha = 0.3$, $\alpha = 0.6$, and $\alpha = 1.0$. The general trend of the results are evident and point to the conclusion that a small turn minimizes the CEP. The time of flight is a significant factor. For $\alpha = 0$, TOF = 100., for $\alpha = 1.0$, TOF = 115.68. During Phase II, the covariances are increasing and every second of flight is significant. Thus, the optimal tradeoff between maneuvering versus TOF, as shown by Case 1 is a small turn that does not increase the TOF significantly. The TOF for $\alpha = 0.1$ is 100.222.

Table 1. Result of Case 1 Analysis

α	TOF	σ_x	σ_y	CEP	COST	P_{18}
0	100.0	8.20	15.62	14.00	14.00	1.0E-4
0.1	100.2	10.91	2.78	8.05	58.11	2.69E-6
0.2	100.9	14.52	3.70	10.71	61.85	5.39E-8
0.3	102.2	15.02	4.64	11.56	65.17	5.83E-7
0.4	102.3	13.89	4.98	11.09	64.81	3.07E-7
0.5	104.7	15.38	6.05	12.61	66.63	2.56E-7
0.6	106.1	13.62	6.37	11.75	66.75	1.80E-7
0.7	109.1	15.40	7.30	13.35	69.86	1.31E-7
0.8	109.9	13.13	7.32	12.02	71.30	9.9EE-8
0.9	112.9	14.73	8.11	13.43	72.20	8.74E-8
1.0	115.6	14.40	8.50	13.47	73.75	7.07E-8

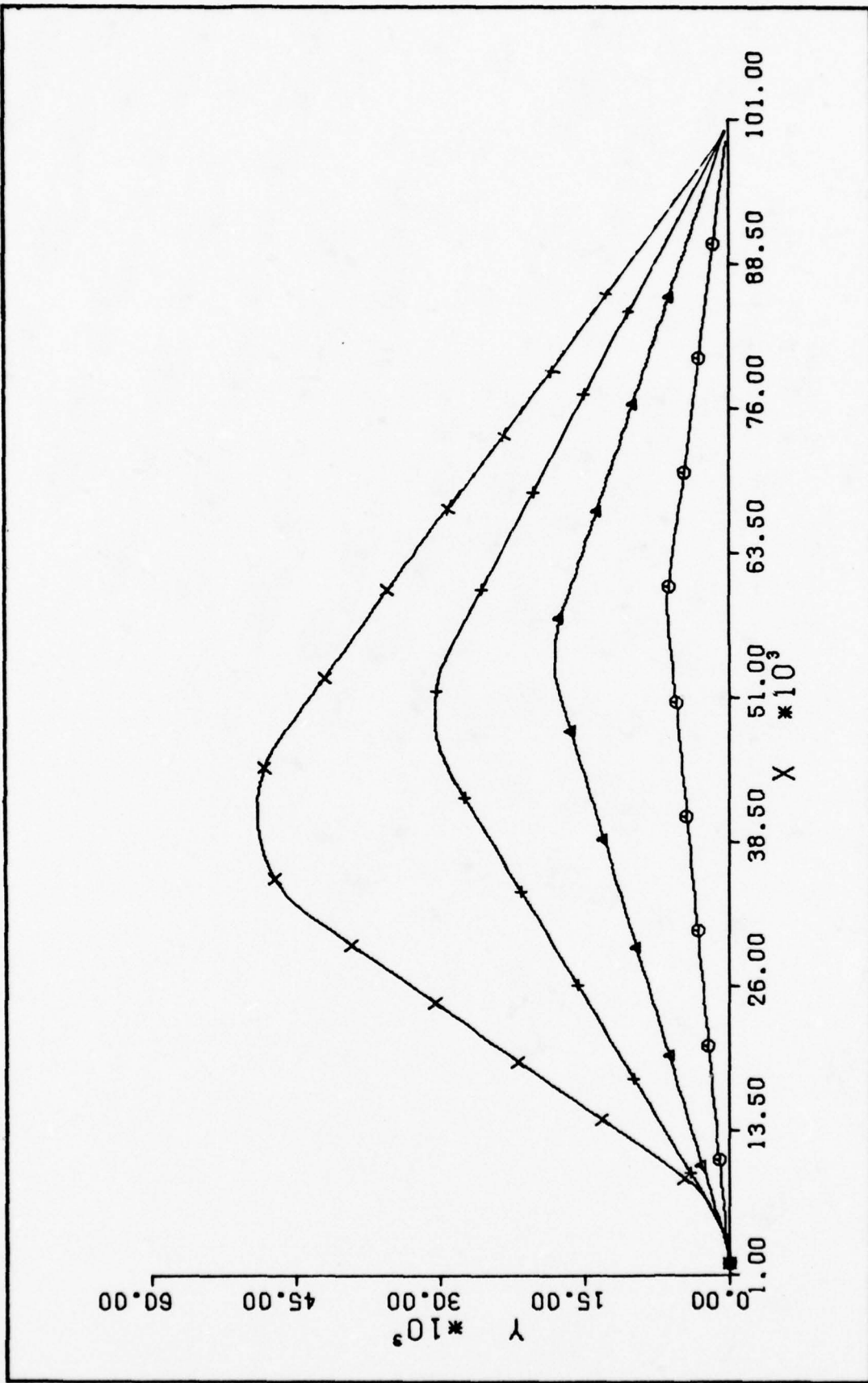


Figure 12. Flight Paths for Case 1

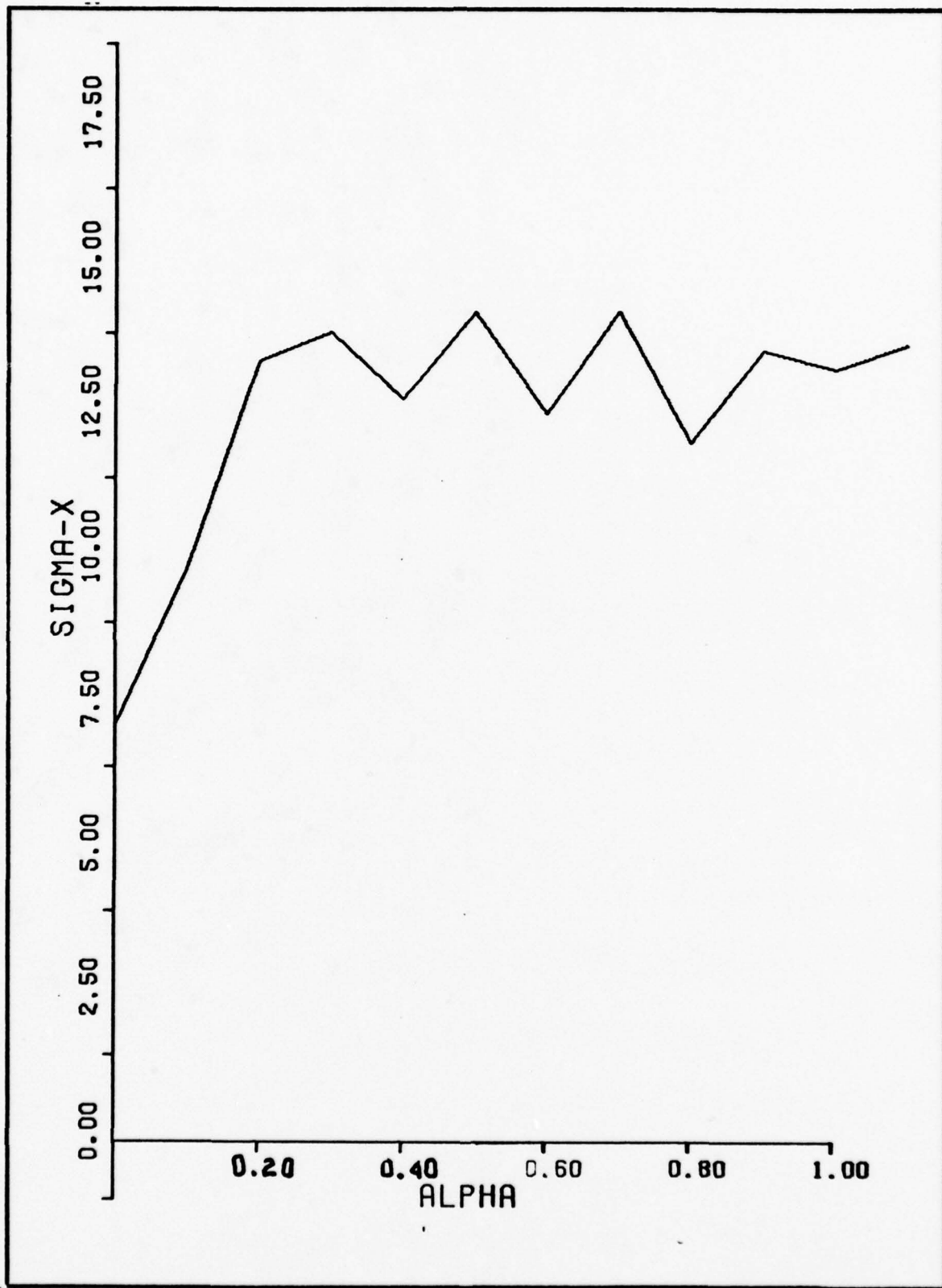


Figure 13. σ_x vs α for Case 1

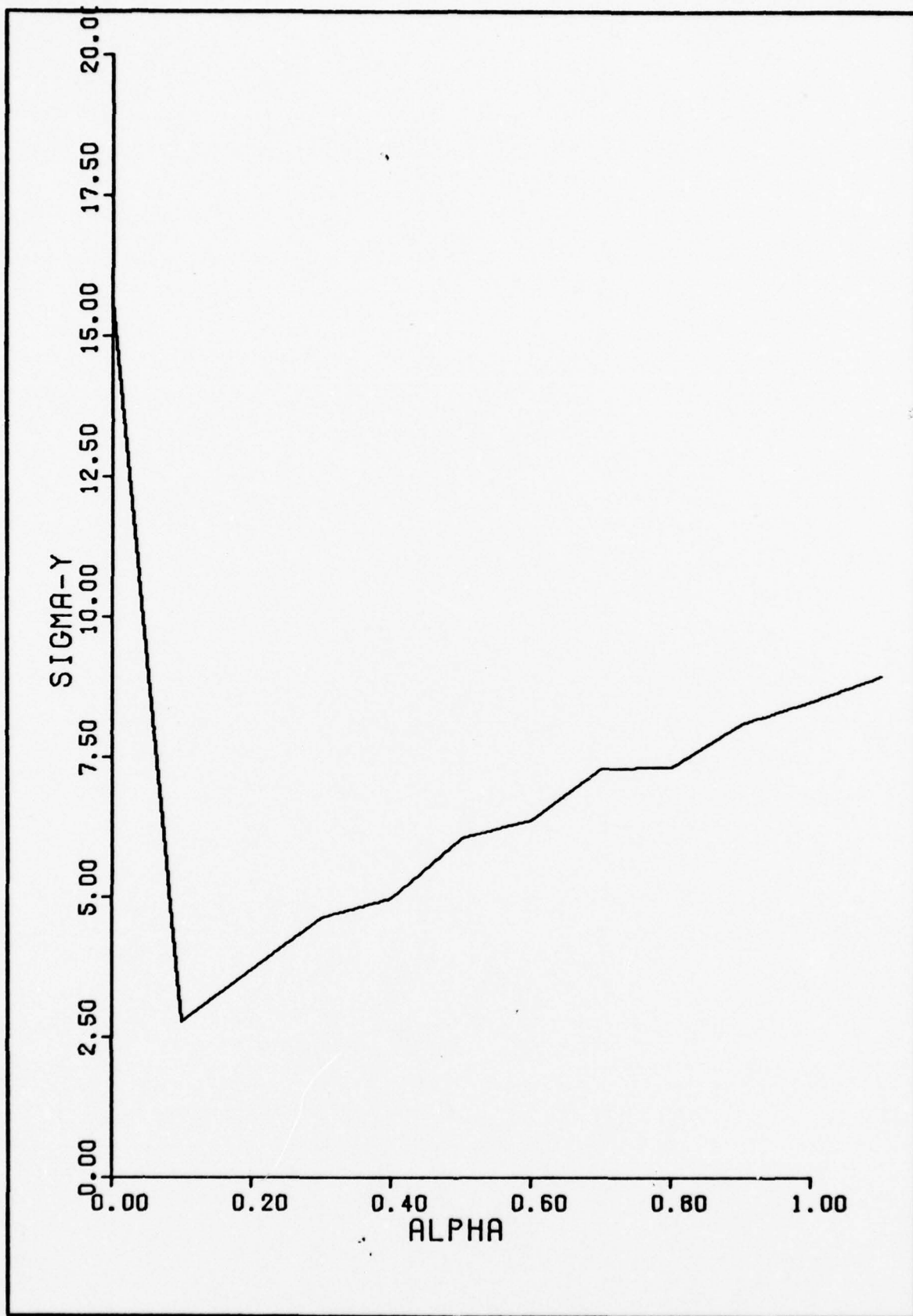


Figure 14. σ_y vs α for Case 1

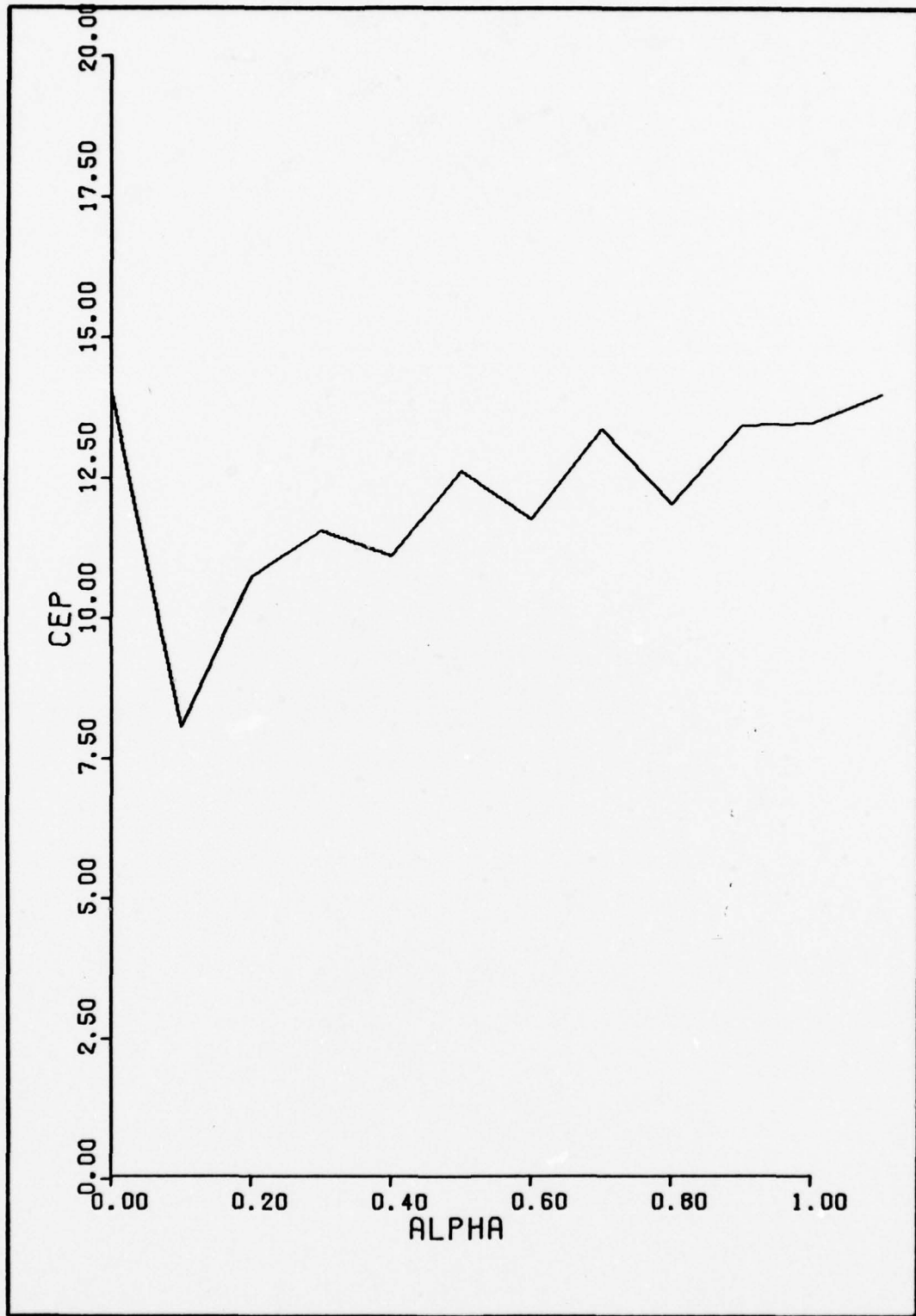


Figure 15. CEP vs α for Case 1

Case 2

Radar Range = 40,000 m.
 $X_f = 201,000$. m.
 $X_0 = 1000$. m.

The major results for Case 2 are presented in Table 2. With no maneuvering, $\alpha = 0$, the terminal CEP is 38.80. This decreases only slightly to 38.16 with $\alpha = 0.1$. The general trend of Case 1 is again evident in Case 2 but to a lesser degree. The minimum CEP is again attained by a small turn and small amount of turning. The σ_y value again shows the sharpest decrease going from 37.72 for $\alpha = 0$, to 14.12 for $\alpha = 0.1$. Figures 16 through 19 show graphically the results of Case 2.

The CEP does not decrease as favorably as in Case 1. This may be due to an increased TOF and less time during Phase I for learning about the misalignment angle. As seen from Table 3, the values of σ_x and σ_y are greater in Case 2 than in Case 1 at the end of Phase I flight. The covariance of the misalignment angle is also greater in Case 2. This coupled with a longer flight time in Phase II in Case 2 diminishes the dual control nature of the problem.

Table 2. Results of Case 2 Analysis

α	TOF	σ_x	σ_y	CEP	COST	P_{18}
0	200.	28.26	37.72	38.80	38.80	1.0E-4
0.1	200.2	50.76	14.12	38.16	88.34	2.1E-6
0.2	200.8	95.09	22.36	69.06	121.8	4.9E-6
0.3	201.8	98.15	26.59	73.34	125.3	3.2E-6
0.4	202.4	93.99	28.57	72.06	125.5	2.1E-6
0.5	203.9	87.98	32.61	70.91	125.2	1.2E-6
0.6	205.2	96.99	40.73	90.98	137.67	1.1E-6
0.7	207.7	111.82	50.97	95.72	153.03	1.0E-6
0.8	208.5	84.21	42.98	74.78	125.19	5.6E-7
0.9	211.0	102.21	53.61	91.62	151.85	6.3E-7
1.0	213.5	97.57	56.33	90.49	151.87	5.0E-7

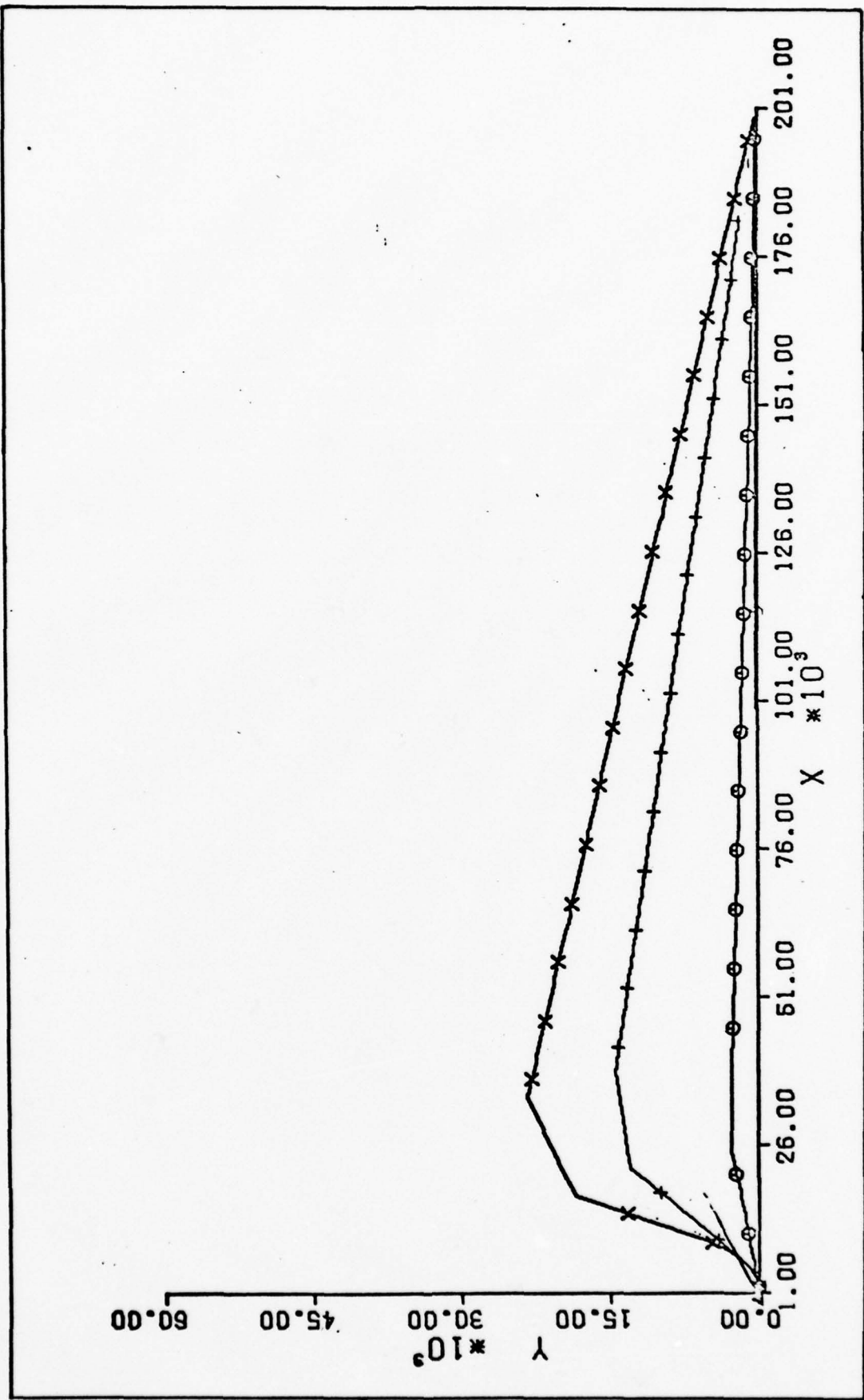


Figure 16. Flight Paths for Case 2

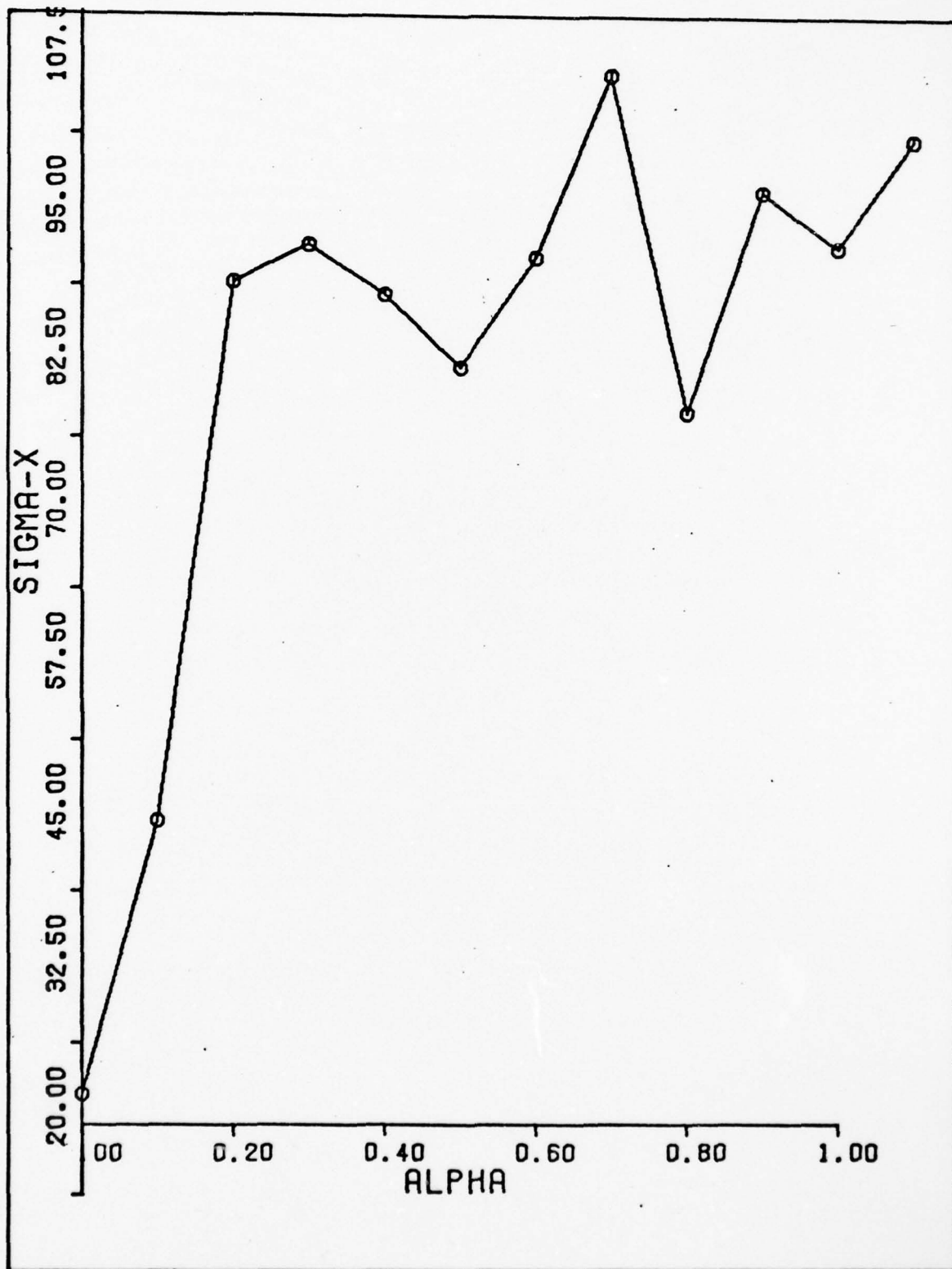


Figure 17. σ_x vs α for Case 2

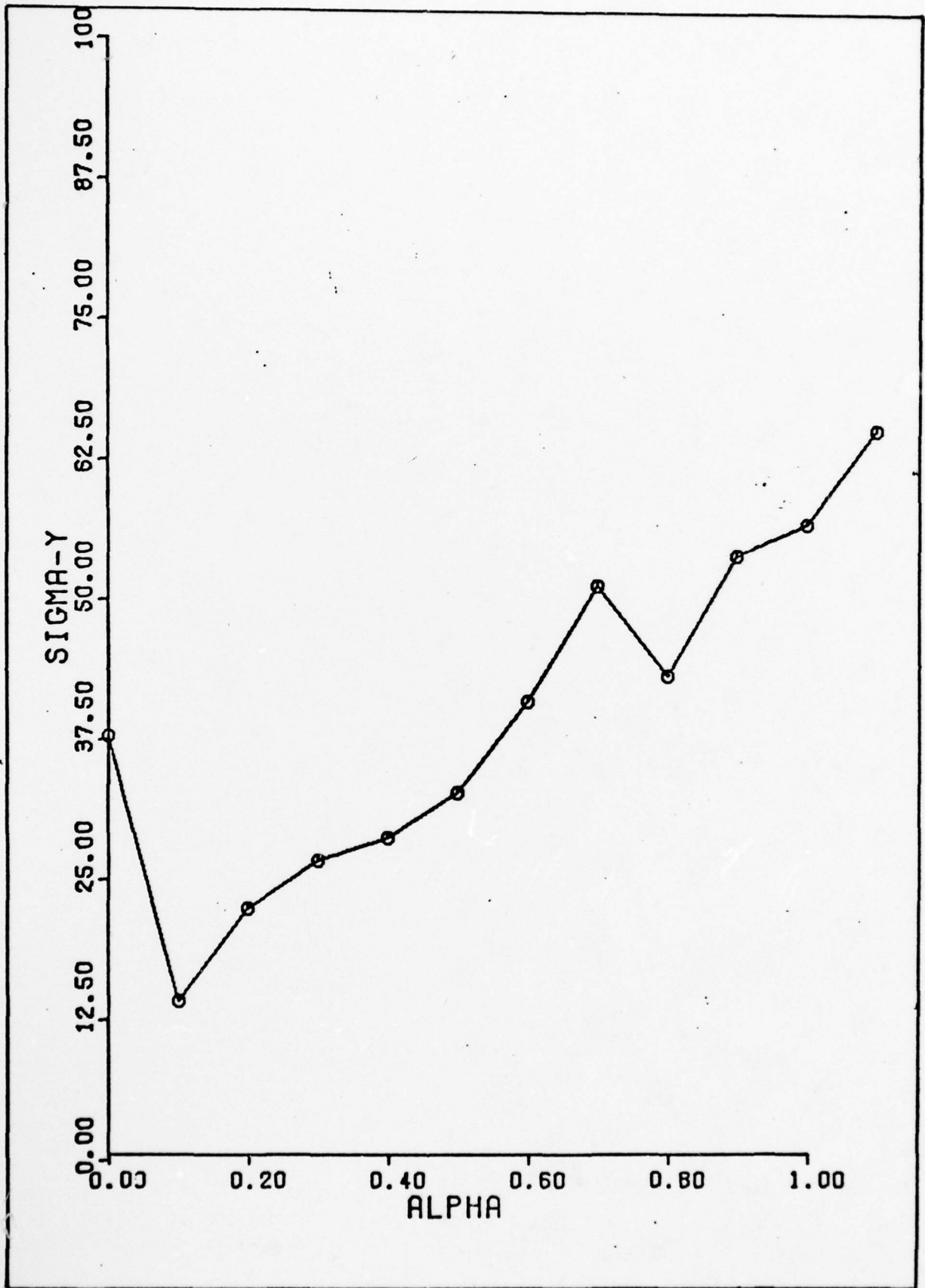


Figure 18. σ_y vs α for Case 2

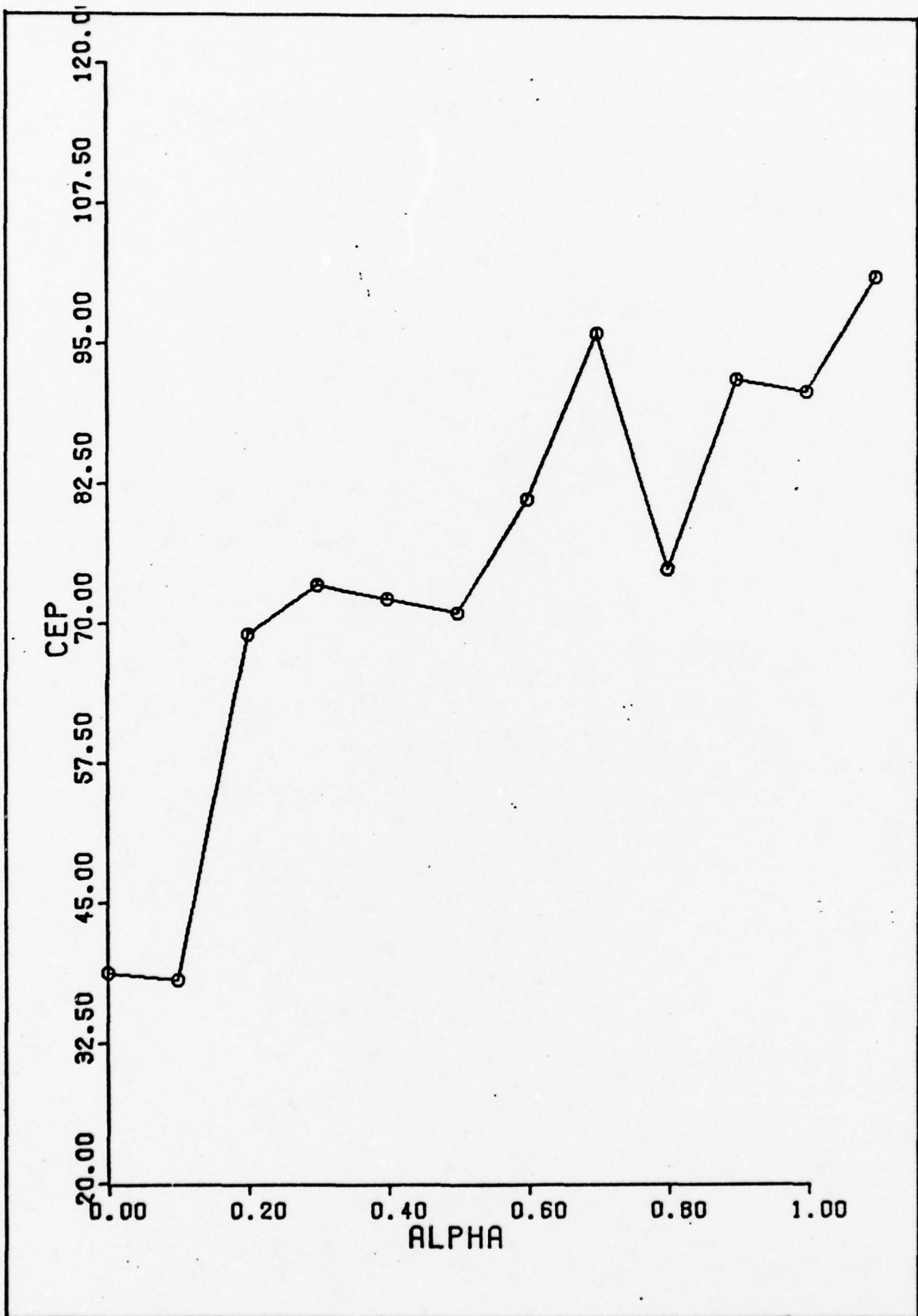


Figure 19. CEP vs α for Case 2

Table 3. Comparison of Case 1 and Case 2 at End of Phase I

α	Case 1				Case 2			
	0	.1	.5	1.0	0	.1	.5	1.0
σ_x	11.8	11.8	13.8	12.3	10.2	15.1	24.6	21.4
σ_y	54.0	0.15	3.0	6.9	44.0	0.2	4.9	12.0
P_{18}	1.0E-4	2.1E-6	2.7E-7	7.4E-8	1.0E-4	2.9E-6	1.4E-6	5.4E-7

These two examples show that dual control can be applied to an air-to-ground missile with a constant misalignment angle. These examples also show significant results for all maneuvering during Phase I. Cases were evaluated for accomplishing the final turn after Phase I. These results are far less encouraging, however, they do show a significant result: that high -g maneuvering during a non-radar environment can increase the terminal CEP. Table 4 shows the results for Case with the final turn initiated during Phase II rather than in Phase I.

Table 4. Results of Case 1, Terminal Maneuvering During Phase II

α	TOF	x	y	CEP	COST	P_{18}
0	100.0	8.19	15.62	14.00	14.00	1.0E-4
0.1	100.9	113.06	6.78	70.46	80.06	9.8E-5
0.2	103.2	215.23	16.35	136.17	148.25	9.1E-5
0.3	106.6	288.28	20.17	181.37	193.61	6.5E-5
0.4	109.6	289.82	22.38	183.57	199.34	4.3E-5
0.5	115.3	243.82	22.26	156.46	175.80	1.8E-5
0.6	118.1	211.13	27.79	140.49	159.46	1.0E-5
0.7	122.8	173.60	32.40	121.13	142.36	4.8E-6
0.8	128.9	149.15	30.25	105.49	130.63	2.7E-6
0.9	136.7	128.20	28.41	92.38	122.38	1.6E-6
1.0	143.9	109.53	30.20	82.17	116.32	9.0E-7

As seen from the table, a small turn will not reduce the terminal CEP when the final turn is completed outside the radar environment.

However, the trend of the data indicates that a large initial turn will offset the maneuvering during Phase II. Note that the CEP reaches a maximum at $\alpha = 0.4$ and then decreases steadily as α increases to 1.0 radian. This is also related to the covariance of the misalignment angle. When the P_{18} state is sufficiently small then the CEP is reduced.

The results of this chapter have demonstrated the feasibility of dual control as applied to an air-to-ground missile. However, the method of maneuvering was severely restricted. Chapter IV investigates the problem using a first order gradient technique which allows more flexibility during Phase I.

IV. Gradient Optimization Technique

Theory

To understand the numerical first-order gradient technique, it is first necessary to develop an understanding of the optimization problem, the general gradient methods, and special variations due to the particular class of problem being considered.

The general problem is to find the control history of the m-dimensional control vector $\bar{u}(t)$ which will bring the performance function J to a minimum. The control function is expressed as:

$$J = \phi[x(t_f), t_f] + \int_{t_0}^{t_f} L[x, u, t] dt \quad (65)$$

The system equations are represented as:

$$\dot{x} = f(x, u, t) \quad (66)$$

where x is an n-vector.

The general method consists of adding Lagrange multipliers to the cost function. This becomes:

$$J = \phi[x(t_f), t_f] + \int [L + \lambda^t (f - \dot{x})] dt \quad (67)$$

Defining the Hamiltonian H as:

$$H = L + \lambda^t f \quad (68)$$

the cost function becomes:

$$\begin{aligned} J &= \phi[x(t_f), t_f] + \int (H - \lambda^t \dot{x}) dt \\ &= \phi + \int H dt - \int \lambda^t \dot{x} dt \end{aligned} \quad (69)$$

Integrating the last term of Equation 69 by parts yields:

$$\int \lambda^t \dot{x} dt = \lambda^t(t_f) x(t_f) - \lambda^t(t_0) x(t_0) - \int \dot{\lambda}^t(t) x(t) dt \quad (70)$$

thus:

$$J = \phi - \lambda^t(t_f)x(t_f) + \lambda^t(t_0)x(t_0) + \int_{t_0}^{t_f} \{H(x,u,t) + \dot{\lambda}^t(t)x(t)\} dt \quad (71)$$

Considering a variation in J due to variations in the control vector $u(t)$ for fixed t_0 and t_f :

$$\begin{aligned} \delta J = & \left[\left(\frac{\partial \phi}{\partial x} \quad \lambda^t \right) S_x \right]_{t_f} + [\lambda^t S_x]_{t_0} \\ & + \int_{t_0}^{t_f} \left[\left(\frac{\partial H}{\partial x} + \dot{\lambda}^t \right) S_x + \frac{\partial H}{\partial u} S_u(t) \right] dt \end{aligned} \quad (72)$$

A necessary condition for a minimum to exist is that $\delta J = 0$ for arbitrary $\delta u(t)$. Therefore, from Equation 72 a necessary condition is that

$$\dot{\lambda}^t = - \frac{\partial H}{\partial x} \quad (73)$$

with

$$\lambda(t_f) = \frac{\partial \phi}{\partial x}(t_f) \quad (74)$$

and

$$\frac{\partial H}{\partial u} = \frac{\partial L}{\partial u} + \lambda^t \frac{\partial f}{\partial u} \quad (75)$$

In summary, a two-point boundary value problem must be solved to find the minimizing value of J. The differential equations that must be solved are:

$$\dot{x} = f(x,u,t) \quad (76)$$

$$\dot{\lambda} = - \frac{\partial H}{\partial x} = - \left(\frac{\partial f}{\partial x} \right) \lambda - \left(\frac{\partial L}{\partial x} \right)^t \quad (77)$$

where $u(t)$ is determined from

$$\frac{\partial H}{\partial u} = 0 \quad (78)$$

Considering no variations in the initial conditions, Equation 72 becomes:

$$\delta J = \int \frac{\partial H}{\partial u} \delta u dt = \int \left(\frac{\partial L}{\partial u} + \lambda^t \frac{\partial f}{\partial u} \right) dt \quad (79)$$

To apply this gradient technique to the problem of this study, it is necessary to consider the terminal constraint $\psi[x(t_f)]$. This constraint may be written as follows:

$$\psi[x(t_f)] = \begin{bmatrix} x_1(t_f) - x_1^f \\ \vdots \\ x(t_f) - x_2^f \end{bmatrix} \quad (80)$$

In a similar manner to the previous development, Lagrange multipliers are added to influence the terminal constraint. This may be developed using a special cost function of the form $J_1 = \psi[x(t_f)]$. Designating the coefficient as R, letting $\psi(x(t_f)) = \phi(x(t_f))$, and considering $\delta x(t_0) = 0$, Equation 72 becomes:

$$\delta J_1 = \left[\left(\frac{\partial \psi}{\partial x} - R^t \right) \delta x \right]_{t_f} + \int \left[\left(\frac{\partial H}{\partial x} + R^t \right) \delta x + \frac{\partial H}{\partial u} \delta u(t) \right] dt \quad (81)$$

choosing R to make the coefficients of δx zero yields

$$R^t = - \frac{\partial H}{\partial x} = - \frac{\partial f}{\partial x} R - \frac{\partial L}{\partial x} \quad (82)$$

However, this coefficient is considering a special performance index, J_1 , where $L = 0$. Therefore,

$$R^t = - \frac{\partial f}{\partial x} R \quad (83)$$

with

$$\tilde{R}^t(t_f) = \frac{\partial \psi}{\partial x}(t_f) \quad (84)$$

Considering the special cost function J_1 , Equation 79 becomes:

$$\delta J_1 = \delta \psi = \int_{t_0}^{t_f} R \frac{\partial f}{\partial u} \delta u(t) dt \quad (85)$$

Now a control history may be formulated that decreased J and satisfies the terminal constraint. Multiplying Equation 85 by a constant ν and adding to Equation 79 yields:

$$\delta J + \nu_i \delta x_i(t_f) = \int_{t_0}^{t_f} \left\{ \frac{\partial L}{\partial u} + [\lambda + \nu_i R]^t \frac{\partial f}{\partial u} \right\} \delta u(t) dt \quad (86)$$

Now choose

$$\delta u(t) = -K \left\{ \left(\frac{\partial f}{\partial u} \right)^t [\lambda + \nu_i R] + \left(\frac{\partial L}{\partial u} \right)^t \right\} \quad (87)$$

This forces the $\delta J + \nu_i \delta x_i(t_f)$ to vanish. The ν 's may be chosen to satisfy the terminal constraint.

Application to Problem

In applying the theory of gradient optimization to the problem of minimizing the terminal CEP of an air-to-ground missile with constant misalignment angle, numerical difficulties are encountered. The first attempt was to use an unspecified final time and allow gradient search during Phase I while commanding the missile to fly toward the target during Phase II. This method had difficulties in the backward integration of the influence functions. Therefore, to make the gradient technique more applicable, the problem was reformulated slightly.

The major change is to project the cost at the end of Phase II based on the system state at the end of Phase I. This can be accomplished since the \dot{P} equation is linear during Phase II. Thus,

$$P(t_f) = \Phi(t, t_g) P \Phi(t, t_g) + \int_{t_r}^{t_0} \Phi(s) Q \Phi(s) ds \quad (88)$$

where

$$t_r = \text{time at end of Phase I}$$

$$t_g = t_f - t_r$$

If the final turn to the target has been accomplished during Phase I, then there will be zero nominal lift during Phase II and the system equations may be expressed as:

$$\begin{bmatrix} \dot{X}_1 \\ \dot{X}_2 \\ \dot{V}_1 \\ \dot{V}_2 \\ \dot{\mu} \end{bmatrix} = \begin{bmatrix} 0 & 0 & 1 & 0 & 0 \\ 0 & 0 & 0 & 1 & 0 \\ 0 & 0 & 0 & 0 & 0 \\ 0 & 0 & 0 & 0 & 0 \\ 0 & 0 & 0 & 0 & 0 \end{bmatrix} \begin{bmatrix} X_1 \\ X_2 \\ V_1 \\ V_2 \\ \mu \end{bmatrix} \quad (89)$$

Thus, during Phase II:

$$\Phi(t, t_g) = e^{At} = \begin{bmatrix} 1 & 0 & t & 0 & 0 \\ 0 & 1 & 0 & t & 0 \\ 0 & 0 & 1 & 0 & 0 \\ 0 & 0 & 0 & 1 & 0 \\ 0 & 0 & 0 & 0 & 1 \end{bmatrix} \quad (90)$$

Substituting Equation 90 into Equation 88 yields:

$$P(t_f) = \begin{bmatrix} P_{11} + 2t_g + t_g^3 P_{33} & P_{12} + t_g P_{25} + t_g P_{14} + t_g^2 P_{34} & " \\ P_{12} + t_g P_{14} + t_g P_{23} + t_g^2 P_{34} & P_{22} + 2t_g P_{24} + t_g^2 P_{44} & " \end{bmatrix} \quad (91)$$

$$+ \int_{t_r}^{t_f} \begin{bmatrix} t^2 \cdot 10^{-4} & 0 \\ 0 & t^2 \cdot 10^{-4} \end{bmatrix} dt$$

The cost at the terminal time may now be written as a function of the state at the end of Phase I. This becomes

$$J(t_f) = 0.588 \left[\sqrt{P_{11} + 2t_g P_{13} + t_g^2 P_{33} + t_g^3 / 3 \cdot 10^{-4}} \right. \\ \left. + \sqrt{P_{22} + 2t_g P_{24} + 2t_g^2 P_{44} + \frac{t_g^3}{3} \cdot 10^{-4}} \right. \quad (92) \\ \left. + \int_0^{t_r} W U^2 dt \right]$$

By choosing $\psi[x(t_r)]$ to satisfy the constraint of the terminal guidance used in Chapter III, all maneuvering will be accomplished during Phase I. Thus,

$$\psi[x(t_r)] = [\theta_{req} - x_3] \quad (93)$$

To make the problem more realistic for an air-to-ground scenario, the final target position was increased from 101,000. m., as used in Chapter III to 601,000. m. The maneuvering time for this method was chosen at a constant 60.0 seconds. Thus, Phase I flight will continue for 60. seconds then the projected cost will be evaluated.

Bryson and Ho (1:222) outline a method for a first-order gradient technique for problems with some state variables specified at a fixed terminal time. By specifying the terminal constraint as a function of the θ or x_3 state this method is applicable to the problem. The general method is as follows:

1. Estimate a set of control histories, $u(t)$.
2. Integrate the system equations forward with the specified initial conditions $x(t_0)$ and estimate from Step 1. Record $x(t)$, $u(t)$, $\psi[x(t_f)]$, J .
3. Determine the n -vector of influence functions, $c(t)$, and the $n \times q$ matrix of influence functions, $R(t)$, by backward integration of the influence functions.

$$\dot{c} = -\left(\frac{\partial f}{\partial x}\right)^t c - \left(\frac{\partial L}{\partial x}\right)^t$$

$$c(t_f) = \left(\frac{\partial \phi}{\partial x_i}\right)_{t_f}$$

$$\dot{R} = -\left(\frac{\partial f}{\partial x}\right)R \quad R(t_f) = \begin{cases} 1 & i = j \\ 0 & i \neq j \end{cases}$$

4. Compute the following integrals.

$$I_{\psi\psi} = \int_{t_0}^{t_f} R^t \left(\frac{\partial f}{\partial u}\right)^{-1} \left(\frac{\partial f}{\partial u}\right)^t R dt$$

$$I_{J\psi} = \int_{t_0}^{t_f} \left[c^t \left(\frac{\partial f}{\partial u}\right) + \frac{\partial L}{\partial u} \right]^{-1} \left(\frac{\partial f}{\partial u}\right)^t R dt$$

$$I_{JJ} = \int_{t_0}^{t_f} \left[c^t \left(\frac{\partial f}{\partial u}\right) + \frac{\partial L}{\partial u} \right]^{-1} \left[\left(\frac{\partial f}{\partial u}\right)^t c + \left(\frac{\partial L}{\partial u}\right)^t \right] dt$$

5. Choose values of $\delta\psi$ to cause the next nominal solution to be closer to the specified $\psi[x(t_f)]$.

$$\delta\psi = -E\psi[x(t_f)]$$

$$v = -[I_{\psi\psi}]^{-1} (\delta\psi + I_{\psi J})$$

6. Repeat Steps 1 through 5 using an improved estimate of $u(t)$

where

$$\delta u(t) = [w(t)]^{-1} \left[\frac{\partial L}{\partial u} + (p(t) + r(t)v)^t \frac{\partial f}{\partial u} \right]^t$$

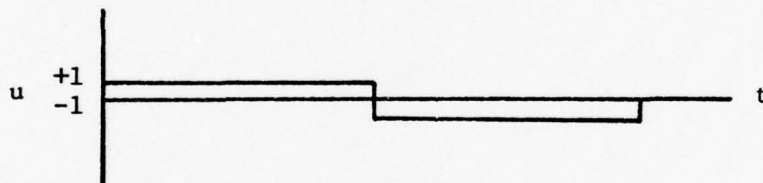
stop when

$$\psi[x(t_j)] = 0 \quad \text{and} \quad I_{JJ} - I_{J\psi} I_{\psi\psi}^{-1} I_{\psi J} = 0$$

This algorithm was applied to the thesis problem. Appendix A contains the details of the influence functions, Step 3, and the 18 x 18 matrix, $\partial f / \partial x$. Figure 20 presents a flow chart of the first-order gradient method. The actual computer listing is contained in Appendix B.

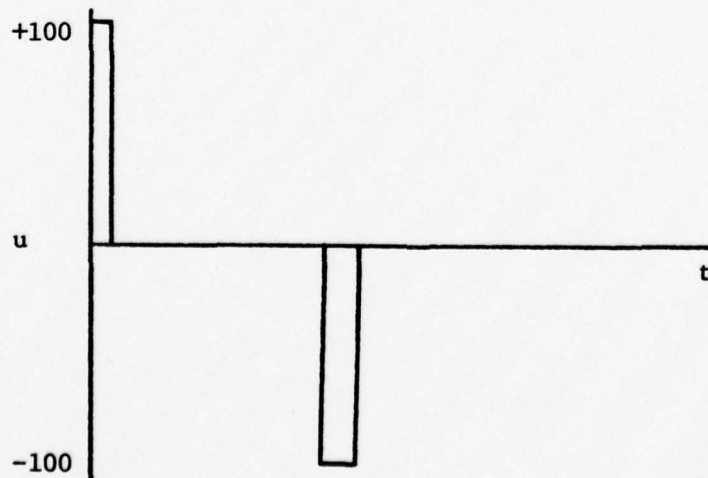
Three cases were evaluated using this method. The cases differ in the initial guess of the control history for $u(t)$. The three cases evaluated were:

Case 1



This case was chosen because of its simplicity and minimum trajectory to initialize the gradient algorithm.

Case 2



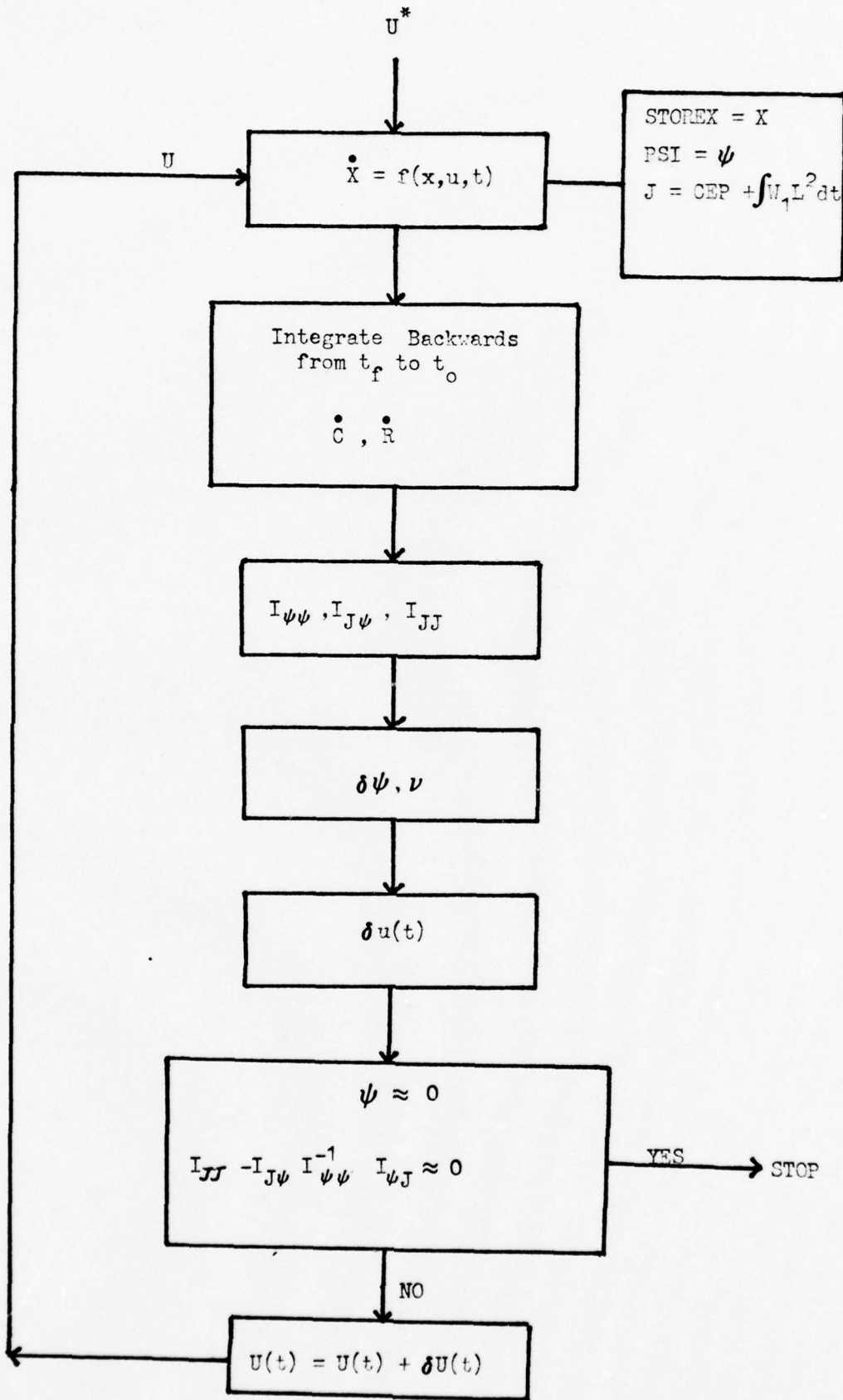
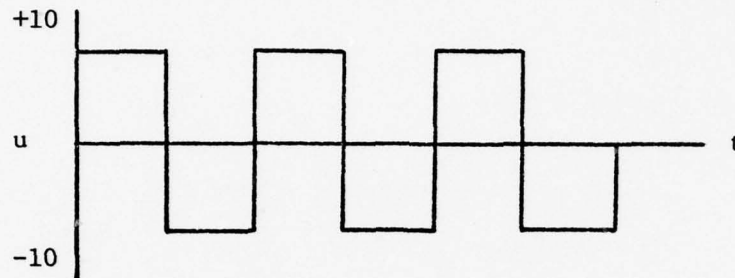


Figure 20. Flow Chart for First Order Gradient Technique

This case represents the minimum from Chapter III. Perhaps this trajectory can be improved by the gradient algorithm.

Case 3



It was felt that perhaps a series of maneuvers would be the ideal trajectory for a global minimum. This initial guess should be able to demonstrate the effects of a constant turning trajectory.

The following values were computed and reported for results:

TOF = Time of flight, this includes the predicted time of flight during Phase II.

σ_x = Covariance of x-estimate. For this method, it is recorded as the value at the end of Phase I.

σ_y = Covariance of y-estimate. For this method, it is recorded as the value at the end of Phase I.

CEP = Circular Error Probable. The area where 50% of the trajectories should terminate. As explained earlier, this is the projected value at the end of Phase II.

Cost = Total performance function. This is also the projected cost at the end of Phase II.

σ_μ = Covariance of misalignment angle. For this method, it is recorded as the value at the end of Phase I.

PSI = The terminal constraint at the end of Phase I. $\psi = (\theta_{req} - x_3)$.

Case 1

The major results of Case 1 are summarized in Table 5. The results are interesting in that the initial reduction of CEP by almost 100 m.

is achieved by turning the missile at a negative 2g turn at about 10 seconds into Phase I. Only slight changes are made in this flight path after the initial gradient search. After ten cycles, the CEP is reduced to 121.65 m. This is a substantial reduction from the initial CEP of 227.23 m. The method diverges quickly for the $\psi[x(t_g)]$ but slowly is trying to bring the ψ value to a minimum. In cycle 10, the ψ value is $-.1323$ rad. or about 7° off a straight-in shot to the final target.

Case 2

The major results of Case 2 are summarized in Table 6. The results do not show such a significant change in control history as in Case 1 but there is still a substantial amount of maneuvering at approximately $t = 10$. seconds. The algorithm produces almost no changes after $t = 25$ seconds.

After eight cycles, the CEP has been reduced to approximately 130 m. The major changes are to reduce ψ . This verifies the results of Chapter III in that a small initial maneuver substantially reduces the CEP. As seen from Table 6, the CEP has only been reduced by 3 m. while in Case 1 the CEP was reduced by 100 m.

Case 3

The major results of Case 3 are summarized in Table 7. The results show a substantial decrease in CEP from an initial 308.44 to 123.77 in Cycle 7. This is mostly from a modification of the input value.

An interesting result of this case is the large jump seen in Cycle 8. The algorithm seems to be searching for a method to reduce σ_μ . The algorithm finally commands an opposite lift vector at $t = 10$. seconds. This increases the CEP slightly. The method then ran into numerical

integration problems and stopped.

Table V. Results of Gradient Technique - Case 1

CYCLE	TOF	σ_x	σ_y	CEP	COST	σ_μ	PSI
1	600.01	3.78	8.25	227.23	227.23	.0255	-.0010
2	601.20	3.52	8.04	130.41	130.44	.0031	-.2507
3	601.06	3.43	8.04	128.85	128.91	.0031	-.2328
4	600.91	3.37	8.11	127.77	127.85	.0031	-.2144
5	600.77	3.31	8.08	127.24	127.34	.0036	-.1977
6	600.69	3.26	8.03	126.34	126.46	.0038	-.1846
7	600.58	3.18	8.15	124.43	124.56	.0041	-.1666
10	600.40	3.02	8.18	121.47	121.65	.0048	-.1323

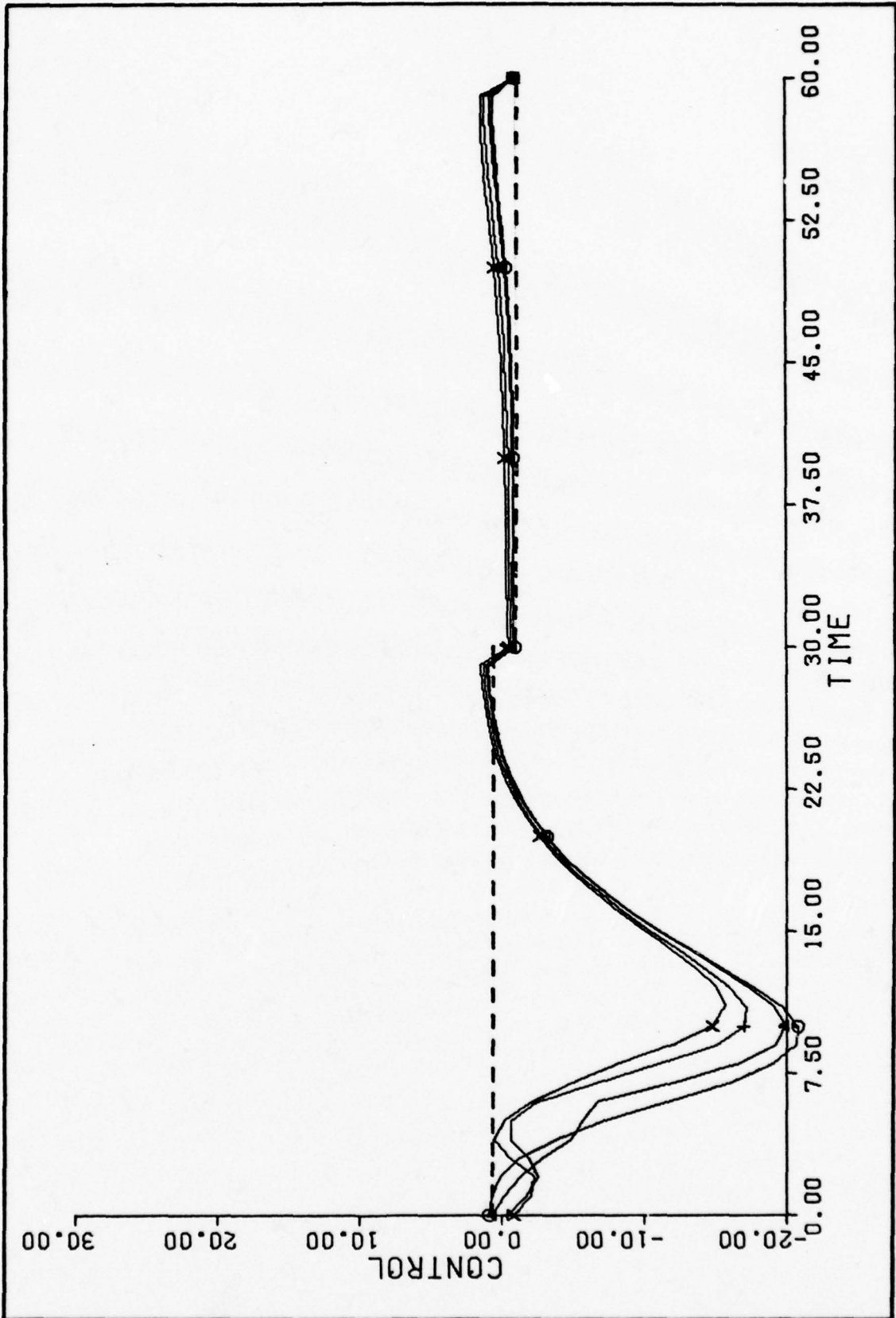


Figure 21. Control History for Case 1

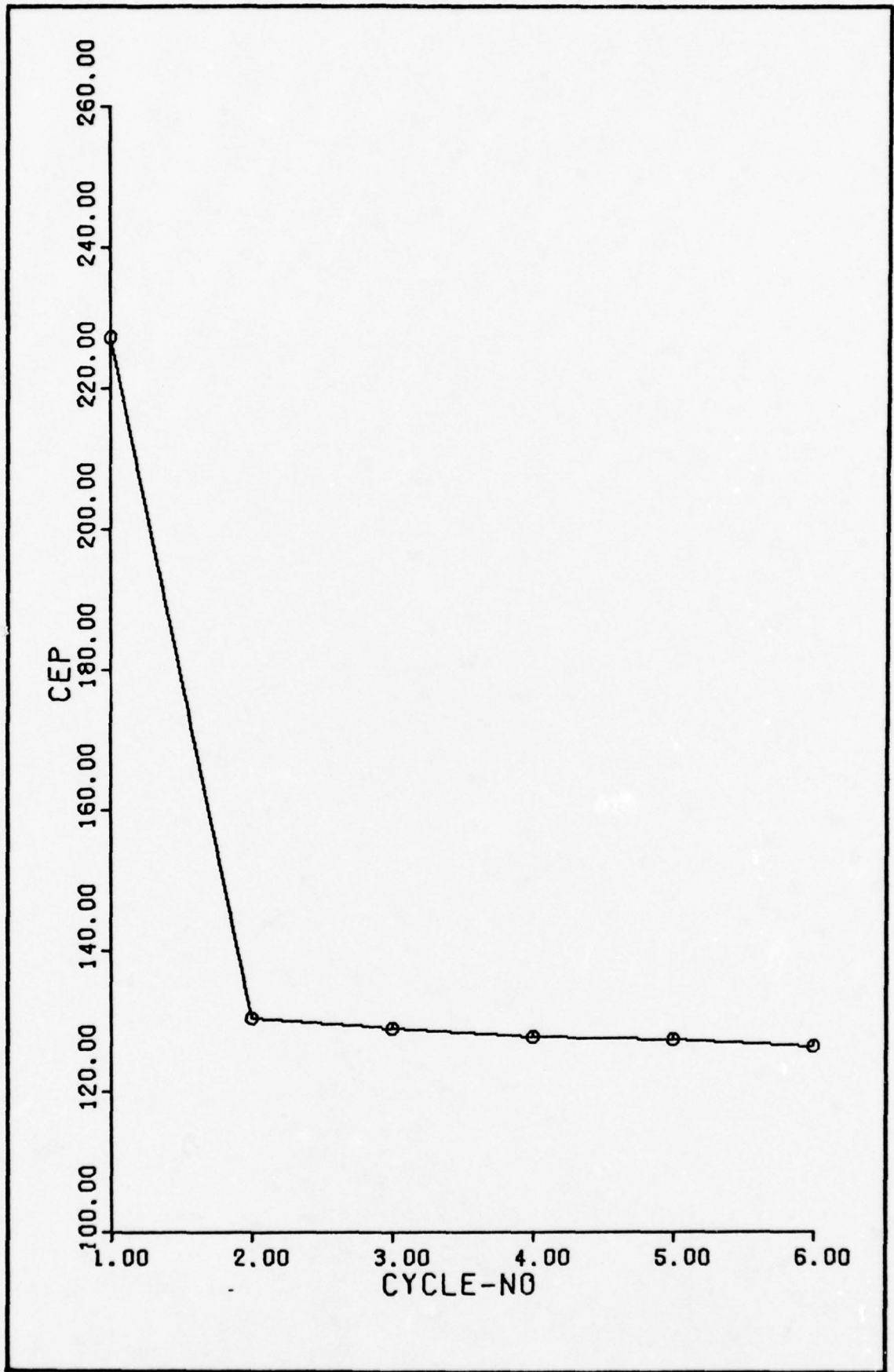


Figure 22. CEP vs Cycle-No. for Case 1

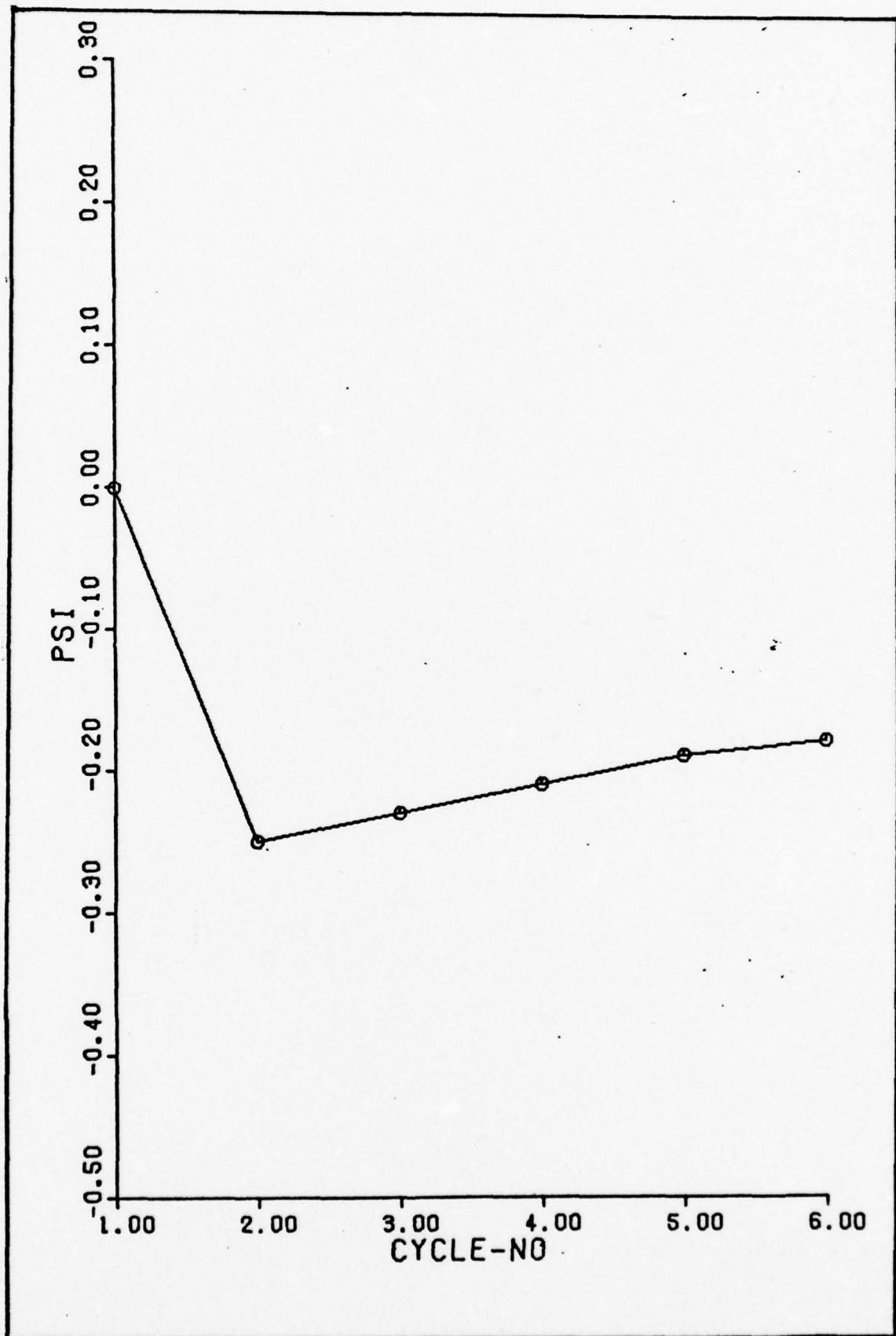


Figure 23. PSI vs Cycle-No. for Case 1

Table VI. Results of Gradient Technique - Case 2

CYCLE	TOF	σ_x	σ_y	CEP	COST	σ_μ	PSI
1	600.15	3.25	8.24	133.04	133.28	1.526E-3	-.0363
2	600.52	3.54	8.14	132.10	132.56	1.461E-3	-.1747
3	603.20	4.50	7.68	131.78	132.47	1.058E-3	-.4259
4	602.56	4.27	7.79	131.12	132.06	1.158E-3	-.3801
5	602.58	4.32	7.75	131.26	132.42	1.090E-3	-.3846
6	601.76	3.95	7.86	129.71	131.09	1.320E-3	-.3150
7	601.36	3.82	7.98	129.92	131.51	1.357E-3	-.2773
8	601.14	3.76	8.04	130.22	132.22	1.327E-3	-.2548

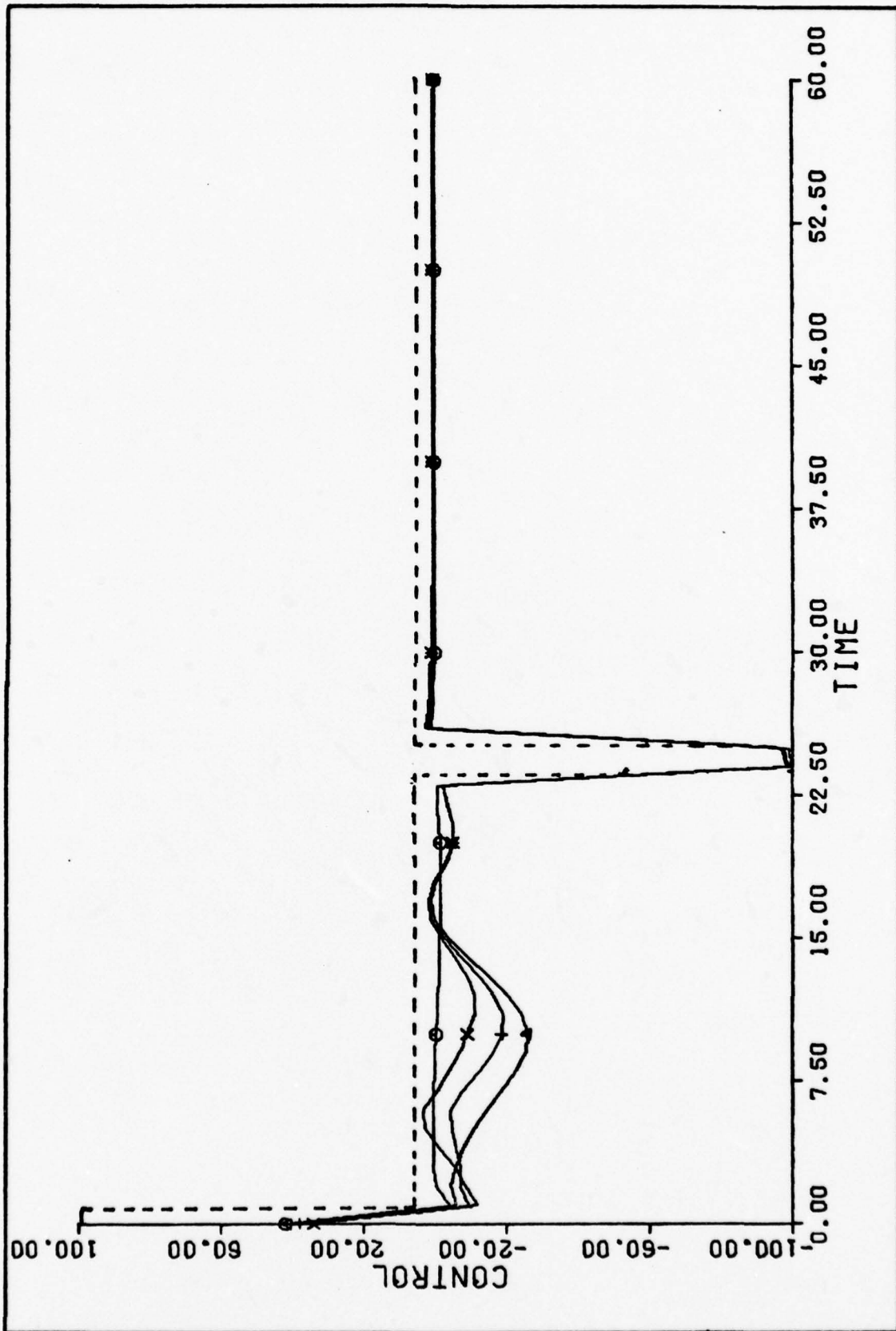


Figure 24. Control History for Case 2

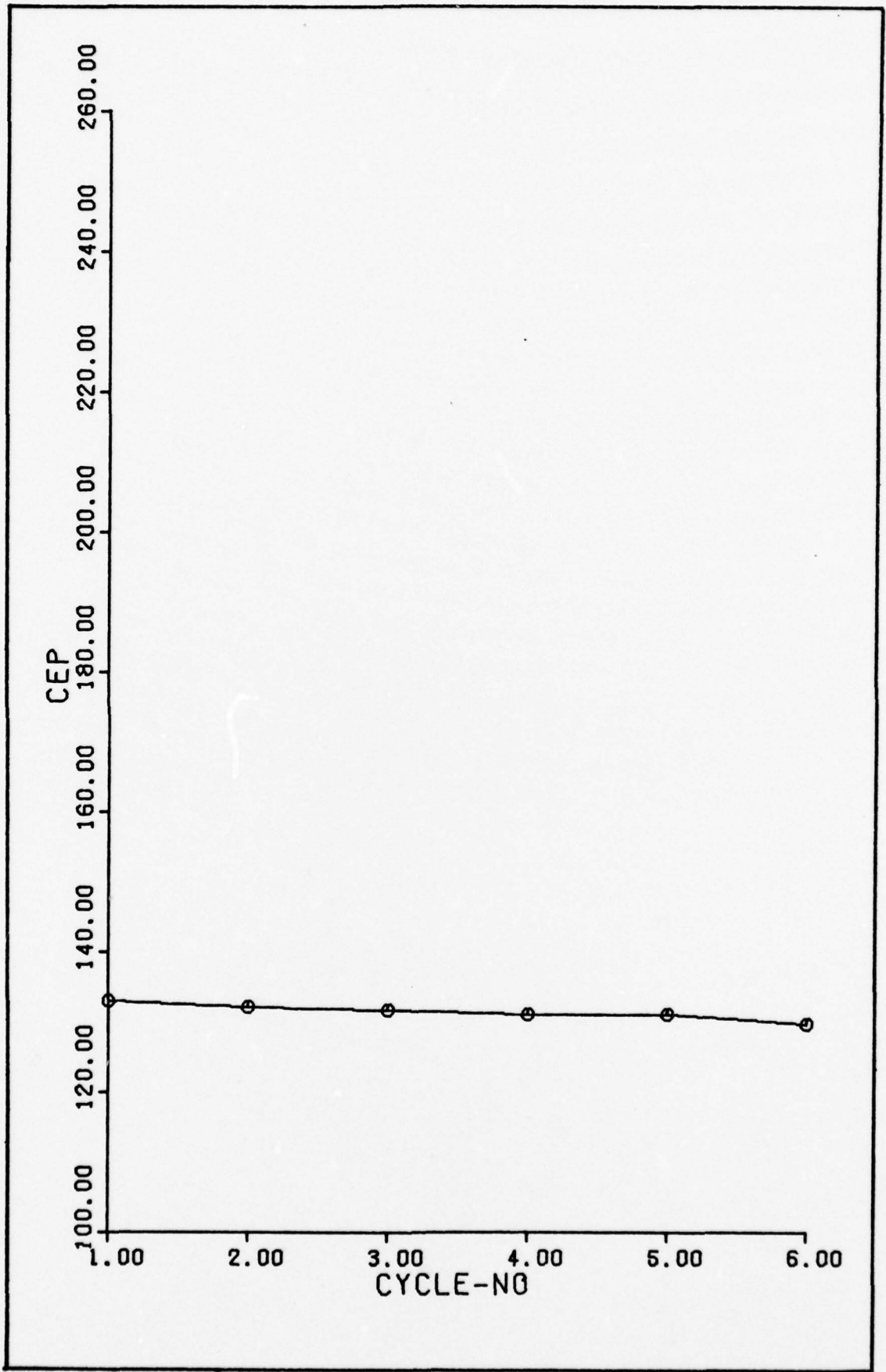


Figure 25. CEP vs Cycle-No. for Case2

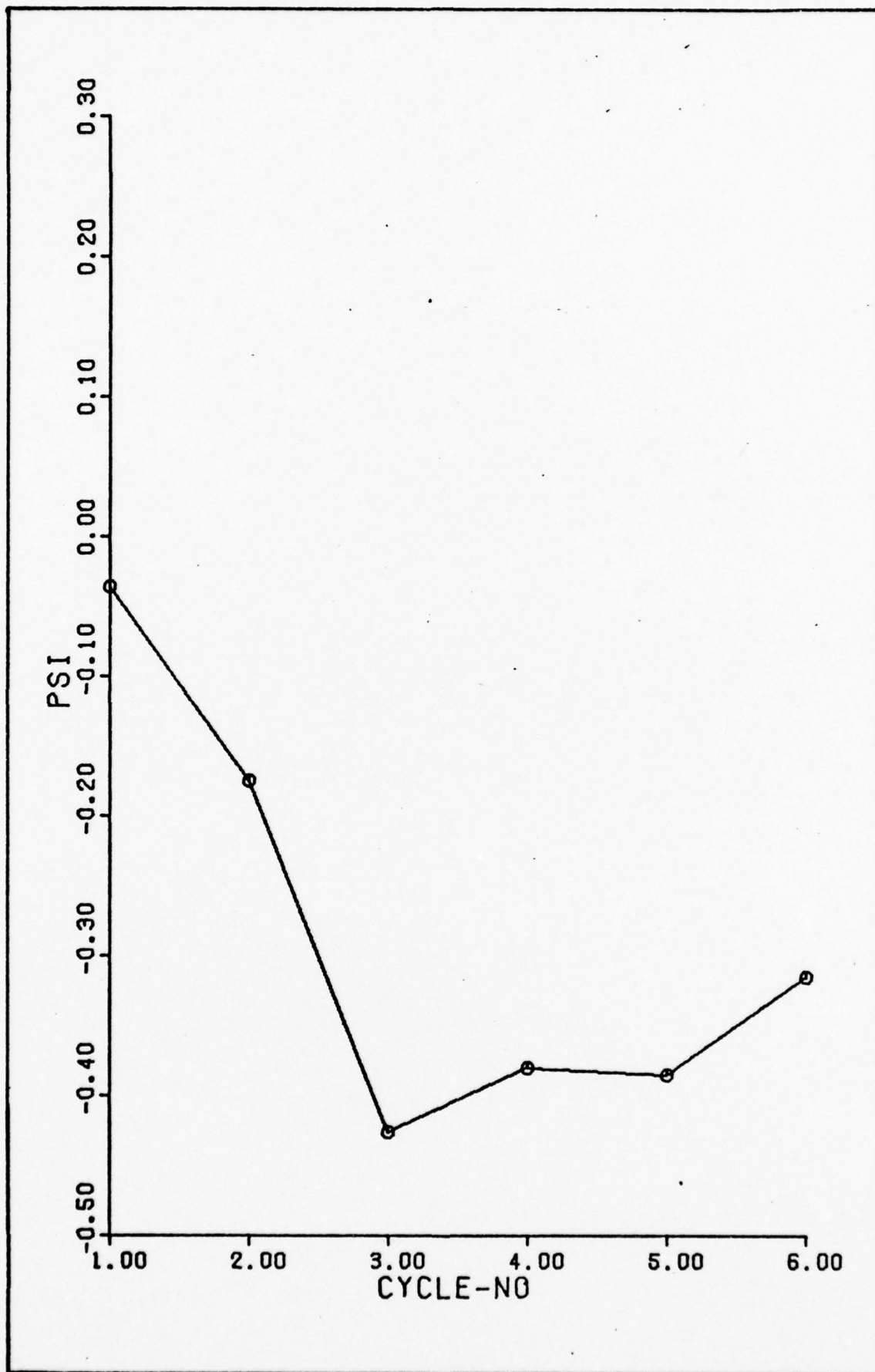


Figure 26. PSI vs Cycle-No. for Case 2

Table VII. Results of Gradient Technique - Case 3

CYCLE	TOF	σ_x	σ_y	CEP	COST	σ_μ	PSI
1	600.09	3.17	8.42	308.38	308.44	.0125	-.0160
2	600.04	2.73	8.41	258.97	259.09	.0118	-.0297
3	600.03	2.67	8.40	207.57	207.75	.0111	-.0379
4	600.03	2.58	8.42	213.62	213.85	.0108	-.0543
5	600.03	3.06	8.40	148.36	148.64	.0087	-.0340
6	600.03	3.10	8.38	144.75	144.09	.0078	-.0332
7	600.07	3.35	8.35	123.40	123.77	.0058	.0153
8	600.55	2.83	8.25	144.64	145.09	.0036	.0684

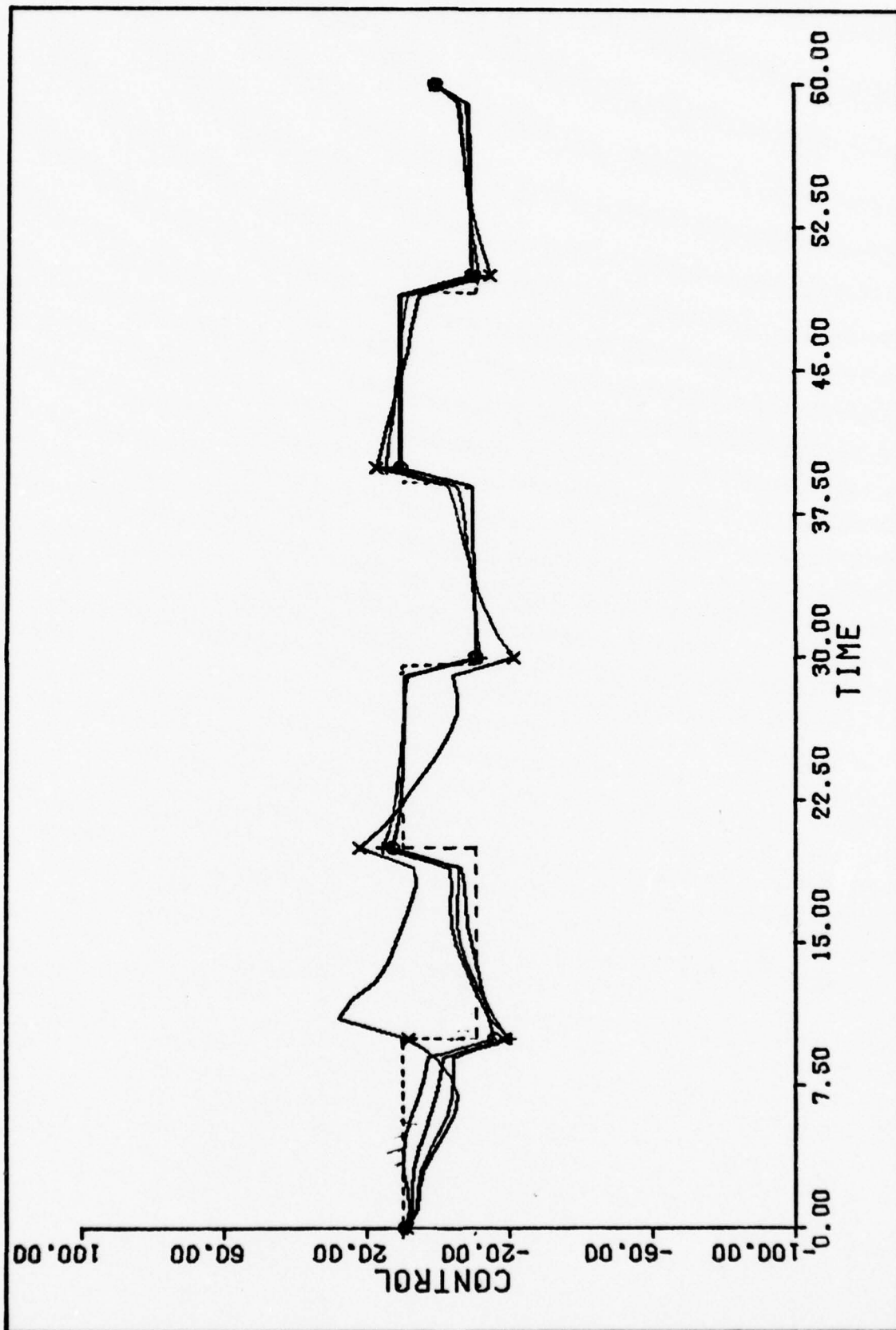


Figure 27. Control History for Case 3

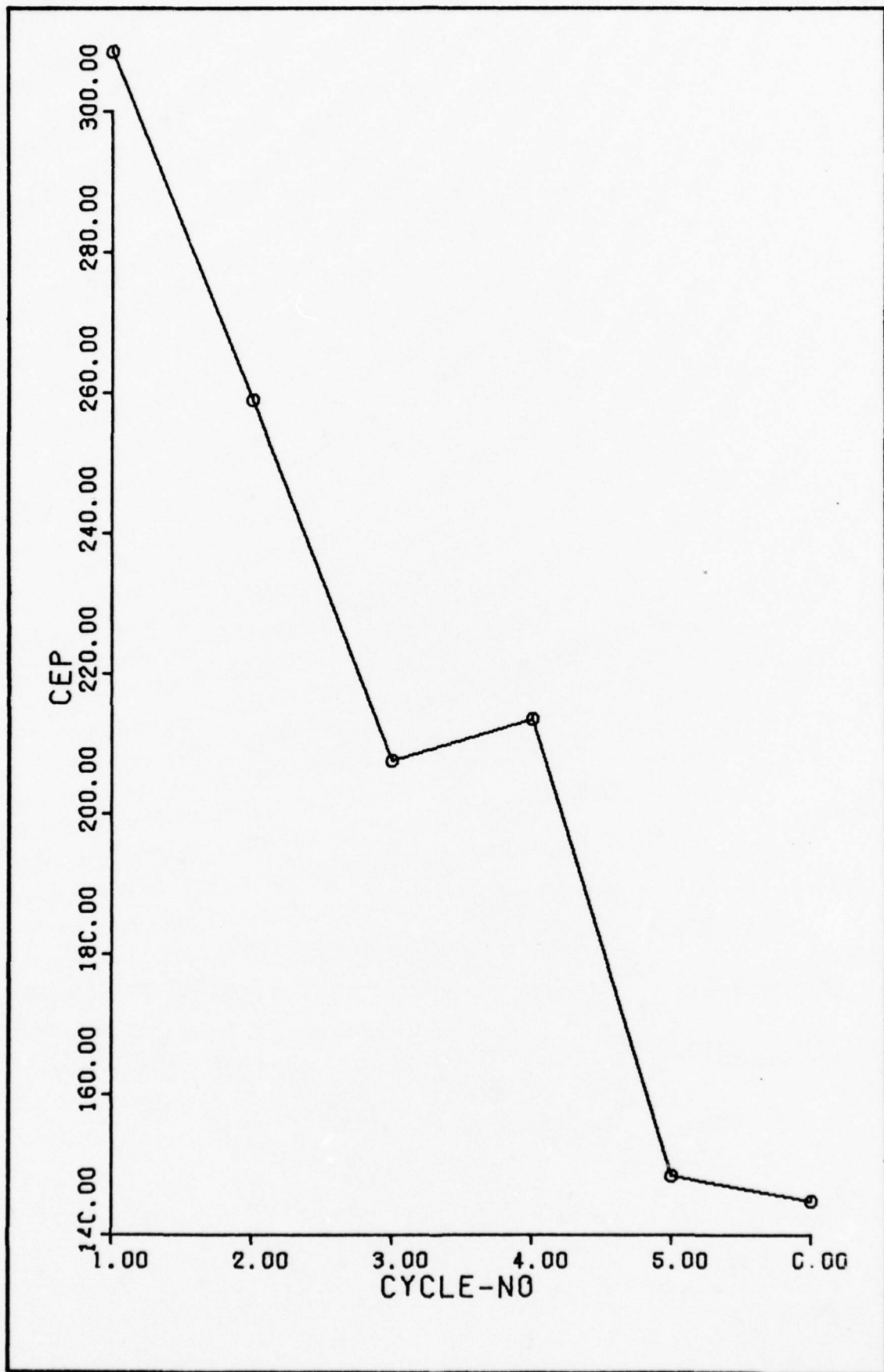


Figure 28. CEP vs Cycle-No. for Case 3

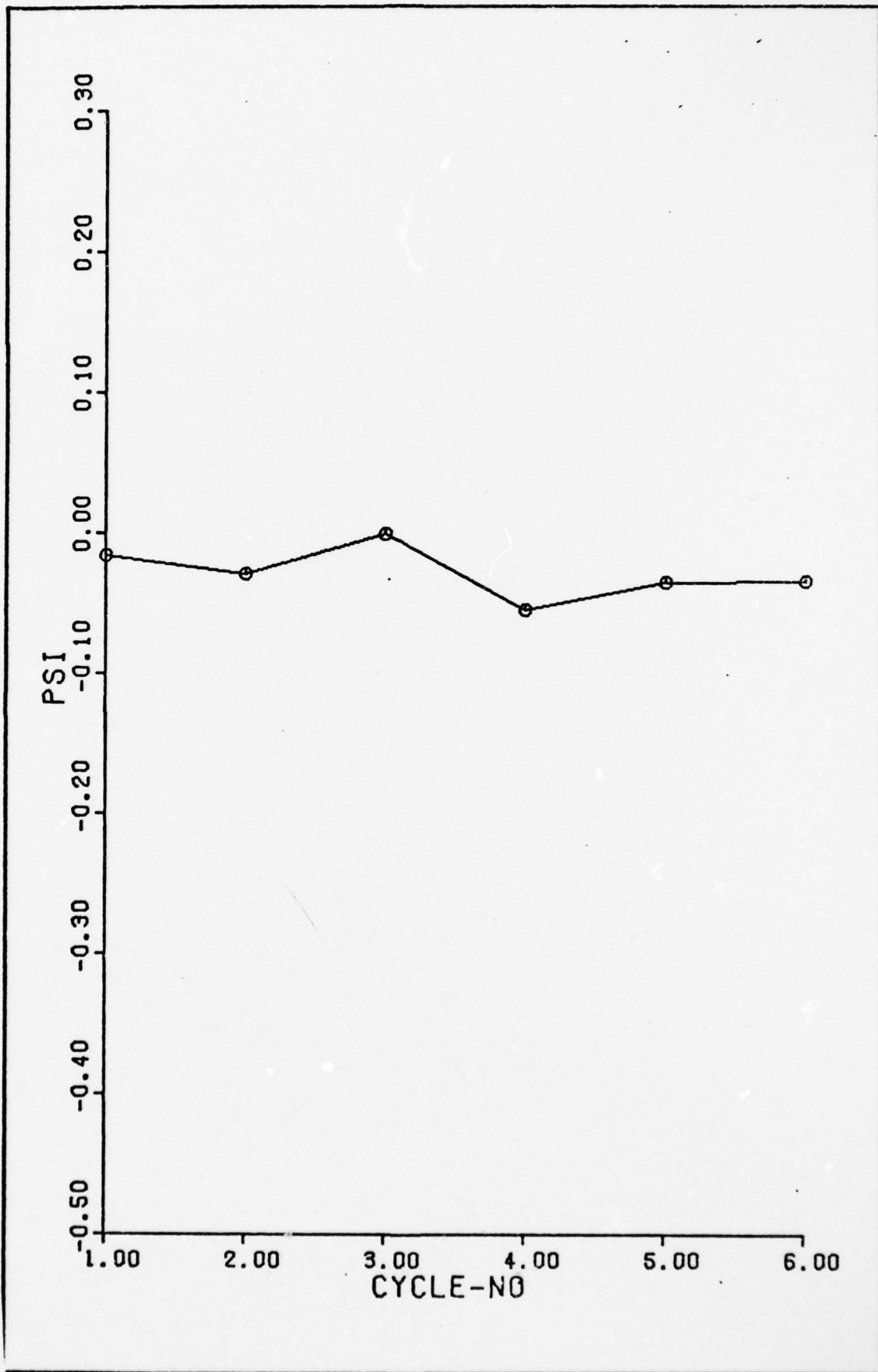


Figure 29. PSI vs Cycle-No. for Case 3

V. Conclusions and Recommendations

The theory of dual control has been applied to an air-to-ground missile with a constant misalignment angle. The analysis, although modeled simply, has shown significant results. The data from Chapter III and Chapter IV show the inherent correlation between the knowledge of the error parameter and the terminal CEP of the missile.

There are two major conclusions that can be drawn.

1. Maneuvering during a radar environment decreases the covariance of the unknown misalignment parameter.
2. Because of this learning about the error parameter, the CEP of the missile can be substantially reduced.

From Chapter III, it was also learned that high-g maneuvers outside the radar environment can amplify the navigation errors greatly. It is therefore recommended that any air launched ballistic missile perform its required maneuvering, especially high-g turns, while it is still in the radar environment of the carrier aircraft. The tracking information from the radar system will aid greatly in reducing the terminal state of INS systems.

From Chapter IV, it is evident that there may be many local minimums. Hence, it may not be concluded that this research has discovered an absolute best trajectory for a minimum CEP. Many more cases of input control guesses can be made which may further reduce the CEP. However, the basic concept of dual control has been successfully applied.

Further research in this area is needed for a more comprehensive and complete understanding of this theory. The following recommendations are made for future study:

1. Radar measurements should be modeled as discrete measurements.

2. Three dimensional analysis would allow greater maneuverability and more error parameters to be identified.
3. Initial boost phase could be modeled. This is an area of increased observability.

The theory of dual control may be able to make significant contributions to inertial navigation systems. It will certainly aid in getting the best performance that each system is capable of producing.

Bibliography

1. Bryson, A. E., and Ho, Yu-Chi. Applied Optimal Control, Washington, D.C.: Hemisphere Publishing Corporation, 1975.
2. Dayan, R. Application of a Maximum Likelihood Parameter Estimator to an Advanced Missile Guidance and Control System, Thesis, Wright-Patterson Air Force Base, Ohio: Air Force Institute of Technology, December, 1977.
3. Eykoff, P. System Identification. London: John Wiley and Sons, 1974.
4. Feldbaum, A. Optimal Control Systems. New York: Academic Press, 1965.
5. Hornbeck, R. W. Numerical Methods, New York, N.Y.: Quantum Publishers, Inc., 1975.
6. Lipshutz, S. Probability, New York: McGraw-Hill Book Company, 1965.
7. Maybeck, P. S. Stochastic Estimation and Control, Part I, Unpublished Notes. Wright-Patterson Air Force Base, Ohio: Air Force Institute of Technology, February, 1975.
8. Reid, J. G. Sensitivity Operators and Associated System Concepts for Linear Dynamic Systems, Technical Report AFAL-TR-76-118. Wright-Patterson Air Force Base, Ohio: Air Force Institute of Technology, July, 1976.
9. Tse, E. and Y. Bar-Shalom. "Wide-Sense Adaptive Dual Control for Nonlinear Stochastic Systems," IEEE Trans. Auto. Control, AC-18: 98-108, April, 1973.

Appendix A

This appendix presents the 18×18 matrix, $\frac{\partial f}{\partial x}$. This is shown on pages 81 through 89. Also influence function equations are presented. These are described in Chapter IV as:

$$\dot{c} = - \left(\frac{\partial f}{\partial x} \right)^t c - \left(\frac{\partial L}{\partial x} \right)^t$$

$$c(t_f) = \left(\frac{\partial \phi}{\partial x_i} \right) t_f$$

and

$$\dot{R} = - \left(\frac{\partial f}{\partial x} \right)^t R$$

$$R(t_f) = \begin{cases} 1 & i = j \\ 0 & i \neq j \end{cases}$$

where

c is a n -vector

R is a $n \times q$ matrix

$$\dot{c} = - \left(\frac{\partial f}{\partial x} \right)^t c - \left(\frac{\partial L}{\partial x} \right)^t$$

$$\dot{c}_1 = 0$$

$$\dot{c}_2 = 0$$

$$\dot{c}_3 = c_1 \cdot v \cdot \sin(X_3) - c_2 \cdot v \cdot \cos(X_3)$$

$$\dot{c}_4 = c_4 \cdot (2AX_4 + 2BX_5) + c_5 (AX_5 + BX_9) + c_6 (AX_6 + BX_{10}) + c_7 (AX_7 + BX_{11}) + c_8 (AX_8 + BX_{12})$$

$$\dot{c}_5 = c_4 (2BX_4 + 2DX_5) + c_5 (AX_4 + 2BX_5 + DX_9) + c_6 (BX_6 + DX_{10}) + c_7 (BX_7 + DX_{11}) + c_8 (BX_8 + DX_{12}) + c_9 (2AX_5 + 2BX_9) + c_{10} (AX_6 + BX_{10}) + c_{11} (AX_7 + BX_{11}) + c_{12} (AX_8 + BX_{12})$$

$$\dot{c}_6 = -2c_4 + c_6 (AX_4 + BX_5) + c_{10} (AX_5 + BX_9) + c_{13} (2AX_6 + 2BX_{10}) + c_{14} (AX_7 + BX_{11}) + c_{15} (AX_8 + BX_{12})$$

$$\dot{c}_7 = -c_5 + c_7 (AX_4 + BX_5) + c_{11} (AX_5 + BX_9) + c_{14} (AX_6 + BX_{10}) + c_{16} (2AX_7 + 2BX_{11}) + c_{17} (AX_8 + BX_{12})$$

$$\dot{c}_8 = L_2 c_6 - L_1 c_7 + c_8 (AX_4 + BX_5) + c_{12} (AX_5 + BX_9) + c_{15} (AX_6 + BX_{10}) + c_{17} (AX_7 + BX_{11}) + c_{18} (2AX_8 + 2BX_{12})$$

$$\dot{c}_9 = c_5 (BX_4 + DX_5) + c_9 (2BX_5 + 2DX_9) + c_{10} (BX_6 + DX_{10}) + c_{11} (BX_7 + DX_{11}) + c_{12} (BX_8 + DX_{12})$$

$$\dot{c}_{10} = -c_5 + c_6 (BX_4 + DX_5) + c_{10} (BX_5 + DX_9) + c_{13} (2BX_6 + 2DX_{10}) + c_{14} (BX_7 + DX_{11}) + c_{15} (BX_8 + DX_{12})$$

$$\dot{c}_{11} = c_7 (BX_4 + DX_5) - 2c_9 + c_{11} (BX_5 + DX_9) + c_{14} (BX_6 + DX_{10})$$

$$+ C_{16}(2BX_7 + 2DX_{11}) + C_{17}(BX_8 + DX_{12})$$

$$\dot{C}_{12} = C_8(BX_4 + DX_5) + L_2 C_{10} - L_1 C_{11} + C_{12}(BX_5 + DX_9) + C_{15}(BX_6 + DX_{10}) + C_{17}(BX_7 + DX_{11}) + C_{18}(2BX_8 + 2DX_{12})$$

$$\dot{C}_{13} = -C_6$$

$$\dot{C}_{14} = -C_7 - C_{10}$$

$$\dot{C}_{15} = C_8 + 2L_2 C_{13} - L_1 C_{14}$$

$$\dot{C}_{16} = -C_{11}$$

$$\dot{C}_{17} = -C_{12} + L_2 C_{14} - 2L_1 C_{16}$$

$$\dot{C}_{18} = L_2 C_{15} - L_1 C_{17}$$

$$\dot{R} = - \left(\frac{\partial f}{\partial x} \right)^T R$$

$$\dot{R}_1 = 0$$

$$\dot{R}_2 = 0$$

$$\dot{R}_3 = -V \sin(X_3)$$

all remaining \dot{R} 's will equal zero because of initial conditions.

	x_1	x_2	x_3	x_4	x_5	x_6
f_1	0	0	$-V \sin(x_3)$	0	0	0
f_2	0	0	$V \cos(x_3)$	0	0	0
f_3	0	0	0	0	0	0
f_4	0	0	0	$-2Ax_4 - 2Bx_5$	$-2Bx_4 - 2Dx_5$	2
f_5	0	0	0	$-Ax_5 - Bx_9$	$-Ax_4 - 2Bx_5 - Dx_9$	0
f_6	0	0	0	$-Ax_6 - Bx_{10}$	$-Bx_6 - Dx_{10}$	$-Ax_4 - Bx_5$

x_1 x_2 x_3 x_4 x_5 x_6

f_7	0	0	0	$-Ax_7 - Bx_{11}$	$-Bx_7 - Dx_{11}$	0
f_8	0	0	0	$-Ax_8 - Bx_{12}$	$-Bx_8 - Dx_{12}$	0
f_9	0	0	0	0	$-2Ax_5 - 2Bx_9$	0
f_{10}	0	0	0	0	$-Ax_6 - Bx_{10}$	$-Ax_5 - Bx_9$
f_{11}	0	0	0	0	$-Ax_7 - Bx_{11}$	0
f_{12}	0	0	0	0	$-Ax_8 - Bx_{12}$	0

	x_1	x_2	x_3	x_4	x_5	x_6
f_{13}	0	0	0	0	0	$-2Ax_6 - 2Bx_{10}$
f_{14}	0	0	0	0	0	$-Ax_7 - Bx_{11}$
f_{15}	0	0	0	0	0	$-Ax_8 - Bx_{12}$
f_{16}	0	0	0	0	0	0
f_{17}	0	0	0	0	0	0
f_{18}	0	0	0	0	0	0

	x_7	x_8	x_9	x_{10}	x_{11}	x_{12}
f_1	0	0	0	0	0	0
f_2	0	0	0	0	0	0
f_3	0	0	0	0	0	0
f_4	0	0	0	0	0	0
f_5	1	0	$-Bx_4 - Dx_5$	1	0	0
f_6	0	$-L_2$	0	$-Bx_4 - Dx_5$	0	0

	x_7	x_8	x_9	x_{10}	x_{11}	x_{12}
f_7	$-Ax_4 - Bx_5$	L_1	0	0	$-Bx_4 - Dx_5$	0
f_8	0	$-Ax_4 - Bx_5$	0	0	0	$-Bx_4 - Dx_5$
f_9	0	0	$-2Bx_5 - 2Dx_9$	0	2	0
f_{10}	0	0	$-Bx_6 - Dx_{10}$	$-Bx_5 - Dx_9$	0	$-L_2$
f_{11}	$-Ax_5 - Bx_9$	0	$-Bx_7 - Dx_{11}$	0	$-Bx_5 - Dx_9$	L_1
f_{12}	0	$-Ax_5 - Bx_9$	$-Bx_8 - Dx_{12}$	0	0	$-Bx_5 - Dx_9$

	x_7	x_8	x_9	x_{10}	x_{11}	x_{12}
f_{13}	0	0	0	$-2Bx_6 - 2Dx_{10}$	0	0
f_{14}	$-Ax_6 - Bx_{10}$	0	0	$-Bx_7 - Dx_{11}$	$-Bx_6 - Dx_{10}$	0
f_{15}	0	$-Ax_6 - Bx_{10}$	0	$-Bx_8 - Dx_{12}$	0	$-Bx_6 - Dx_{10}$
f_{16}	$-2Ax_7 - 2Bx_{11}$	0	0	0	$-2Bx_7 - 2Dx_{11}$	0
f_{17}	$-Ax_8 - Bx_{12}$	$-Ax_7 - Bx_{11}$	0	0	$-Bx_8 - Dx_{12}$	$-Bx_7 - Dx_{11}$
f_{18}	0	$-2Ax_8 - 2Bx_{12}$	0	0	0	$-2Bx_8 - 2Dx_{12}$

	x_{13}	0	0	0	0	0	0
	x_{14}	0	0	0	0	0	0
	x_{15}	0	0	0	0	0	0
	x_{16}	0	0	0	0	0	0
	x_{17}	0	0	0	0	0	0
	x_{18}	0	0	0	0	0	0
f_1							
f_2							
f_3							
f_4							
f_5							
f_6						1	

AD-A058 515

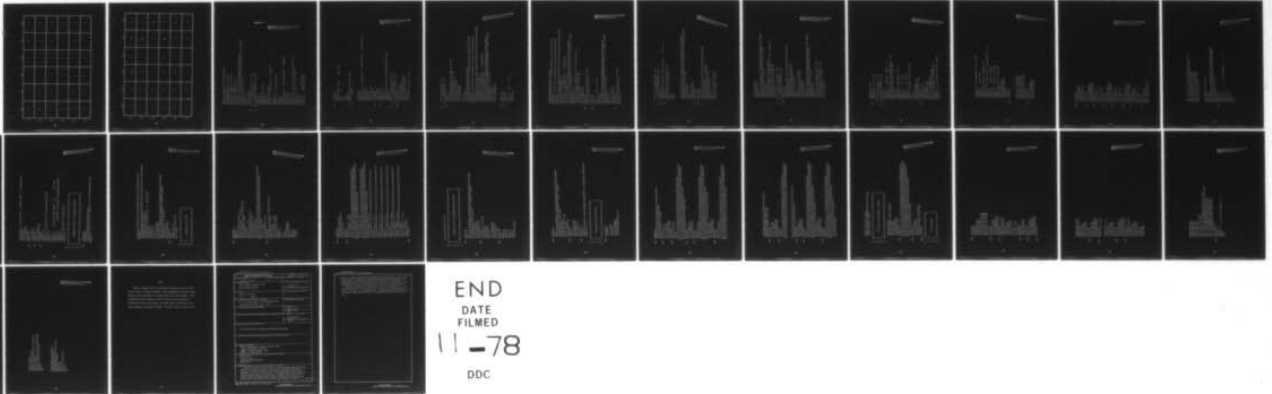
AIR FORCE INST OF TECH WRIGHT-PATTERSON AFB OHIO SCH--ETC F/0 16/4.1
DUAL CONTROL ANALYSIS OF AN AIR TO GROUND MISSILE.(U)
MAR 78 J P KAUPPILA

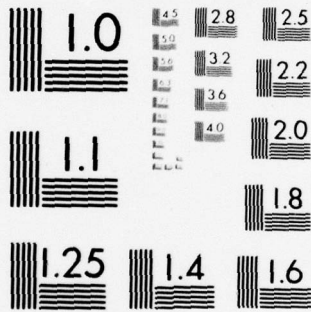
UNCLASSIFIED

AFIT/0A/EE/78-1

NL

2 OF 2
AD
A058515





MICROCOPY RESOLUTION TEST CHART
NATIONAL BUREAU OF STANDARDS-1963-A

	x_{13}	x_{14}	x_{15}	x_{16}	x_{17}	x_{18}
f_7	0	1	0	0	0	0
f_8	0	0	1	0	0	0
f_9	0	0	0	0	0	0
f_{10}	0	1	0	0	0	0
f_{11}	0	0	0	1	0	0
f_{12}	0	0	0	0	1	0

	x_{13}	x_{14}	x_{15}	x_{16}	x_{17}	x_{18}
f_{13}	0	0	$-2L_2$	0	0	0
f_{14}	0	0	L_1	0	$-L_2$	0
f_{15}	0	0	0	0	0	$-L_2$
f_{16}	0	0	0	0	$2L_1$	0
f_{17}	0	0	0	0	0	L_1
f_{18}	0	0	0	0	0	0

THIS PAGE IS BEST QUALITY PRACTICABLE
FROM COPY FURNISHED TO DDC

```
C *****  
C * COMMAND TURN *  
C *****  
102 CONTINUE  
  I=I+1  
  IF(AFS(X(3)-ALPHA).LT.0.005) GO TO 110  
  IF(X(3).GT.ALPHA) GO TO 110  
  L=1000.*(ALPHA-X(3))  
  IF(L.GT.100) L=100.  
  L1=-1.*SIN(X(3))  
  L2=L.*COS(X(3))  
  U(I)=L  
  THETA=Y(3)  
  P=(X(1)+X(1)+X(2)+X(2))*(.5)  
  SIGX1=((((COS(THETA))**2)+SIGR2)+((R**2)*((SIN(THETA))**2)  
  @*SIGT2))  
  SIGY2=((((SIN(THETA))**2)+SIGR2)+((R**2)*((COS(THETA))**2)  
  @*SIGT2))  
  SIGXY=COS(THETA)*SIN(THETA)*SIGR2-R**2*COS(THETA)*SIN(THETA)*SIGT2  
  DEN=SIGX1+SIGX2-SIGXY**2  
  IF(DEN.EQ.0.0) DEN=1.0  
  A=SIGX2/DEN $R=-SIGX/DEN $ 0=SIGX1/DEN  
  IF(I.EQ.1) PRINT,"A=",A  
  CALL ODE(F1,NEQN,X,T,TOUT,PELER,ARSER,IFLAG,WORK,IWORK)  
  IF(IFLAG.GT.2) PRINT,"ABORT--ABORT--ABORT----- IFLAG=",IFLAG  
  IF(IFLAG.GT.2) GO TO 909  
  TOUT=TOUT+1.  
  DO 115 K=1,18  
  STOREX(I,K)=X(K)  
  
105 CONTINUE  
  GO TO 102  
107 CONTINUE  
  I=I+1  
  L=0. $ L1=0. $ L2=0.  
  U(I)=0.  
  THETA=X(3)
```

```
P=(X(1)+X(2)+X(2))*X(2)**(C.5)
SIGY1=((COS(THETA))**2)*SIGR2+((R**2)*((SIN(THETA))**2)
@*SIGT2)
SIGX2=(((SIN(THETA))**2)*SIGR2+((R**2)*((COS(THETA))**2)
A*SIGT2))
SIGXY=COS(THETA)*SIN(THETA)*SIGR2-R**2*COS(THETA)*SIN(THETA)*SIGT2
DEN=SIGX1+SIGX2-SIGXY**2
IF(DEN.EC.0.0) DEN=1.0
A=SIGX2/DEN 3R=-SIGXY/DEN $ D=SIGX1/DEN
IF(J.EC.1) PRINT,"A=",A
CALL ODE(F1,NFON,X,T,TOUT,PELERR,ABSEPR,IFLAG,WORK,IMORK)
IF(IFLAG.GT.2) PRINT,"ABORT---ABORT----- IFLAG=",IFLAG
IF(IFLAG.GT.2) GO TO 999
TOUT=TOUT+1.0
IF(X(1).GT.49999) PRINT,"AT THE END OF PHASE I: "
IF(Y(1).GT.+9999) PRINT 1,Y
IF(X(1).GT.+9999.) GO TO 106
DO 104 K=1,18
STOPFX(I,K)=X(K)
CONTINUE
104 IF(ABS(X(1)-XF).LT.200) GO TO 300
IF(X(1).GT.XF) GO TO 300
GO TO 107
CONTINUE
105 I=I+1
L=0. $ L1=0. $ L2=0.
U(I)=0.
THETA=Y(3)
CALL ODE(F2,NEON,X,T,TOUT,PELERR,ABSEPR,IFLAG,WORK,IMORK)
IF(IFLAG.GT.2) PRINT,"ABORT---ABORT----- IFLAG=",IFLAG
IF(IFLAG.GT.2) GO TO 999
TOUT=TOUT+1.0
I=I+1
DO 107 K=1,18
STOPFX(I,K)=X(K)
CONTINUE
107 IF(ABS(X(1)-XF).LT.200) GO TO 300
IF(X(1).GT.XF) GO TO 300
GO TO 106
```

THIS PAGE IS BEST QUALITY PRACTICABLE
FROM COPY FURNISHED TO DDC

```
C *****  
C * FLY TO RADAR LIMIT *  
C *****  
110 CONTINUE  
PRINT*, "TURN COMPLETE X(3)= ", X(3), " AT T= ", T  
CONTINUE  
R=(X(1)+X(1)+X(2)+X(2))* (0.5)  
IF(R.GT.25000.) GO TO 130  
L=0.  
L1=0.  
L2=0.  
  
CALL ONE(F1,NEON,X,T,TOUT,RELEP2,ABSERR,IFLAG,WORK,IWORK)  
IF(IFLAG.GT.2) PRINT*, "ABORT--ABORT--ABORT----- IFLAG= ", IFLAG  
IF(IFLAG.GT.2) GO TO 999  
TOUT=TOUT+1.0  
I=I+1  
DO 100 K=1,18  
STOPX(I,K)=X(K)  
CONTINUE  
GO TO 112  
CONTINUE  
THETA=X(3)  
RAD=(T**2-4*(T**2-((XF-X(1))**2+X(2)**2)/V**2)  
TF=T+RAD** (0.5)/2  
TRC=ACOS((XF-X(1))/((TF-T)*V))  
IF(X(2).GT.0.) TRC=-TRC  
LREQ=(TRC-X(3))*V  
L=LREQ  
IF(LREQ.GT.100.) L=100.  
IF(LREQ.LT.-100.) L=-100.
```

```

L1=-1 *SIN(X(3))
L2=L *CCS(X(3))
U(I)=L
CALL ODE(F1,NEON,X,T,TOUT,RELEP,ARSEPR,IFLAG,WORK,IWORK)
IF(IFLAG.GT.2) PRINT*, " ABORT--IFAG= ",IFLAG
IF(IFLAG.GT.2) GO TO 999
TOUT=TOUT+1.0
PANCE=(X(1)+X(2)+X(3))**(0.5)
IF(RANGE.GT.50000.) PRINT*, "AT THE END OF PHAZE I: "
IF(RANGE.GT.50000.) PRINT 1,X
IF(RANGE.GT.50000.) GO TO 200
GO TO 130
C *****
C * TERMINAL GUIDANCE *
C *****
200 CONTINUE
THETA=X(3)
PAD= *T**2-4*(T**2-((XF-X(1))**2+X(2)**2)/V**2)
TF= *RAD***(0.5)/2
TREQ=ACOS((XF-X(1))/((TF-T)+V))
IF(X(2).GT.0.) TREQ=-TREQ
LREQ=(TREQ-X(3))*V
L=LREQ
IF(LREQ.GT.100.) L=100.
IF(LREQ.LT.-100.) L=-100.
L1=-1 *SIN(X(3))
L2=L *CCS(X(3))
U(I)=L
CALL ODE(F2,NEON,X,T,TOUT,RELEP,ARSEPR,IFLAG,WORK,IWORK)
IF(IFLAG.GT.2) PRINT*, " ABORT--IFAG= ",IFLAG
IF(IFLAG.GT.2) GO TO 999
TOUT=TOUT+1.0
I=I+1
PTT=((X(1)-XF)**2+X(2)**2)**(0.5)
IF(RTT.LT.10.) GO TO 300
IF(APS(X(1)-XF).LT.500) GO TO 300
IF(X(1).GT.XF) GO TO 300
GO TO 200 K=1,18

```

THIS PAGE IS BEST QUALITY PRACTICABLE
FROM COPY FURNISHED TO DDC

```
202 STORFX(I,K)=X(K)
    CONTINUE
    IF(I.EQ.200) GO TO 999
    GO TO 200
C *****
C * IMPACT TARGET *****
C *****
300 CONTINUE
    PRINT*, " "
    PRINT*, " * * MISSILE IMPACT * * "
    PRINT*, " "
    PRINT*, "THE TOTAL TIME FOR FLIGHT= ", TF
    PRINT*, "AT THE END OF PHASE II: "
    PRINT 1, X
    PRINT*, " "
    PRINT*, "THE COORDINATES ARE: "
    PRINT*, " "
    PRINT*, " X= ", X(1)
    PRINT*, " "
    PRINT*, " Y= ", X(2)
    PRINT*, " "
    PRINT*, "THE MISS DISTANCE= ", RTT
    M=1
M1=M-1
DO 310 I=2, M1
    F=ABS(W3*U(I)**2)+F
    IF(ALPHA.EQ.0.0) F=0.
310 CONTINUE
    PSI(1)=X(1)-XF
    PSI(2)=X(2)
    SGMX=X(4)**(0.5)
    SGMY=X(9)**(0.5)
    CEP=(.588*(SGMX+SGMY)
    J=CEP+F*.5*(U(1)+U(M))*W3
    PRINT*, "ADDITIONAL INFORMATION: "
    PRINT*, " "
    PRINT*, " THE COVARIANCE FOR X= ", SGMX
    PRINT*, " "
```

THIS PAGE IS BEST QUALITY PRACTICABLE
FROM COPY FURNISHED TO DDC

```
PRINT*, " THE COVARIANCE FOR V= ", SGMY
PRINT*, " "
PRINT*, " CEP= ", CEP
PRINT*, " "
PRINT*, "THE CONTROL INTEGRAL= ", F
PRINT*, " "
PRINT*, " THE TOTAL COST AT THIS POINT IS ", J
PRINT*, " "
PRINT*, " PSI(1)= ", PSI(1)
PRINT*, " "
PRINT*, " PSI(2)= ", PSI(2)
PRINT*, " "
PRINT*, "*****"
AL(N) = ALPHA
SX(N) = X(4)**(0.5)
SY(N) = Y(9)**(0.5)
CE(N) = CEP
J1(N) = J
500 CONTINUE
```

```
IF(N.EQ.2) GO TO 510
IF(N.EQ.4) GO TO 520
IF(N.EQ.7) GO TO 530
IF(N.EQ.11) GO TO 540
IF(N.EQ.12) GO TO 550
GO TO 10
CONTINUE
DO 511 K=1,100
X1(K)=STOREX(K,1)
Y1(K)=STOREX(K,2)
```

510

THIS PAGE IS BEST QUALITY PRACTICABLE
FROM COPY FURNISHED TO DDC

```
511 CONTINUE
    X1(101)=1000.
    X1(102)=12500.
    Y1(101)=0.
    Y1(102)=15000.
    GO TO 10

520 CONTINUE
    DO 521 K=1,100
    X2(K)=STOREX(K,1)
    Y2(K)=STOREX(K,2)
521 CONTINUE
    X2(101)=1000.
    Y2(102)=12500.
    Y2(101)=0.
    Y2(102)=15000.
    GO TO 10

530 CONTINUE
    DO 531 K=1,100
    X3(K)=STOREX(K,1)
    Y3(K)=STOREX(K,2)
531 CONTINUE
    X3(101)=1000.
    Y3(102)=12500.
    Y3(101)=0.
    Y3(102)=15000.
    GO TO 10

540 CONTINUE
    DO 541 K=1,100
    X4(K)=STOREX(K,1)
    Y4(K)=STOREX(K,2)
541 CONTINUE
    X4(101)=1000.
    Y4(102)=12500.
    Y4(101)=0.
    Y4(102)=15000.
    GO TO 10

550 CONTINUE
    CALL PLOTS(30)
    CALL PLOT(0,,-3,,-3)
    CALL PLOT(0,3,,-3)
```


THIS PAGE IS BEST QUALITY PRACTICABLE
FROM COPY FURNISHED TO DDC

```
PROGRAM N03(INPUT, OUTPUT, PLOT)
EXTFNAL F1, F2, F3
COMMON/PARARA/X(18)
COMMON/MARY/STORA(100), STOREB(100), STORED(100), STOREX(100, 18)
COMMON/SANDY/V, A, B, D, L, L1, L2
COMMON/CAROL/W1, W2
DIMENSION U(100)
DIMENSION DU(100)
DIMENSION C(18), STOREC(100, 18)
DIMENSION RS(3), STORER(100)
DIMENSION WORK(500), IWORK(5)
DIMENSION WORK2(500), IWORK2(5)
DIMENSION WORK3(500), IWORK3(5)
DIMENSION DC(18)
DIMENSION STOREJ(15), STOREP(15), CY(15), STORET(75)
DIMENSION STOREL1(75), STOREL2(75), STOREL3(75), STOREL4(75)
DIMENSION X1(75), X2(75), X3(75), X4(75), Y1(75), Y2(75), Y3(75), Y4(75)
DIMENSION CE(15)
INTEGER M, Q
REAL L, L1, L2, LTF
FORMAT(9E12.4)

*****
* INITIAL VALUES *
*****
V=100. $ THETA=0. $ TF=60.
N=60
W=10.
SIGR2=100. $ SIGT2=1.0E-6
O=C
EPS=C.01
W1=100. $ W2=100. $ W3=1.0E-5
NEQN=18
T=C.
TOUT=1.0
```

1
C
C
C
C
C
C

THIS PAGE IS BEST QUALITY PRACTICABLE
FROM COPY FURNISHED TO DDC

```
200 CONTINUE
PRINT*, " "
PRINT*, " "
PRINT*, "END OF PHASE I "
PRINT*, "I= ", I, " T= ", T
DIST=(X(2)**2+(XF-X(1))**2)**(0.5)
PRINT*, "DIST= ", DIST
TG=DIST/V
PRINT*, "TG= ", TG
TREQ=ACCS((XF-X(1))/DIST)
PRINT*, "TREQ= ", TREQ
PSI=(X(3)-TREQ)
PRINT*, "PSI= ", PSI
PHI=0.585*((X(4)+2.*TG*X(5)+TG**2*X(13)+(TG**3/3)*1.0E-4)**(0.5)
@+(X(9)+2.*TG*X(11)+TG**2*X(16)+(TG**3/3)*1.0E-4)**(0.5)
PRINT*, "PHI= ", PHI
DO 201 K=2,59
EYEL=EYEL+U(K)**2*W3
CONTINUE
EYEL=EYEL+0.5*(U(1)**2+W3*U(N))**2*W3
PRINT*, "EYEL= ", EYEL
COST=PHI+EYEL
PRINT*, "COST= ", COST
IF(Q.EQ.5) GO TO 800
PRINT*, " "
PRINT*, " "
I=61
L=U(61)
L1=-L*SIN(X(3))
L2=L*COS(X(3))
T=60.
TOUT=59.
IFLAG=1
NEQN=18
```

```

300 CONTINUE
    TGX2=X(2)/(V*DIST)
    TGX1=(X(1)-XF)/(V*DIST)
    DO 305 K=1,18
    C(K)=0.
305 CONTINUE
    PRINT*, "TGX2= ", TGX2
    PRINT*, "TGX1= ", TGX1
    C(1)=0.294*(X(4)+2*TG*X(6)+TG**2*X(13)+TG**3*(1/3)*1.0E-4)**
    @(-0.5)*(2*X(6)*TGX1+2*TG*X(13)+TG**2*1.0E-4*TGX1)+0.294*(
    @X(9)+2*TG*X(11)+TG**2*X(16)+TG**3*(1/3)*1.0E-4)*(2*X(11)
    @+TGX1+2*TG*X(16)+TGX1+TG**2*1.0E-4*TGX1)
    PRINT*, "C(1)= ", C(1)
    C(2)=0.294*(X(4)+2*TG*X(5)+TG**2*X(13)+TG**3*(1/3)*1.0E-4)**
    @(-0.5)*(2*X(5)*TGX2+2*TG*X(13)+TG**2*1.0E-4*TGX2)+0.294*(
    @X(9)+2*TG*X(11)+TG**2*X(16)+TG**3*(1/3)*1.0E-4)*(2*X(11)
    @+TGX2+2*TG*X(16)+TGX2+TG**2*1.0E-4*TGX2)
    PRINT*, "C(2)= ", C(2)
    C(4)=0.294*(X(4)+2*TG*X(6)+TG**2*X(13)+TG**3*(1/3)*1.0E-4)**
    @(-0.5)
    PRINT*, "C(4)= ", C(4)
    C(6)=0.588*TG*(X(4)+2*TG*X(6)+TG**2*X(13)+(1/3)*TG**3*1.0E-4)**
    @(-0.5)
    PRINT*, "C(6)= ", C(6)
    C(9)=0.294*(X(9)+2*TG*X(11)+TG**2*X(16)+(1/3)*TG**3*1.0E-4)**
    @(-0.5)
    PRINT*, "C(9)= ", C(9)
    C(11)=0.588*TG*(X(9)+2*TG*X(11)+TG**2*X(16)+(1/3)*TG**3*1.0E-4)
    @*(-0.5)
    PRINT*, "C(11)= ", C(11)
    C(13)=0.294*(X(4)+2*TG*X(6)+TG**2*X(13)+(1/3)*TG**3*1.0E-4)**
    @(-0.5)*TG**2
    PRINT*, "C(13)= ", C(13)
    C(16)=0.294*(X(9)+2*TG*X(11)+TG**2*X(16)+(1/3)*TG**3*1.0E-4)**
    @(-0.5)*TG**2
    PRINT*, "C(16)= ", C(16)
    DO 306 K=1,18
    STOREC(61,K)=C(K)
306 CONTINUE

```



```
330 CONTINUE
    I=I-1
    CALL CDE(F3,NEQN,PS,T,TOUT,RELER?,ARSEPP,IFLAG,WORK3,IMORK3)
    IF(IFLAG.GT.2) PRINT*, "ARORT--- IFLAG= ",IFLAG
    IF(IFLAG.GT.2) GO TO 999
    STORP(I)=RS(3)
    IF(I.EC.1) GO TO 380
    DO 335 K=1,18
    X(K)=STORP(I,K)
335 CONTINUE
    L=U(I)
    L1=-1.*SIN(X(3))
    L2=L*CCS(X(3))
    TOUT=TOUT-1.0
    GO TO 330
380 CONTINUE
    PRINT*, " "
    PRINT*, "INFLUENCE COEFFICIENTS SUCCESSFULLY CALCULATED--PRESS ON"
    PRINT*, " "
C *****
C *
C *
C *
C *
C *
C *
C *
C *****
          CALCULATE THE INTEGRALS
C *****
C *
C *
C *
C *
C *
C *
C *****
400 CONTINUE
    EYEPSI=0.
    EYEJFSI=0.
    EYEJJ=0.
    DO 410 K=2,60
    PS(3)=STORP(K)
    EYEPSI=EYEPSI+RS(3)**2
```

```
410 CONTINUE
EYEPSI=EYEPSI+0.5*(STORER(1)**2+STORER(61)**2)
EYEPSI=(1/(V**2))*(1/W)*EYEPSI
PRINT*, "EYEPSI= ", EYEPSI
420 CONTINUE
DO 425 I=2,60
DO 430 K=1,18
X(K)=STOREX(I,K)
C(K)=STOREC(I,K)
430 CONTINUE
PS(3)=STORER(I)
L=U(I)
PTFU=C(3)*(1/V)-C(6)*X(8)*COS(X(3))-C(7)*X(8)*SIN(X(3))
@-C(10)*X(12)*COS(X(3))-C(11)*X(12)*SIN(X(3))-C(13)*2*X(15)*COS(X(3))
@)-C(14)*X(17)*COS(X(3))-X(15)*SIN(X(3))-C(15)*X(18)*COS(X(3))
@-C(16)*2*X(17)*SIN(X(3))-C(17)*X(18)*SIN(X(3))
EYEJFSI=EYEJFSI+(PTFU+2.*W3*L)*RS(3)
425 CONTINUE
DO 435 K=1,18
X(K)=STOREX(1,K)
C(K)=STOREC(1,K)
435 CONTINUE
L=U(1)
RS(3)=STORER(1)
PTFU=C(3)*(1/V)-C(6)*X(9)*COS(X(3))-C(7)*X(8)*SIN(X(3))
@-C(10)*X(12)*COS(X(3))-C(11)*X(12)*SIN(X(3))-C(13)*2*X(15)*COS(X(3))
@)-C(14)*X(17)*COS(X(3))-X(15)*SIN(X(3))-C(15)*X(18)*COS(X(3))
@-C(16)*2*X(17)*SIN(X(3))-C(17)*X(18)*SIN(X(3))
EYEJFSI=EYEJFSI+0.5*(PTFU+2.*W3*L)*RS(3)
DO 440 K=1,18
X(K)=STOREX(61,K)
C(K)=STOREC(61,K)
440 CONTINUE
L=U(61)
PS(3)=STORER(61)
PTFU=C(3)*(1/V)-C(6)*X(8)*COS(X(3))-C(7)*X(8)*SIN(X(3))
@-C(10)*X(12)*COS(X(3))-C(11)*X(12)*SIN(X(3))-C(13)*2*X(15)*COS(X(3))
@)-C(14)*X(17)*COS(X(3))-X(15)*SIN(X(3))-C(15)*X(18)*COS(X(3))
@-C(16)*2*X(17)*SIN(X(3))-C(17)*X(18)*SIN(X(3))
```

```
450 EYEJPSI=EYEJPSI+0.5*(PTFU*2.*W3*L)*RS(3)
    EYEJFSI=EYEJPSI*(1/W)*(1/V)
    PRINT*,"EYEJPSI=",EYEJPSI
    CONTINUE
    DO 460 I=2,50
    DO 465 K=1,18
    X(K)=STOREX(I,K)
    C(K)=STOREC(I,K)
    CONTINUE
    L=U(I)
    PTFU=C(3)*(1/V)-C(6)*X(9)*COS(X(3))-C(7)*X(8)*SIN(X(3))
    @-C(10)*X(12)+COS(X(3))-C(11)*X(12)*SIN(X(3))-C(13)*2*X(15)*COS(X(3)
    @)-C(14)*X(17)*COS(X(3))-X(15)*SIN(X(3))-C(15)*X(18)*COS(X(3))

465 @-C(16)*2*X(17)*SIN(X(3))-C(17)*X(19)*SIN(X(3))
    EYEJ= EYEJ+ (PTFU+2.*W3*L)**2
    CONTINUE
    DO 470 K=1,18
    X(K)=STOREX(1,K)
    C(K)=STOREC(1,K)
    CONTINUE
    L=U(1)
    PTFU=C(3)*(1/V)-C(6)*X(8)*COS(X(3))-C(7)*X(8)*SIN(X(3))
    @-C(10)*X(12)*COS(X(3))-C(11)*X(12)*SIN(X(3))-C(13)*2*X(15)*COS(X(3)
    @)-C(14)*X(17)*COS(X(3))-X(15)*SIN(X(3))-C(15)*X(18)*COS(X(3))
    @-C(16)*2*X(17)*SIN(X(3))-C(17)*X(18)*SIN(X(3))
    EYEJ= EYEJ+0.5*(PTFU+2.*W3*L)**2
    DO 480 K=1,18
    X(K)=STOREX(61,K)
    C(K)=STOREC(61,K)
    CONTINUE
    L=U(61)
    PTFU=C(3)*(1/V)-C(6)*X(8)*COS(X(3))-C(7)*X(8)*SIN(X(3))
    @-C(10)*X(12)*COS(X(3))-C(11)*X(12)*SIN(X(3))-C(13)*2*X(15)*COS(X(3)
    @)-C(14)*X(17)*COS(X(3))-X(15)*SIN(X(3))-C(15)*X(18)*COS(X(3))
    @-C(16)*2*X(17)*SIN(X(3))-C(17)*X(18)*SIN(X(3))
    EYEJ= EYEJ+0.5*(PTFU+2.*W3*L)**2
    EYEJ= EYEJ*(1/W)
```

THIS PAGE IS BEST QUALITY PRACTICABLE
 FROM COPY FURNISHED TO DDC

```

PRINT*, "EYEJ= ", EYEJ
TERM=EYEJ-(EYEJPSI*(1/EYEPSI)+EYEJPSI)
PRINT*, "TERM= ", TERM

```

```

C *****
C *
C *
C *
C *
C *
C *
C *
C *****

```

CALCULATE NEW CONTROL HISTORY

```

DPSI=-EPS*PSI
NU=- (1/EYEPSI) * (DPSI+EYEJPSI)
DO 510 I=1,61
DO 515 K=1,18
X(K)=STOREX(I,K)
C(K)=STOREC(I,K)
515 CONTINUE
CRFU= (C(3)+RS(3)) * (1/V) - C(6) * COS(X(3)) * X(8) - C(7) * SIN(X(3)) * X(8)
a-C(10) * COS(X(3)) * X(12) - C(11) * SIN(X(3)) * X(12) - C(13) * 2 * COS(X(3)) * X(1
a5) - C(10) * COS(X(3)) * X(12) - C(11) * SIN(X(3)) * X(12) - C(13) * 2 * COS(X(3)) *
aY(15) - C(14) * COS(X(3)) * X(17) - SIN(X(3)) * X(15) - C(15) * COS(X(3)) *
aX(18) - C(16) * 2 * SIN(X(3)) * X(17) - C(17) * SIN(X(3)) * X(18)
DU(I)=- (1/W) * (2 * U(I) * W3 + CRFU)

```

```

510 CONTINUE
NO 520 I=1,61
U(I)=U(I)+DU(I)
IF(U(I).GT.100.) U(I)=100.
IF(U(I).LT.-100.) U(I)=-100.
520 CONTINUE

```

```

C *****
C *
C *
C *
C *
C *
C *
C *****

```

PLOT RESULTS

THIS PAGE IS BEST QUALITY PRACTICABLE
FROM COPY FURNISHED TO DDC

```
800 CONTINUE
    CY(0)=0
    CE(0)=PHI
    STOREJ(0)=COST
    STORCP(0)=PSI
    IF(0.E0.1) GO TO 810
    IF(0.E0.2) GO TO 820
    IF(0.E0.5) GO TO 830
    IF(0.E0.8) GO TO 840
    GO TO 50
810 CONTINUE
    DO 811 I=1,61
    STOREL1(I)=U(I)
    X1(I)=STOREX(I,1)
    Y1(I)=STOREX(I,2)
811 CONTINUE
    STOREL1(62)=-100.
    STOREL1(63)=40.
    X1(62)=0.
    Y1(63)=7500.
    Y1(62)=-30000.
    Y1(63)=10000.
    T=-1.0
    DO 815 I=1,61
    T=T+1.0
    STORFT(I)=T
815 CONTINUE
    STORFT(62)=0.
    STORFT(63)=7.5
    GO TO 50
820 CONTINUE
    DO 821 I=1,61
    STORFL2(I)=U(I)
    X2(I)=STOREX(I,1)
    Y2(I)=STOREX(I,2)
821 CONTINUE
```

THIS PAGE IS BEST QUALITY PRACTICABLE
FROM COPY FURNISHED TO DDC

STOREL2(62)=-100.
STOREL2(63)=40.
X2(62)=0.
X2(63)=7500.
Y2(62)=-30000.
Y2(63)=10000.
GO TO 50
CONTINUE
DO 831 I=1,61
STOREL3(I)=U(I)
X3(I)=STOREX(I,1)
Y3(I)=STOREX(I,2)
CONTINUE
831 STOREL3(62)=-100.

STOREL3(63)=40.
X3(62)=0.
X3(63)=7500.
Y3(62)=-30000.
Y3(63)=10000.
GO TO 50
CONTINUE

DO 841 I=1,61
STOREL4(I)=U(I)
X4(I)=STOREX(I,1)
Y4(I)=STOREX(I,2)
CONTINUE

841 STOREL4(62)=-100.
STOREL4(63)=40.
X4(62)=0.
X4(63)=7500.
Y4(62)=-30000.
Y4(63)=10000.
CY(9)=1.
CY(10)=1.
CE(9)=100.
CE(10)=20.

THIS PAGE IS BEST QUALITY PRACTICABLE
FROM COPY FURNISHED TO DDC

```
STORFJ(9)=100.  
STOREJ(10)=20.  
STOREP(9)=-0.5  
STOREP(10)=0.1  
CALL PLOTS(30)  
CALL PLOT(0.,-3.,-3)  
CALL PLOT(0.,2.,-3)  
CALL AXIS(0.,0.,4HTIME,-4,8,0,0,0.,7.5)  
CALL AXIS(0.,0.,7HCONTPOL,7,5,0,90.,-100.,40.)  
CALL LINE(STORET,STOREL1,61,1,10,1)  
CALL LINE(STORET,STOREL2,61,1,10,2)  
CALL LINE(STORET,STOREL3,61,1,10,3)  
CALL LINE(STORET,STOREL4,61,1,10,4)  
CALL PLOTE(Q)  
CONTINUE  
PRINT*, " "  
PRINT*, " "  
PRINT*, " * * * END OF PROGRAM * * * "  
STOP  
END
```

999

THIS PAGE IS BEST QUALITY PRACTICABLE
FROM COPY FURNISHED TO DDC

```
C THIS IS DURING THE PADAR ENVIRONMENT
SUBROUTINE F1(T,X,DX)
COMMON/SANDY/V,A,B,D,L,L1,L2
REAL L,L1,L2
DIMENSION DX(18),X(18)
DX(1)=V*COS(X(3))
DX(2)=V*SIN(X(3))
DX(3)=L/V
DX(4)=2*X(6)-X(4)*(A*X(4)+R*X(5))-X(5)*(R*X(4)+D*X(5))
DX(5)=X(10)+X(7)-X(4)*(A*X(5)+B*X(9))-X(5)*(B*X(5)+D*X(9))
DX(6)=X(13)-L2*X(8)-X(4)*(A*X(6)+B*X(10))-X(5)*(B*X(6)+D*X(10))
DX(7)=X(14)+L1*X(8)-X(4)*(A*X(7)+B*X(11))-X(5)*(B*X(7)+D*X(11))
DX(8)=X(15)-X(4)*(A*X(8)+B*X(12))-X(5)*(B*X(8)+D*X(12))
DX(9)=2*X(11)-X(5)*(A*X(5)+B*X(9))-X(9)*(B*X(5)+D*X(9))
DX(10)=X(14)-L2*X(12)-X(5)*(A*X(6)+B*X(10))-X(9)*(B*X(6)+D*X(10))
DX(11)=X(16)+L1*X(12)-X(5)*(A*X(7)+B*X(11))-X(9)*(B*X(7)+D*X(11))
DX(12)=X(17)-X(5)*(A*X(8)+B*X(12))-X(9)*(B*X(8)+D*X(12))
DX(13)=-2*L2*X(15)-X(6)*(A*X(6)+B*X(10))-X(10)*(B*X(6)+D*X(10))
@+1.0F-4
DX(14)=-L2*X(17)+L1*X(15)-X(6)*(A*X(7)+B*X(11))-X(10)*(B*X(7)+D*X(11))
@X(11)
DX(15)=-L2*X(18)-X(6)*(A*X(8)+B*X(12))-X(10)*(B*X(8)+D*X(12))
DX(16)=2*L1*X(17)-X(7)*(A*X(7)+B*X(11))-X(11)*(B*X(7)+D*X(11))
@+1.0F-4
DX(17)=L1*X(18)-X(7)*(A*X(8)+B*X(12))-X(11)*(B*X(8)+D*X(12))
DX(18)=-X(8)*(A*X(8)+B*X(12))-X(12)*(B*X(8)+D*X(12))
RETURN
END
```

```

SUBROUTINE F2(T,C,DC)
COMMON/BARBARA/X(18)
COMMON/MARY/STORER(100),STORER(100),STORED(100),STOREX(100,18)
COMMON/SANDY/V,A,B,D,L,L1,L2
COMMON/CAROL/W1,W2
DIMENSION DC(18),C(18)
REAL L,L1,L2
DC(1)=C.
DC(2)=C.
DC(3)=C(1)*V*SIN(X(3))-C(2)*V*COS(X(3))
DC(4)=(2*A*X(4)+2*B*X(5))*C(4)+(A*X(5)+R*X(9))*C(5)+(A*X(6)+B*X(10)
a) )+C(6)+(A*X(7)+R*X(11))*C(7)+(A*X(8)+B*X(12))*C(8)
DC(5)=C(4)*(2*B*X(4)+2*D*X(5))+C(5)*(A*X(4)+2*B*X(5)+D*X(9))
a) +C(6)*(B*X(5)+D*X(10))+C(7)*(B*X(7)+D*X(11))+C(8)*(B*X(8)+D*X(12))
a) +C(9)*(2*A*X(5)+2*B*X(9))+C(10)*(A*X(6)+B*X(10))+C(11)*(A*X(7)+B*X
a) (11))+C(12)*(A*X(8)+B*X(12))
DC(6)=-2*C(4)+(A*X(4)+B*X(5))*C(5)+(A*X(5)+R*X(9))*C(10)
a) +(2*B*X(6)+2*B*X(10))*C(13)+(A*X(7)+B*X(11))*C(14)+(A*X(8)+B*X(12)
a) *C(15)
DC(7)=-C(5)+(A*X(4)+B*X(5))*C(7)+(A*X(5)+R*X(9))*C(11)
a) +(A*X(6)+B*X(10))*C(14)+(2*A*X(7)+2*B*X(11))*C(16)+(A*X(8)+B*X(12)
a) *C(17)
DC(8)=L2*C(6)-L1*C(7)+(A*X(4)+B*X(5))*C(8)+(A*X(5)+D*X(9))*C(12)
a) +(A*X(5)+B*X(10))*C(15)+(A*X(7)+B*X(11))*C(17)+(2*A*X(8)+2*B*X(12)
a) *C(18)
DC(9)=(B*X(4)+D*X(5))*C(5)+(2*B*X(5)+2*D*X(9))*C(9)+(B*X(5)+D*
a) X(10))+C(10)+(B*X(7)+D*X(11))*C(11)+(B*X(8)+D*X(12))*C(12)
DC(10)=-C(5)+(B*X(4)+D*X(5))*C(6)+(B*X(5)+D*X(9))*C(10)
a) +(2*B*X(6)+2*D*X(10))*C(13)+(B*X(7)+D*X(11))*C(14)
a) +(B*X(8)+D*X(12))*C(15)
DC(11)=(B*X(4)+D*X(5))*C(7)-2*C(9)+(B*X(5)+D*X(9))*C(11)
a) +(B*X(6)+D*X(10))*C(14)+(2*B*X(7)+2*D*X(11))*C(16)
a) +(2*B*X(8)+D*X(12))*C(17)
DC(12)=(B*X(4)+D*X(5))*C(8)+L2*C(10)-L1*C(11)+(B*X(5)+D*X(9))*
a) C(12)+(B*X(6)+D*X(10))*C(15)+(B*X(7)+D*X(11))*C(17)+(2*B*X(8)
a) +2*D*X(12))*C(18)

```

THIS PAGE IS BEST QUALITY PRACTICABLE
FROM COPY FURNISHED TO DDG

```
DC(13)=-C(6)
DC(14)=-C(7)-C(10)
DC(15)=-C(8)+2*L2*C(13)-L1*C(14)
DC(16)=-C(11)
DC(17)=-C(12)+L2*C(14)-2*L1*C(16)
DC(18)=L2*C(15)-L1*C(17)
RETURN
END
```

```
SUBROUTINE F3(T,RS,DRS)
COMMON/BARBARA/X(18)
COMMON/SANDY/V,A,B,D,L,L1,L2
DIMENSION DRS(3)
DRS(1)=0.
DRS(2)=0.
DRS(3)=-V*SIN(X(3))
RETURN
END
```

VITA

James P. Kauppila was born in Hancock, Michigan on June 15, 1948. He was raised in Jackson, Michigan. After graduating from Jackson High School, he was appointed to the United States Air Force Academy. After graduation from the Academy in 1970, he went to pilot training at Williams Air Force Base, Arizona. He then became a B-52H copilot and later upgraded to Aircraft Commander. He came to AFIT in June of 1976.

UNCLASSIFIED

SECURITY CLASSIFICATION OF THIS PAGE (When Data Entered)

REPORT DOCUMENTATION PAGE		READ INSTRUCTIONS BEFORE COMPLETING FORM
1. REPORT NUMBER AFIT/GA/EE/78-1 ✓	2. GOVT ACCESSION NO.	3. RECIPIENT'S CATALOG NUMBER
4. TITLE (and Subtitle) DUAL CONTROL ANALYSIS OF AN AIR TO GROUND MISSILE		5. TYPE OF REPORT & PERIOD COVERED MS Thesis
		6. PERFORMING ORG. REPORT NUMBER
7. AUTHOR(s) James P. Kauppila Capt USAF		8. CONTRACT OR GRANT NUMBER(s)
9. PERFORMING ORGANIZATION NAME AND ADDRESS Air Force Institute of Technology (AFIT-EN) Wright-Patterson AFB, Ohio 45433		10. PROGRAM ELEMENT, PROJECT, TASK AREA & WORK UNIT NUMBERS
11. CONTROLLING OFFICE NAME AND ADDRESS		12. REPORT DATE March 1978
		13. NUMBER OF PAGES 117
14. MONITORING AGENCY NAME & ADDRESS (if different from Controlling Office)		15. SECURITY CLASS. (of this report) Unclassified
		15a. DECLASSIFICATION/DOWNGRADING SCHEDULE
16. DISTRIBUTION STATEMENT (of this Report) Approved for public release; distribution unlimited		
17. DISTRIBUTION STATEMENT (of the abstract entered in Block 20, if different from Report)		
18. SUPPLEMENTARY NOTES Approved for public release; IAW AFR 190-17 <i>Jerry F. Guess</i> JERRAL F. GUESS, Captain, USAF Director of Information		
19. KEY WORDS (Continue on reverse side if necessary and identify by block number) Dual Control Optimal Control Parameter Identification Sensitivity		
20. ABSTRACT (Continue on reverse side if necessary and identify by block number) Many errors are known to exist in Inertial Navigation Systems of modern air-to-ground missiles. These error sources, if undetected, contribute to navigation errors of position and velocity. This study analyses one source of INS errors -- the misalignment of the accelerometer reference frame. By maneuvering a missile, the error source becomes more observable. Thus, a better estimate can be made of the error source. This directly influences the estimate of position. ← CONF →		

UNCLASSIFIED

SECURITY CLASSIFICATION OF THIS PAGE(When Data Entered)

→ Hence, in order to minimize the terminal navigation error, some control energy must be expended to identify the error source. This dual control problem may be viewed as an optimization problem. By formulating a performance index of the terminal error and control energy appropriate mathematical techniques should yield an optimal flight trajectory.

This thesis seeks to analyze the dual control nature of an air-to-ground missile. Two methods are used. The first uses a predetermined flight path which is incremented until a minimum is reached. The second is a first-order gradient which allows greater freedom in the control law.

UNCLASSIFIED

SECURITY CLASSIFICATION OF THIS PAGE(When Data Entered)